The Role of the Non-neuronal Cholinergic System in Immune Regulation

By

Danika Roy

A thesis submitted in partial fulfillment
of the requirements for the degree of
Master of Science (MSc) in Chemical Sciences

The Faculty of Graduate Studies
Laurentian University
Sudbury, Ontario, Canada

THESIS DEFENCE COMMITTEE/COMITÉ DE SOUTENANCE DE THÈSE
Laurentian Université/Université Laurentienne
Faculty of Graduate Studies/Faculté des études supérieures

Title of Thesis Titre de la thèse	The Role of the Non-neuronal Cholinergic System in Immune Regulation
Name of Candidate Nom du candidat	Roy, Danika
Degree Diplôme	Master of Science
Department/Program Département/Programme	Chemical Sciences
Date of Defence Date de la soutenance	February 22, 2022

APPROVED/APPROUVÉ

Thesis Examiners/Examinateurs de thèse:

Dr. Alain Simard
(Supervisor/Directeur(trice) de thèse)

Dr. Eric Gauthier
(Committee member/Membre du comité)

Dr. Sujeenthar Tharmalingam
(Committee member/Membre du comité)

Approved for the Office of Graduate Studies
Approuvé pour le Bureau des études supérieures
Tammy Eger, PhD
Vice-President, Research (Office of Graduate Studies)
Vice-rectrice à la recherche (Bureau des études supérieures)

Dr. Clinton S. Robbins
(External Examiner/Examinateur externe)

ACCESSIBILITY CLAUSE AND PERMISSION TO USE

Abstract

Activation of nicotinic acetylcholine receptors (nAChRs) by agonists like acetylcholine (ACh) can have anti-inflammatory properties via the regulation of cytokines. A recent novel class of nAChR specific molecules termed silent agonists are also thought to induce nAChR-dependent metabotropic signaling cascades, while causing very little channel opening. These molecules may therefore be potent immune regulators. This study assessed the expression of cholinergic genes in human macrophages and gained insights on the anti-inflammatory properties of nAChR agonists, silent agonists and cholinergic inhibitors in human macrophages. For both aims, two human monocytic cell lines (THP-1 and U937) were cultured and differentiated into macrophages using phorbol 12-myristate 13-acetate (PMA) to obtain Mo macrophages and in some cases, further polarized into M1 (INF-γ) or M2 (IL-13 and IL-4). Expression of cholinergic genes were first determined via Western Blot and PCR. Secondly, experiments assessing expression of cell markers, cytokine expression, and viability were carried out following treatment with various conditions in the presence of LPS. It was hypothesized that macrophages would express cholinergic proteins and that nAChR agonists/silent agonists would result in anti-inflammatory responses whereas cholinergic inhibitors would result in pro-inflammatory responses. Overall, we found that differentiated macrophages expressed most cholinergic proteins and that the inhibition of cholinergic proteins and nAChR agonism modulated LPS-induced cytokine release. These experiments gave pertinent information regarding the presence of cholinergic genes and the anti-inflammatory properties of agonists/silent agonists in human macrophages.

Key Words
Nicotinic acetylcholine receptors, acetylcholine, silent agonists, cholinergic system, cytokines, macrophages, anti-inflammatory, immune system, cell markers, Western Blots

Acknowledgements

My academic experience here at the Northern Ontario School of Medicine and at Laurentian University has been unforgettable thanks to many individuals who have helped me throughout my journey. First, I would like to thank Dr. Alain Simard, my supervisor at the Northern Ontario School of Medicine for his guidance and for all of his help in the lab. Dr. Simard always made himself available to meet with me regarding any of my questions and concerns. He taught me many lab techniques including cell culturing, flow cytometry, Western Blotting and qPCR. Overall, I am extremely thankful to have had such a great supervisor throughout my MSc.

I would also like to acknowledge and thank my committee members Dr. Eric Gauthier and Dr. Sujeenthar Tharmalingam for their time, support and helpful advice. They have been important in ensuring my progress throughout my MSc by attending meetings and reviewing my MSc thesis.

Furthermore, I would like to thank Dr. Natalie Lefort, the Research Laboratory Coordinator at the Northern Ontario School of Medicine for her assistance and helpful advice. I also owe special thanks to Dr. Ramya Narendrula. Ramya worked in Dr. Simards laboratory during my first year of my master's degree, and she always went above and beyond to lend a hand when I needed it. Moreover, I would like to thank my lab colleagues, Maryse Lachapelle, Eduardo Soto Espinosa, Manon Valiquette, Gabriella Rumball, Doretha Thompson and Bailey Laforest for their constant support and all of their help throughout my master's thesis.

Finally, I would like to thank Dr. Nicole Hornstein and Dr. Roger Papke at the University of Florida for the synthesis of the synthetic silent agonists tested in this study.

Table of Contents

List of Figures

List of Tables

List of Appendices

List of Abbreviations

α-BGT: α-bungarotoxin

α-NETA: 2-(alpha-Naphthoyl)ethyltrimethylammonium idodide

Aβ: Beta Amyloid

ACh: Acetylcholine

AChE: Acetylcholinesterase

AChRs: Acetylcholine Receptors

AD: Alzheimer's Disease

AP-1: Activator Protein 1

APCs: Antigen Presenting Cells

BChE: Butyrylcholinesterase

BM: Bone Marrow

BMDM: Bone Marrow Derived Macrophage

CFA: Complete Freund's Adjuvant

ChAT: Choline Acetyltransferase

ChT: Choline Transporter

CLR: C-type Lectin Receptors

CNS: Central Nervous System

COX: Cyclooxygenase

CTLs: Choline Transporter-like Proteins

DMDs: Disease-modifying Drugs

DMSO: Dimethylsulfoxide

EAE: Experimental Auto-immune Encephalomyelitis

ECL: Enhanced Chemiluminescence

GSH: Glutathione

IL: Interleukin

IL-1R: Interleukin-1 Receptor

IL-6R: Interleukin-6 Receptor

IL-10R: Interleukin-10 Receptor

INF: Interferon

IRF3: Interferon Regulatory Factor 3

KO: Knockout

LBP: Ligand Binding Pocket

LDH: Lactate Dehydrogenase

LPS: lipopolysaccharide

mAChRs: Muscarinic Acetylcholine Receptors

MAPK: Mitogen-activated Protein Kinase

MNL: Mononuclear Leukocytes

MS: Multiple Sclerosis

nAChR: Nicotinic Acetylcholine Receptor

NF-kB: Nuclear Factor Kappa-light-chain-enhancer of Activated B Cells

NK: Natural Killer

NLRs: NOD-like Receptors

NNCS: Non-neuronal Cholinergic System

NOD: Nucleotide-binding Oligomerization Domain

NRTC: No Reverse Transcriptase Control

NSAIDS: Non-steroidal Anti-inflammatory Drugs

NTC: No Template Control

OCT: Organic Cation Transporter

PAM: Positive Allosteric Modulator

PBS: Phosphate Buffered Saline

PAMPs: Pathogen Associated Molecular Patterns

PBMC: Peripheral Blood Mononuclear Cell

PMA: Phorbol 12-myristate 13-acetate

PRRs: Pattern Recognition Receptors

RA: Rheumatoid Arthritis

RLR: RIG-1 like Receptors

RNS: Reactive Nitrogen Species

ROS: Reactive Oxygen Species

SEM: Standard Error Mean

TBE: Tris/Borate/EDTA

TCR: T-cell Receptor

TGFβ: Transforming Growth Factor Beta

TLRs: Toll-like receptors

TNF-α: Tumor Necrosis Factor alpha

TNFR: Tumor Necrosis Factor Receptor

Tregs: Regulatory T cells

VAChT: Vesicular Acetylcholine Transporter

Introduction

1.0 The Immune System

The immune system consists of various cells (macrophages, dendritic cells, lymphocytes, etc.) that tightly regulate and trigger immune responses against invasive and dangerous pathogens[1]. Such pathogens may include microbes, viruses, cancer cells and toxins[2]. Although this is the immune system's main role, it is also very much involved in other processes including homeostasis, reproduction, wound healing and metabolism amongst many others[3]. The immune system is made up of two fundamental lines of defense: innate immunity and adaptive immunity.

1.0.1 Innate Immunity

The innate immune response represents the first line of defense against pathogens. It is considered a less specific defense mechanism than the adaptive immune response as it recognizes conserved features of pathogens known as pathogen associated molecular patterns (PAMPs) like bacterial and fungal cell wall components (ex. gram negative cell walls)[4]. The recognition of PAMPS is mediated by pattern-recognition receptors (PRRs)[4]. PPRs can be further divided into four families: the Toll-like receptors (TLRs), nucleotide-binding oligomerization domain (NOD)-like receptors (NLRs), C-type lectin receptors (CLR) and RIG-1 like receptors (RLR)[5–7].

Several types of defensive barriers make up the innate immune system; these include anatomical, physiological, inflammatory as well as endocytic and phagocytic barriers[8]. The main goal of the innate immune system is to rapidly recruit immune cells in hopes of eliminating the

stimuli and initiating the healing process. More specifically, the immune cells that make up the innate immunity include phagocytes (macrophages, dendritic cells (DCs), monocytes, neutrophils and mast cells), Natural Killer (NK) cells, basophils, dendritic cells and eosinophils[2]. Since macrophages play vital roles in immunity and participate in many inflammatory disorders, macrophages are of particular interest in this study.

1.0.2 Macrophages

Macrophages are an essential component of the innate response [9–11]. Macrophages have an extensive range of cell surface receptors and intracellular components allowing them to not only interact with host cells, but also engulf and destroy invading pathogens[12]. Macrophages have a high plasticity and therefore, depending on their surrounding environment, can be polarized into a spectrum of activity-related phenotypes, which are dogmatically described by two main subsets: pro-inflammatory macrophages (M1 or classically activated macrophages) and anti-inflammatory macrophages (M2 or alternatively activated macrophages)[13,14]. Some features that distinguish M1 and M2 macrophages include their role in inflammation, their expression of cell markers and the cytokines they release. Although some markers are more highly expressed in one phenotype than the other, the extreme polarities are uncommon therefore resulting in a 'spectrum' of macrophage populations[15].

M1 macrophages contribute to local inflammation and tissue injury by promoting pro-inflammatory immune responses[16] as well as antiproliferative and cytotoxic activities[17]. These functions are completed through the release of pro-inflammatory cytokines, such as Interleukin (IL)-1β, IL-12, IL-23 and Tumor Necrosis Factor-α (TNF-α)[16], and production of reactive oxidants[18]. Macrophages can be polarized into M1 macrophages upon stimulation by type I

cytokines (ex. Interferon (INF)- and TNF-α) or upon binding of PAMPs (ex. Lipopolysaccharide (LPS)) to their respective receptors[17]. M1 macrophages can identified by their high expression of CD80 and CXCL10[19–22] cell markers.

In contrast, M2 macrophages are mainly involved in downregulating inflammation and promoting tissue repair[17]. Since M2 macrophages have a diverse set of responses, they are further subdivided into three subpopulations: M2a (stimulated by IL-4 and IL-13), M2b (stimulated by different immune signals along with IL-1β or LPS) and M2c (stimulated by IL-10, Transforming Growth Factor Beta (TGFβ), or glucocorticoids)[17]. Briefly, M2a macrophages are associated with the encapsulation and destruction of parasites as well as allergic responses[23]. They release polyamines and IL-10 which in return inhibit pro-inflammatory cytokine production[24]. M2b macrophages are responsible for the selective upregulation of phagocytosis and modulating immune responses[23]. They release very high levels of IL-10 while also secreting very little pro-inflammatory cytokines[23]. Finally, M2c macrophages play major roles in tissue and extracellular matrix repair as well as the downregulation of M1 immune responses[25,26]. M2c macrophages also release IL-10 which in turn, deactivates M1 immune responses[23]. IL-10 secretion from these cells also stimulates the release of CXCL13 and CXCL4[23]. M2 macrophages express different cell markers in comparison to M1 macrophages, which include MRC1 (CD206) and CD163[27].

Because of the high plasticity that macrophages possess, they can continuously switch phenotypes upon stimulation with different molecules and proteins[15,28]. For example, monocytic cell lines like THP-1 and U937 have been shown to display M1 macrophage characteristics upon stimulation with INF-γ and LPS whereas they showed M2 macrophage characteristics upon stimulation with IL-13 and IL-4[29,30].

1.0.3 Cytokines

Cytokines are small messenger proteins primarily produced by macrophages and helper T cells[31]. Cytokines initiate signaling cascades by either acting on the cells that secreted them (autocrine), on other nearby cells (paracrine) or on some distant cells (endocrine)[31]. Cytokines may be produced in response to PAMPs[32], PRRs involving TLRs and NLRs[33]. An example of a microbial molecule that induces the release of cytokines includes LPS, a major membrane component of Gram-negative bacteria. The main surface receptor for LPS is CD14, a membrane receptor that is highly expressed on macrophages[34]. LPS is first recognized by the LPS-binding protein that transports LPS and brings it to CD14. This facilitates the transfer of LPS to the TLR4/MD-2 receptor complex on the cell surface[35]. Afterwards, numerous intracellular signaling pathways become activated, which include nuclear factor kappa-light-chain-enhancer of activated B cells (NF-kB), interferon regulatory factor 3 (IRF3) and mitogen-activated protein kinase (MAPK) kinase pathways, further resulting in the expression of various pro-inflammatory genes[36].

Two types of cytokines exist: pro-inflammatory cytokines and anti-inflammatory cytokines. Pro-inflammatory cytokines upregulate inflammatory responses[31] whereas anti-inflammatory cytokines down-regulate inflammatory responses mainly by inhibiting the release of pro-inflammatory cytokines[31]. Cytokines typically initiate cascades via autocrine and paracrine signaling, resulting in a complex network of interactions[33]. Autocrine signaling occurs when a cytokine acts on the cell it was released by and amplifies or modulates gene expression of that cell whereas paracrine signaling occurs when a cytokine controls or amplifies changes in genes in nearby cells[37]. Paracrine signaling functions are important for inflammatory responses within a tissue or organ[37].

Amongst all pro-inflammatory cytokines, TNF-α, IL-6, and IL-1β appear to be the most important in the process of inflammation, being among the first cytokines to be released during such processes[31]. These cytokines signal through the type I cytokine receptors and initiate various signaling pathways as well as contribute to human disease[33].

TNF-α is a potent inflammatory mediator that plays important roles in the innate immune response mainly via the production of additional cytokines, the expression of adhesion molecules and the stimulation of growth[33]. TNF-α also stimulates the proliferation of cells, has cytolytic and inhibitory effects on tumor cells and is implicated in antiviral and inflammatory activities[33]. It is mainly secreted by activated macrophages but may also be secreted by other cell types like monocytes, T cells, mast cells and NK cells[33]. TNF-α initiates molecular signaling via binding to one of two receptors: tumor necrosis factor receptor (TNFR) 1 and 2. Both TNFRs receptors play similar roles, activating several pathways including MAP kinases and NF-kB, but only TNFR1 is capable of also activating apoptotic pathways (caspases)[38]. Interestingly, TNFR1 has been reported to be responsible for most cellular responses to TNF-α (cell growth, apoptosis, activation of immune signaling pathways and upregulation of cytokines) whereas TNFR2 has been shown to mostly play vital roles in the proliferation of lymphoid cells[39]. Such receptors are expressed at different concentrations, with TNFR1 being the most potent receptor found on cells and TNFR2 mainly only found on leukocytes and endothelial cells[40]. Overall, TNF-α has been shown to be an important cytokine in infection control, also affecting the activity of multiple other cells[33].

Similarly, IL-6 is also a pleiotropic cytokine expressed by a variety of cells including macrophages, T and B cells, fibroblasts, endothelial cells, keratinocytes, hepatocytes and bone marrow cells[41]. It is involved in haematopoiesis, the maturation of B cells[42] and the activation

and differentiation of T cells[33]. IL-6 initiates signal transduction via binding to the ligand-binding IL-6 receptor (IL-6R) and CD130[43]. The IL-6R expression is mostly restricted to lymphocytes and hepatocytes whereas CD130 is universally expressed[44,45].

IL-1β is made by various cells including monocytes, macrophages, neutrophils, and hepatocytes[46]. IL-1β mainly targets NK cells, and B and T cells with major functions in fever and pro-inflammatory responses essential for the host's response to pathogens[33,47]. IL-1β is also responsible for aggravating damage during tissue injury and chronic diseases[47] as well as activating T lymphocytes and B lymphocytes[48]. To induce its effects, it must first bind to one of two IL-1 receptors (IL-1R): IL-1R1 and IL-1R2[33]. Binding of IL-1a and IL-1β to IL-1R1 results in a signaling complex, initiating inflammatory responses[49]. In contrast, IL-1R2 acts as a decoy receptor, therefore does not initiate signal transduction and acts as an endogenous inhibitor of IL-1 signaling[49,50].

Finally, regarding anti-inflammatory cytokines, IL-10 is of particular interest. It is one of the most potent anti-inflammatory cytokines, supressing the expression of pro-inflammatory cytokines like TNF-α, IL-6 and IL-1β. Additionally, IL-10 promotes the secretion of the anti-inflammatory IL-1 receptor antagonist as well as the proliferation of various immune cells[51]. IL-10 initiates its immunosuppressive effects by binding to IL-10 receptor-1 (IL-10R1) a ligand binding subunit and IL-10 receptor-2 (IL-10R2), an accessory subunit necessary for signal transduction[51,52]. By down regulating immune responses, IL-10 prevents damage to tissues and promotes homeostasis within the host[51].

While the production of cytokines is essential in the fight against pathogens, unregulated cytokine release may lead to autoimmune diseases and chronic inflammation (or inflammatory diseases).

1.0.4 Inflammation

Inflammation is a non-specific mechanism generated by a local immune response to an infectious, physical or chemical agent[53]. Immune cells and peripheral leukocytes are recruited to the injury site where they release inflammatory mediators like bradykinin, histamine, prostaglandins and cytokines[54]. These inflammatory mediators help dilate and increase the permeability of blood vessels thus increasing local blood flow and allowing more immune cells to reach the injured tissue[55]. This is characterized as localized redness, swelling, heat and pain. Some other inflammatory mediators like cytokines also help in mediating immune responses and recruiting other immune cells to the injured tissues. Inflammation may be short-term (acute inflammation), lasting from hours to a couple weeks, where the stimuli is quickly removed, and tissue repair takes place[56]. On the contrary, long-term inflammation (chronic inflammation), lasts longer than two weeks and results from unregulated immune responses. Chronic inflammation triggers active inflammation and may cause permanent tissue damage[56].

1.0.5 Adaptive Immunity

The adaptive immune system, unlike the innate immune system, is specific in targeting the type of pathogen and is therefore slower to respond to newly encountered pathogens[57]. The adaptive immune system has an immunological memory, hence subsequent infections of the same pathogen are cleared faster. Because of this, efficient immunization against various diseases is possible[58]. The adaptive immune system is made up of lymphocytes, more specifically T and B cells.

T cells mature in the thymus and express a variety of antigen-binding receptors called T-cell receptors (TCR). T cells activate cell-mediated immune responses in which T cells act

directly against foreign antigens with the help of antigen presenting cells (APCs) like macrophages, dendritic cells and B cells amongst others[2,59]. Moreover, T cells also produce signal molecules initiating the destruction of phagocytosed microbes[59]. Different subsets of T cells exist, including follicular helper T cells which provide help to B cells in the production of antibodies, cytotoxic T cells which eliminate substances deemed harmful by the immune system and regulatory T cells (Tregs) that suppress immune responses and maintain homeostasis[60,61].

Conversely, B cells mature in the bone marrow and express antigen-binding receptors therefore do not require the help of APCs[2]. The main function of B cells is to release antibodies that circulate in the bloodstream and bind specifically to foreign antigens[59]. More specifically, when a naïve or memory B cell becomes activated by an antigen, it will proliferate and differentiate into an effector B cell, which secretes antibodies[62]. The binding of antibodies to the antigens results in either the inactivation of the antigen, the inhibition of the antigen to bind to other host cells, or the marking of the antigen for destruction[59]. Effector B cells eventually mature into large plasma cells, continuously secreting even more antibodies[62]. Although most plasma cells die after a few days, some may survive and reside in the bone marrow for many months to years, secreting antibodies into the blood[62].

Although these two lines of defense work synergistically in eliminating pathogens, flaws in any of these systems can result in numerous disorders such as inflammatory and autoimmune diseases, immunodeficiencies and hypersensitivities[2].

1.1 Autoimmune Diseases

Autoimmune diseases arise from the immune system attacking self-molecules as a result of a decline in immunologic tolerance[63]. All autoimmune diseases vary in their target organs and

clinical manifestations. However, they are thought to undergo a similar series of sequential stages: initiation, propagation, and resolution[64]. Genetic, infectious and environmental factors are responsible for initiating and contributing to autoimmunity[63,64]. Throughout the propagation phase, epitope spreading occurs, immune cells produce cytokines, and the numbers of both effector T cells and Tregs become imbalanced[64–67]. Furthermore, autoantigens may be generated. Autoantigens are endogenous antigens recognized by the immune system as non-self, resulting in autoimmune responses such as the production of autoantibodies[68]. Consequently, this results in progressive inflammation and tissue damage[64]. During the resolution phase, extrinsic and intrinsic mechanisms are activated which includes the activation of Tregs and various inhibitory receptors[64]. Given the complexity of autoimmune diseases, the symptoms and the progression of the disease may vary between individuals. Some examples of common autoimmune diseases include multiple sclerosis (MS) and rheumatoid arthritis (RA).

MS is one of the most common neurological disease in young adults, affecting 1 in 1,000 individuals[69]. This chronic inflammatory disease results in the individual's immune system mistakenly attacking the myelin surrounding the nerve fibers creating miscommunication between the brain and the body[70]. These lesions within the central nervous system (CNS) may lead to severe physical and cognitive dysfunctions as well as neurological deficits[71]. Similarly, RA is another common autoimmune disease characterized by the immune system's destruction of body tissue and other parts of the body (skin, eyes, lung, heart and blood vessels)[72]. This disease is most seen in the elderly, affecting approximately 1% of the population[73].

1.1.1 Current Therapies

Although many therapies against autoimmune diseases exist, the efficacy of the treatments strictly varies between individuals and is dependent on the progression of the disease[74]. Conventional therapies against autoimmune diseases include non-steroidal anti-inflammatory drugs (NSAIDS), glucocorticoids and disease-modifying drugs (DMDs)[74].

First, NSAIDS are one of the most widely used medications in the world because of their efficacy to relieve pain and inflammation[75]. NSAIDS achieves anti-inflammatory and analgesic effects via the inhibition of cyclooxygenase (COX) enzymes[76]. COX is involved in the production of lipids termed prostaglandins which promote inflammation and pain[76]. While NSAIDS are often effective in alleviating pain and inflammation, chronic use of NSAIDs may result in various side effects including gastrointestinal disorders (bleeding, ulcers and perforation)[77], renal toxicity[77,78] and cardiovascular conditions (congestive heart failure and myocardial fraction)[79,80].

Secondly, another treatment option for individuals suffering from autoimmune diseases is glucocorticoids. Glucocorticoids bind to their specific receptor and inhibit immune signaling pathways (activator protein 1 (AP-1), NF-kB) subsequently inhibiting cytokine expression[81]. Although they have been found to be effective in the treatment of some chronic diseases, glucocorticoids may induce several side effects similar to those of NSAIDS which include gastrointestinal ulcers and bleeding, infection, immunosuppression and bone damage[82].

Lastly, the third conventional therapy against autoimmunity, more specifically in MS, consists of DMDs. There are several different types of DMDs, each with different mechanisms of action, but they all function by targeting the underlying disease instead of the symptoms. To

date, 11 classes of DMDs are being used to help treat MS, most of these being antibodies. Examples of DMDs include alemtuzumab, daclizumab and INF-beta-1a[83]. Both alemtuzumab (also known as Lemtrada) and daclizumab (also known as Zinbryta) are antibodies that selectively bind to CD52 and CD25 respectively, reducing lymphocyte activation and migration[83]. On the other hand, INF-beta-1a works by binding to its receptor to prevent T cell proliferation, reduce antigen presentation and modulate cytokine secretion[84].

Hence, it is clear that DMDs, being immunomodulatory, may help in decreasing tissue and organ damage caused by inflammatory responses[85]. However, considering most of these DMDs reduce overall immune responses, the side effects can become very severe ranging from headaches, skin rashes and flu-like symptoms to autoimmune hepatitis, cancer and cardiac disorders[86–88]. These agents target the terminal phase of inflammation and are therefore not effective against the fundamental problem that is responsible for these autoimmune diseases[64]. For this reason, patients are often required to take them for life, increasing their chances of malignant and infectious complications[64].

Despite advances in drug development, many patients with autoimmune diseases like MS and RA do not effectively respond to current therapies and may have serious adverse effects[69,89]. For this reason, more effective and safer therapies need to be developed to allow individuals affected by autoimmune diseases to live a longer and healthier life.

1.1.2 Roles of Macrophages in Autoimmunity

Considering the effectiveness of the DMDs in the treatment of some autoimmune diseases like MS, it is therefore evident that immune cells like lymphocytes have major roles in tissue damage. Since macrophages are important modulators of both the innate and adaptive

immune system, they must also play a vital role in the pathogenesis of autoimmune disorders such as MS and RA[90].

It is known that macrophages accumulate at the site of injury and participate in ongoing inflammation[17]. During phagocytosis of cell debris and pathogens, macrophages produce and release reactive oxygen species (ROS) and reactive nitrogen species (RNS)[17,18]. ROS and RNS release at controlled normal levels is necessary in maintaining tissue homeostasis as well as the destruction of pathogens and foreign materials[17]. However, during chronic inflammation, macrophages may occasionally produce excessive amounts of ROS resulting in oxidative stress[17,18]. The resulting oxidative stress, if not quickly regulated, can then lead to various detrimental outcomes. First, oxidative stress itself can cause local tissue damage[18]. Oxidative stress and excessive ROS production can generate an imbalance in antioxidants, more specifically in glutathione (GSH) therefore inducing cell death[91]. Additionally, the ROS generated by these macrophages can modify proteins, lipids and DNA[92]. These modifications may cause modified function, necrosis, apoptosis and the generation of autoantigens[93]. This may result in the initiation and progression of autoimmune diseases.

Furthermore, the importance of myeloid cells like macrophages in MS disease progression has become increasingly clear[16]. In active MS brain lesions, macrophages were found to be one of the most dominant cells[94–96]. As previously discussed, macrophages have different functions and release different molecules and proteins depending on their phenotypes. The balance of macrophage phenotypes has a big influence on the outcomes of many autoimmune diseases[97]. M1 macrophages can provoke inflammation and their uncontrolled release of pro-inflammatory cytokines and oxidative products can lead to autoimmune disease progression[28]. A previous study on experimental autoimmune encephalomyelitis (EAE), an

animal model for MS, reported the importance of M1/M2 balance in the progression and relapse of the disease[98]. Remarkably, they demonstrated that in the EAE rat model, relapsing Dark Agouti rats had a more balanced M1/M2 population in brain lesions and peripheral blood during spontaneous disease recovery[98]. However, during their disease relapse, the rats showed greater pro-inflammatory responses, suggesting that M1 macrophages are involved in the relapsing of the disease[98]. Interestingly, administration of M2-activated macrophages exhibited suppression of disease relapse[98], thus, restoring M2 cell populations may have critical therapeutic value in the progression of autoimmune diseases.

Despite knowledge advancements of the contribution of macrophages in autoimmune diseases, the exact mechanisms and role that macrophages have in autoimmune diseases remains to be elucidated.

1.2 The Cholinergic System

The cholinergic system refers to cells capable of producing the required elements for acetylcholine (ACh) synthesis, storage, transport and degradation[99]. The major cholinergic system components include choline acetyltransferase (ChAT), acetylcholinesterase (AChE), butyrylcholinesterase (BChE), vesicular acetylcholine transporter (VAChT) and choline transporter (ChT). ChAT is the enzyme responsible for the synthesis of ACh from choline and acetyl coenzyme A (acetyl-CoA). On the other hand, AChE and BChE are hydrolytic enzymes that both degrade ACh into choline and acetate. In neurons, the degraded choline is then transported back into the cell by ChT, and is considered essential for the continuous ACh synthesis[100]. Three types of choline transport proteins exist which includes an organic cation transporter (OCT) (low affinity for choline), choline transporter-like proteins (CTLs) (moderate

affinity for choline) and ChTs (high affinity for choline)[101]**.** VAChT is a specific vesicular ACh transporter that mediates the storage of ACh in synaptic vesicles[102]. A summary of the roles of these cholinergic proteins are shown in Figure 1.

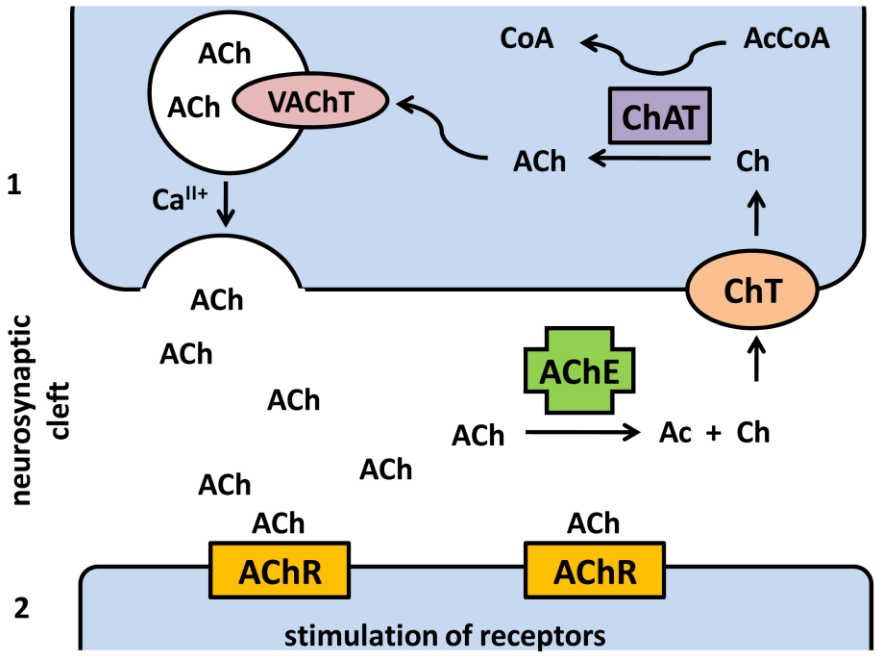

Figure 1. Overview of the Roles of Various Cholinergic Proteins
Obtained from Pohanka, M., 2012.

The cholinergic system is a branch of the autonomic nervous system, with major roles in memory, digestion, heart rate, blood pressure and movement amongst many other functions[103]. These roles are accomplished through the release of ACh and its binding to acetylcholine receptors (AChRs). Although ACh is more commonly known for its role as a neurotransmitter, it may also be released by and act on non-neuronal cells[104], termed the non-neuronal cholinergic system. The system for ACh synthesis, storage, transport and degradation within these cells is called the non-neuronal cholinergic system (NNCS).

1.2.1 The Non-neuronal Cholinergic System

Increasing evidence suggests that the NNCS is dysregulated in various autoimmune and inflammatory diseases[104]. Although modulation of the neuronal cholinergic system (ex. AChE inhibitors) for neuronal diseases like AD is commonly used as treatment against the disease, in non-neuronal cells, our knowledge on the expression and function of the NNCS is limited[104].

Over the years, several studies focusing on the expression of cholinergic markers in immune cells were carried out and it is now evident that immune cells possess an independent cholinergic system. The presence of ACh in immune cells was first determined in the human peripheral blood mononuclear leukocytes (MNL)[105–108]. Shortly after, the presence of ACh was demonstrated in many leukemic cell lines like HSB-2, MOLT-3 and CEM amongst others[109,110]. Additionally, ACh was also found in rat lymphocytes, more specifically T and B cells, where T cells expressed significantly higher ACh expression than B cells[111], likely due to the higher expression of ChAT in T cells[112]. The ACh expression in both macrophages and DCs, however, remains unclear.

As previously mentioned, the protein ChAT is necessary for ACh production. Rinner and Schauenstein[112] were amongst the first to confirm the presence of ACh-synthesizing activity in various immune cells like rat T and B cells from the thymus, spleen and blood. These findings suggest the presence of ChAT in lymphocytes[112]. Furthermore, the expression of ChAT mRNA was detected in activated murine MNLs and DCs but was not detected in neither activated nor resting murine peritoneal macrophages[113]. However, others have determined the presence of ChAT mRNA in human lung and alveolar macrophages as well as monocytes at very high Ct values, suggesting the very low expression of ChAT within these cells[114]. Fujii et al.[115] provided definitive evidence by confirming the presence of ChAT mRNA in human leukemic T cells

using RT-PCR and Western Blots. These discoveries support the idea that ACh within immune cells is mainly produced by the protein ChAT.

There is increasing evidence of immune cells expressing other cholinergic proteins like AChE, VAChT and ChT. In fact, AChE was shown to be present ubiquitously in murine lymphocytes, DCs and macrophages[113]. In line with those findings, AChE mRNA was detected in other immune cells including MNLs, leukemic T cells and B cells[116]. Moreover, VAChT immunoreactivity was determined in human peripheral blood T and B cells but further studies are required to confirm the presence of VAChT within immune cells[117]. Finally, ChT expression, more specifically CHT1 was also detected amongst lymphocytes, more specifically in the human leukemic T cell, MOLT-3, while other T cell lines (CEM and Jurkat) showed no expression[118].Thus, it has become clear that immune cells possess the machinery necessary to produce and degrade ACh. The ACh released by such cells can then initiate signaling cascades by binding nAChRs, another important component of the NNCS.

1.2.2 Nicotinic Acetylcholine Receptors

The nAChR, a type of AChR, is a ligand-gated transmembrane ion channel expressed by both neuronal and non-neuronal cells[119–121]. nAChR history goes back to 1844, when Claude Bernard discovered that curare paralyses rabbits without affecting their hearts[122]. Afterwards, from 1905-1907, John Langley developed the concept of a ‘receptive substance’ where he demonstrated that nicotine could stimulate denervated muscle cells and that this was blocked by curare[123]. In 1914, Dale revealed that both nicotine and muscarine act as agonists to create different effects on AChRs, and proposed that two different types of acetylcholine receptors must therefore exist[124,125]. Then, Otto Loewi discovered a chemical transmission which controls

heart muscles in 1921[126], and in 1936, Sir Henry Dale and coworkers identified acetylcholine to be that chemical transmitter[127].

In the mid-1980s, two important studies led to a great advancement in our knowledge of nAChRs. First, a rich source of nAChRs was discovered in the *Torpedo* electric organ[128,129]. This discovery provided a great source of starting material for isolating and studying nAChRs. Second, was the α-bungarotoxin (α-BGT), a component of krait snake venom that was found to bind irreversibly to nAChRs, blocking the action of ACh[130,131]. α-BGT inhibits nAChR function, promoting paralysis at the neuromuscular junction followed by respiratory failure and death[132]. Collectively, these discoveries significantly advanced our knowledge of nAChR structure and function.

nAChRs belong to the superfamily of Cys-loop ligand-gated ion channel superfamily containing two disulfide linked cysteines separated by 13 highly conserved amino acids[128,133]. Each nAChR subunit is comprised of four transmembrane α-helical domains, denoted M1-M4 and an extracellular amino-terminus and carboxy-terminus[133]. A large intracellular domain of variable length located between M3-M4 is also present[133]. The extracellular amino-terminus is essential for ACh binding[134] while the M2 segment forms the conducting pore determining cation selectivity and conductance[135]. The structure of nAChRs is shown in Figure 2.

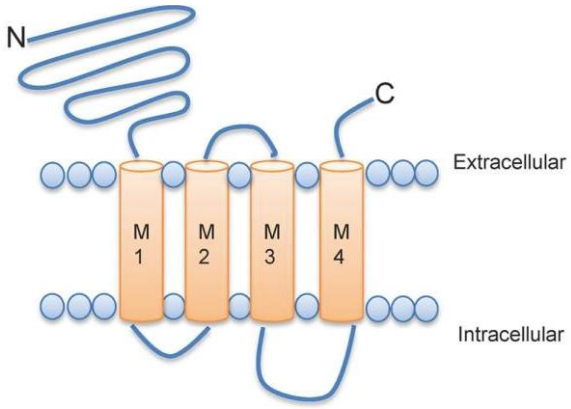

Figure 2. Structure of nAChRs
Modified from Hendrickson, L.M., Guildford, M. J. & Tapper, A. R., 2013.

nAChRs have 17 different nAChRs subunits identified in vertebrates (α1-10, β1-4, γ, δ, ε)[128], however, the α8 has only been shown to be present in avian species[136]. Functional nAChRs consists of five subunits, arranged to form either homomeric or heteromeric channels, although only the α7-9 subunits have been shown to form functional homomeric receptors[137–140]. Examples of functional heteromeric and homomeric nAChRs are shown in Figure 3.

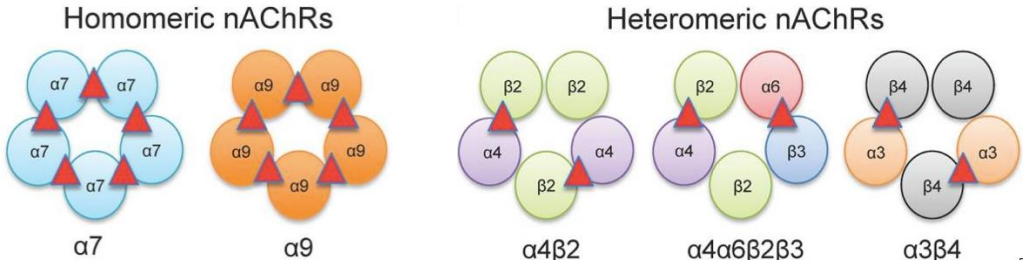

Figure 3. Examples of Homomeric and Heteromeric nAChRs
Acetylcholine binding sites are shown as red triangles. Homomeric receptors bind to five ACh molecules while heteromeric receptors bind to two ACh molecules, between an a subunit and a non-a subunit. Modified from Hendrickson, L.M., Guildford, M. J. & Tapper, A. R., 2013.

As a result of subtype diversity in neuronal nAChRs, the different nAChR subtypes have distinct pharmacological and physical properties[141,142]. nAChRs are divided into two groups: the

muscle-type nAChR and the neuronal-type nAChR[143]. The muscle-type nAChRs are found within skeletal muscles at the neuromuscular junction where they play crucial roles in the transmission of nerve signals to skeletal muscles[143]. The muscle-type nAChRs can only be assembled in two nAChR subtypes which include α1β1γδ found in embryonic muscle and α1β1εδ found in adult muscle. The γ subunit in embryonic muscle is replaced by the ε subunit in adult muscle due to the developmental switch in transcription[136].

The neuronal-type nAChRs on the other hand, are found in the nervous system in peripheral ganglia and in the brain as well as in non-excitable cells like epithelial and immune cells[143]. There is increasing evidence of the presence of at least one type of nAChR subunit in various immune cell types including lymphocytes[144–148], monocytes[149], macrophages[150–152] and endothelial cells[153]. In contrast to the muscle-type nAChRs, the neuronal-type nAChRs have greater diversity, capable of forming many homomeric and heteromeric receptors from the α and β subunits[136]. Neuronal nAChR have various functions depending on their subtype and location. These functions include regulating the release of neurotransmitters (learning, memory and reward pathways), blood pressure and heart rate[143].

1.2.3 nAChR Agonist Binding

As their name suggests, nAChRs can be activated by ligands such as ACh and nicotine, though they can also bind and be activated by various other ligands. The ligand binding pocket (LBP) for an agonist or antagonist of nAChRs is via the α-subunit where Cys-Cys pairing is required[128]. The α-subunit contains a loop, termed C-loop, that is structured to interlock the agonist/antagonist around the face of an adjacent subunit, which can be either an α, β, γ, or ε subunit[128]. The LBP of nAChRs has been conserved throughout evolution, making them great

targets for predatory toxins[128]. Toxins may function as either potent agonists (ex. nicotine, anatoxin) or antagonists (ex. α-BGT, methyllcaconitine)[128]. Upon binding of nAChR to an agonist, the receptor undergoes a conformational change, allowing positively charged ions like calcium, sodium and potassium to flow through[128]. The binding of ligands to nAChRs triggers the receptor to undergo different conformational states which include: the resting state (channel is closed, low affinity for agonists), the active state (channel is open, agonist occupies the ligand binding site) and the desensitized state (channel is closed, agonist still occupies the ligand binding site but is unresponsive to agonists)[120,128]. For the receptor to return to the resting state, all agonists need to be unbound[120,128]. For this reason, in the presence of high agonist concentrations, the receptor will spend most of its time in the desensitized state[120,128]. The different conformational states are shown in Figure 4. Once the agonist binds to the receptor and undergoes channel opening (active state), within seconds or minutes, the channel closes and enters the desensitized state[154].

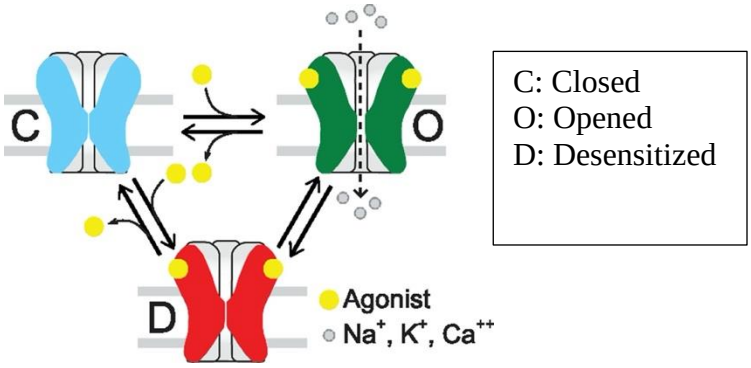

Figure 4. The Three Conformational States of nAChRs
Modified from Corradi, J. & Bouzat C., 2016.

Although nAChRs are traditionally viewed as ligand-gated ion channels with major roles in neurotransmission, two decades ago, the importance of nAChR in the modulation of the immune system was raised[155]. Since then, it has become progressively clear that the activation of nAChRs by ligands such as ACh and nicotine can protect against inflammatory diseases such as MS and RA. Though the anti-inflammatory capabilities of nAChRs was first thought to be caused by the nAChR channel opening, increasing evidence suggest that it is instead caused by prolonged channel desensitization[156]. Amongst all subtypes, the α7 nAChR homomeric receptor have been shown to be involved in anti-inflammatory responses and is therefore of particular interest in studying immune responses and inflammation. In addition, the α9 nAChR homomeric receptor has also recently been shown to be involved in inflammatory and immune responses.

1.2.4 Homomeric Nicotinic Acetylcholine Receptors

The homopentameric α7 nAChR, one of the most abundant subtypes of nAChR in the nervous system, is also expressed in numerous non-neuronal cells[157]. This receptor is highly permeable to calcium, suggesting its significant involvement in intracellular signaling[158]. The α7 homomeric receptor is also less sensitive to nicotine and can become desensitized much faster than the heteromeric receptors[159,160]. In non-neuronal cells like immune cells, the α7 nAChR plays major roles in immunity, inflammation and neuroprotection[161] . Previous studies have shown that nicotine or ACh binding to the α7 nAChR results in the suppression of inflammation[155,165,166], mainly by inhibiting the release of the pro-inflammatory cytokine, TNF-α[166–168]. In fact, inflammatory responses are highly dependent on the expression of α7 nAChRs as it was shown that upon stimulation of the vagus nerve or upon administration of galantamine (an AChE inhibitor) or choline (a nAChR agonist) TNF-α release is attenuated in WT mice but

not in α7-deficient mice[166,169,170]. In line with those findings, it was shown that the expression of TNF-α, INF-ɣ, and IL-6 are much higher in α7-knockout (KO) mice in comparison to the WT-mice[171], suggesting the overall anti-inflammatory role of α7 nAChRs.

In addition, in a study on EAE, nicotine was shown to successfully diminish EAE severity while this effect was partially attenuated in the α7-KO mice[172]. Upon activation of α7 nAChRs, nicotine inhibits immune signaling pathways like MAPK, NF-kB and *c-myc*[173]. The effects of nicotine on EAE were only partially reversed in α7-KO mice, suggesting that other nAChR subunits may also contribute to the anti-inflammatory effects of nicotine on EAE[172]. In fact, recent studies have shown that the α9 nAChR subunit also plays important roles in anti-inflammatory effects upon nAChR agonist binding[174,175]. Likewise, phosphocholine has previously been identified as an unconventional agonist for the α9 nAChR receptor, capable of activating metabotropic functions of α9[176]. Such findings further support the idea that other nAChR subunits, likely the α9 subunit, also contribute to anti-inflammatory effects of nAChR agonists like nicotine.

Taken together, these results demonstrate the important roles of α7 nAChR and potentially α9 nAChR in the modulation of inflammatory responses and has increased their interest in medical and biological research.

1.3 Silent Agonists

There has been increasing evidence suggesting that nAChR desensitization, rather than opening, is responsible for the anti-inflammatory effects of nAChRs and the important roles the α7 subunit plays in anti-inflammatory responses[177,178]. For these reasons, molecules that target α7 and that promotes receptor desensitization may be of great therapeutic potential. A new class of

molecule, termed silent agonist have been developed by Dr. Papke and Dr. Horenstein from the University of Florida[177,178]. The silent agonists are very weak α7 partial agonists[178] that produce little to no channel activation while inducing prolonged receptor desensitization[177]. Recent unpublished evidence also suggests that some of these silent agonists have potent activity on α9-containing receptors as well[175]. These unique molecules are "silent" in an ionotropic sense and considered agonist because when co-applied with a positive allosteric modulator (PAM), a molecule known to increase agonist-mediated receptor activity, the channel opens[179]. This phenomenon is shown in Figure 5.

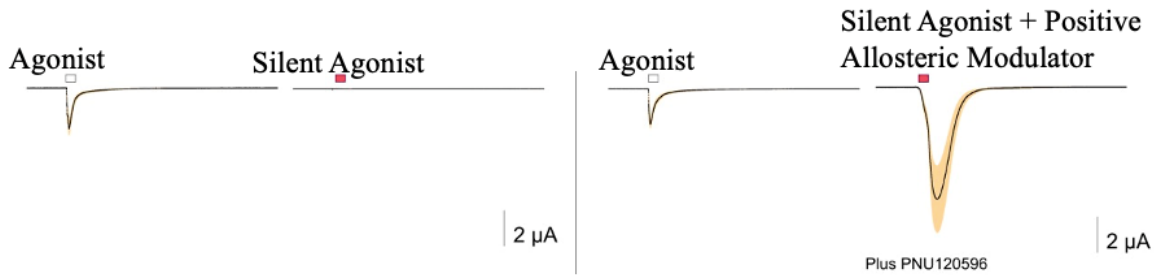

Figure 5. Voltage-Clamped Oocytes in the presence of an agonist, a silent agonist and a silent agonist in the presence of a PAM
Voltage-clamp responses demonstrating the activation of α7 nAChRs upon treatment with a nAChR agonist and silent agonist alone or coapplied with a positive allosteric modulator. When applied alone, the silent agonist showed no activation of the α7 receptor. Modified from Papke, R.L. et *al*., 2018.

Interestingly, unlike most conventional nAChR agonists, the silent agonists specifically bind to the α7 and α9 homomeric nAChR and α9α10 heteromeric nAChR[175,178]. The silent agonists analyzed in this study are p-CF_3 diEPP (6.MQ.39), m-bromo PEP (2.MQ.75) and m-$CONH_2$ diEPP Iodide (2.MQ.103). These silent agonists were chosen based on their selectivity for the α7 nAChR and previous studies demonstrating the efficacy of these molecules to produce anti-inflammatory effects[178,180,181]. Figure 6 shows their chemical structure.

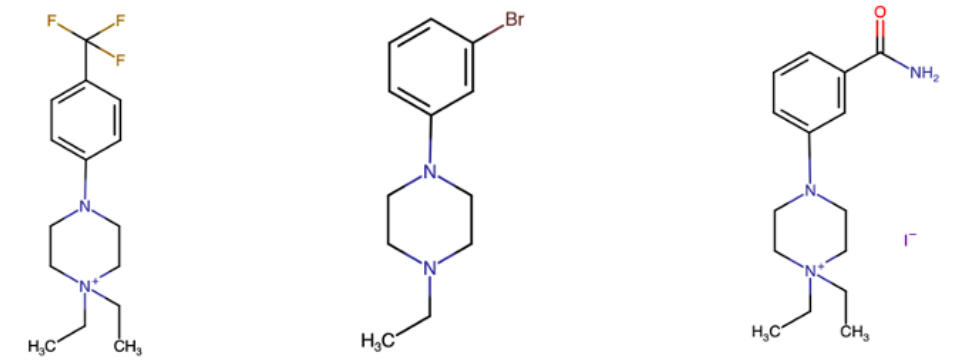

Figure 6. Structure of silent agonists

Recent studies have shown the efficacy of the silent agonists in both *in vivo* and *in vitro* models of inflammation. One study showed that m-bromo PEP protects against EAE[180]. M-bromo PEP effectively diminished immune cell infiltration into the CNS thereby reducing EAE clinical scores[180]. Upon stimulation of bone marrow cells with LPS, m-bromo PEP downregulated TNF-α, IL-6 and IL-10 release[180]. In a different study using the α7-selective silent agonist NS6740, this silent agonist successfully attenuated TNF-α release in LPS-stimulated rat microglial cells[182]. Likewise, Papke *et al.* demonstrated that NS6740 is an effective treatment of inflammatory and neuropathic pain in mouse models while also having analgesic effects[156]. In addition, in a study using complete Freund's Adjuvant (CFA)-induced inflammatory pain model in mice, p-CF_3 diEPP dose dependently reduced CFA-induced mechanical sensitivity[178].

Additional studies performed in our laboratory demonstrated the anti-inflammatory effects of both p-CF_3 diEPP and m-$CONH_2$ diEPP iodide in human whole blood[181]. When pre-treated for 1 hour with p-CF_3 diEPP or m-$CONH_2$ diEPP, p-CF_3 diEPP decreased LPS-induced

IL-6, IL-1β and TNF-α secretion while m-$CONH_2$ diEPP iodide seemed to strongly reduce TNF-α secretion from these cells[181].

Hence, the findings of the silent agonists as anti-inflammatory molecules imply a promising role in a therapeutic context for the treatment of various autoimmune and inflammatory diseases like MS and RA. However, further work is required as there is currently a lack of knowledge on the effects on these molecules on different tissues and cell types.

Objectives/Hypothesis

This study's overall goal was to elucidate the role of the cholinergic system and silent agonists in immune regulation. Our first objective was to determine the expression of cholinergic genes in human macrophages at both the transcript level (PCR) and the protein expression level (Western Blot). It is important to note that both methods were performed with a qualitative approach, to determine the expression of cholinergic genes and not to quantitively compare expression levels of the genes. The second aim of this study was to investigate the anti-inflammatory properties of nAChR silent agonists and various other nAChR agonists and cholinergic inhibitors in human macrophages. The anti-inflammatory responses were measured by assessing cytokine profiles and immune cell phenotype upon stimulation with the various conditions and LPS, an immune stimulant. It was hypothesized that some, if not most cholinergic proteins would be expressed by human macrophages and that the nAChR agonists/silent agonists would result in anti-inflammatory responses whereas cholinergic inhibitors would result in pro-inflammatory responses in LPS-stimulated human macrophages. Moreover, it was also hypothesized that agonists that have anti-inflammatory effects would also decrease the expression of cellular markers more commonly expressed by pro-inflammatory cells while promoting the expression of cellular markers expressed by anti-inflammatory cells.

Materials and Methods

2.0 Chemicals

The silent agonists p-CF_3 diEPP, m-bromo PEP and m-$CONH_2$ diEPP Iodide were synthesized as previously described[183]. The molecules arrived as pure crystalline products and were immediately stored at -20 °C. Stock solutions of each silent agonist were prepared by diluting the crystals in dimethylsulfoxide (DMSO) to a concentration of 100 mM and then, subsequently diluted at a storage concentration of 10 mM in sterile phosphate buffered saline (PBS). Various agonists and cholinergic inhibitors including galantamine hydrobromide (Sigma-Aldrich, Cat#PHR1623), ML352 hydrochloride (Tocris Bioscience, Cat#5725) acetylcholine chloride (Sigma-Aldrich, Cat#A2661) choline chloride (Sigma-Aldrich, Cat#C7527) and nicotine, ditartrate (Sigma-Aldrich, Cat#481975) were purchased and diluted in water. 2-(alpha-Naphthoyl)ethyltrimethylammonium idodide (α-NETA) (Sigma-Aldrich, Cat#SML2731) was also purchased but because of its insolubility in water, it was diluted in DMSO.

2.1 Cell lines and culture conditions

The human monocytic cell lines, THP-1 (ATCC, TIB-202) and U937 (ATCC, CRL-1593.2), were purchased from the American Type Culture Collection (Virginia, USA). The cells were maintained in RPMI-1640 medium (ATCC, Cat#30-2001) supplemented with 10 % fetal bovine serum (Gibco, Cat#12484028) and 1 % penicillin streptomycin (Gibco, Cat#15140122) and incubated at 37 °C with 5 % CO_2 in the Forma Series II Water Jacketed CO_2 Incubator

(ThermoFisher, serial# 304981). The THP-1 cell complete growth medium also contained 0.05mM of 2-mercaptoethanol (Gibco, Cat#21985023)

2.2 Mo, M1 and M2 macrophage differentiation

The cells were seeded at approximately 5×10^5 viable cells per mL into a flask or in a well plate. For differentiation to a macrophage phenotype (Mo), THP-1 and U937 cells were stimulated with 100 ng/mL of phorbol 12-myristate 13-acetate (PMA) (Sigma-Aldrich, P8139) for 48 hours. The media was replaced with PMA-free media to allow the cells to rest for 24 hours. Macrophages were then treated with fresh media supplemented with 10 ng/mL of INF-ɣ (Sigma-Aldrich, Cat#IF005) and 10 pg/mL of LPS (Invitrogen, Cat#LS00497603) or 20 ng/mL of IL-4 (R&D systems, Cat#204-IL-020) and 20 ng/mL of IL-13 (R&D systems, Cat#213-ILB-005) to further polarize into M1 or M2 phenotypes, respectively, or left untreated to maintain the Mo phenotype for an additional 48 hours.

2.2.1 Treatment with various silent agonists

The THP-1 and U937 cell lines were differentiated into macrophages as previously described in section 2.2. After polarization, the macrophages were given fresh media and pre-treated with 100 μM of silent agonists (p-CF_3 diEPP, m-bromo PEP, CONH2 diEPP Iodide) for 1-hour followed by an 8-hour stimulation with 100 ng/mL of LPS. The concentrations for the LPS and the silent agonists were chosen based on previous work performed in our laboratory. Likewise, the 1-hour silent agonist pre-treatment was chosen based on a previous study in our laboratory demonstrating that pro-inflammatory cytokine release was best inhibited at a 1-hour silent agonist pre-treatment[181]. The 8 hours of LPS stimulation was selected based on preliminary

data demonstrating the reduction of cytokine release after 9 hours of LPS stimulation. Vehicle control groups were also included in this study, which included a 0.1 % DMSO (Corning, Cat#25-950-CQC) treated group and a 100 ng/mL LPS + 0.1 % DMSO treated group.

2.2.2 Acute and Chronic agonist/silent agonist/cholinergic inhibitor treatments

The THP-1 and U937 cell lines were differentiated into macrophages as previously described in section 2.2. During the 48-hour polarization (or 48-hour rest for Mo cells), the macrophages were treated with various agonist, silent agonists, or cholinergic inhibitors at varying concentrations (Table 1). After the 48-hour polarization, the macrophages were given fresh media and treated with the same concentration of agonists, silent agonists, or cholinergic inhibitors (as found in table 1) as well as 10 ng/mL of LPS for 5 hours. Control groups included an untreated group and a 10 ng/mL LPS treated group for the treatments diluted in H_2O, as well as a 0.1 % DMSO vehicle control and a 10 ng/mL LPS+ 0.1 % DMSO for the treatments diluted in DMSO. Additionally, one well was reserved for the total release (required for the viability measurements). The concentrations of ACh and nicotine were chosen based on previous literature demonstrating the efficacy of these treatments in inhibiting pro-inflammatory cytokines at 100μm[184–186]. To be able to compare agonist efficacy, the choline concentration was chosen to be the same as ACh and nicotine (100μm). The concentrations for the remaining treatments were chosen based on previous work performed in our laboratory. The 5 hour stimulation of LPS was chosen to be able to compare our data to similar experiments currently being carried out by our collaborators

Table 1. Concentration of the various silent agonist treatments

Well #	Treatment
1	Untreated
2	10 ng/mL LPS
3	10 ng/mL LPS + 100 µM ACh
4	10 ng/mL LPS + 100 µM ACh + 50 µM Gal (AChE Inhibitor)
5	10 ng/mL LPS + 50 µM Gal (AChE Inhibitor)
6	10 ng/mL LPS + 100 µM Ch
7	10 ng/mL LPS + 100 µM Nicotine
8	10 ng/mL LPS + 10 µM ML352 (ChT Inhibitor)
9	10 ng/mL LPS + 0.1 % DMSO
10	10 ng/mL LPS + 100 µM p-CF_3 diEPP
11	10 ng/mL LPS + 5 µM α-NETA (ChAT Inhibitor)
12	Total Release

2.3 Protein Extraction

Proteins from the differentiated macrophages were extracted by first removing the culture media from the adherent cells and washed twice with ice cold PBS. Then, cold radioimmunoprecipitation assay buffer (RIPA) (Thermo Scientific, Cat#89900) buffer was added to the cells and kept on ice for 5 min, swirling the plate/flask occasionally. The lysate was gathered to one side of the plate/flask using a cell scraper and transferred to a microcentrifuge tube. Samples were then centrifuged at 14,000 x g for 15 min to pellet the cell debris and the supernatant was transferred to a new labeled tube for further analysis.

2.4 BCA Assay

To ensure the equal loading of proteins in Western Blotting, the concentration of the extracted proteins was determined using the Pierce™ BCA Protein Assay Kit (Thermo Scientific, Cat#23225), in which the manufacturer's microplate protocol was closely followed. Briefly, 25 µL of standards and samples and 200 µL of working reagent were added to the microplate wells. The working reagent was prepared by mixing 50 parts of BCA Reagent A with 1 part BCA Reagent B. RIPA buffer and 1X PBS were used as protein blanks. The plate was covered and incubated for 30 min at 37 ^{o}C and the absorbance was then read at a wavelength of 562 nm using the PowerWave XS plate reader (BioTek, serial# 198303) and Gen5 software (v2.0).

2.5 Western Blot

Extracted protein samples were diluted with RIPA buffer and 4X reducing Laemmli SDS sample buffer (Alfa Aesar, Cat#J60015) to the desired concentration of 1 µg/µL. These diluted samples were then heated at 95 ^{o}C on a block heater for 6 minutes. Positive control lysates including IMR-32 (human neuroblastoma) whole cell lysate (Abnova, Cat#L008V1) and 293T (human kidney cells) whole cell lysate (Abcam, Cat#ab95494) were purchased and prepared according to the manufacturer's protocol. The module containing the 4-15 % precast polyacrylamide gels (Bio-Rad, Cat#4568085) were placed in electrophoresis tanks and the inner chamber as well as the electrophoresis tank were filled with 1X running buffer. The running buffer consists of a 1X diluted solution of 10X Tris-Glycine SDS Buffer (Thermo Fisher Scientific, Cat#28362). The comb was carefully removed and 10 µL of the ladder (FroggaBio,

Cat#PM007-0500), positive control lysates and heated samples were added to the wells using gel loading tips. Once all the samples were successfully added to the wells, the lid was placed on the electrophoresis tank and the gel ran at 110 V for 1 hour.

Afterwards, the precast gels were removed, and the gels were imaged on the ChemiDoc Imaging system (Bio-Rad, serial# 733BR2507) under UV transillumination to ensure successful separation of proteins in the gel. Then, the protein transfer from the gel onto a PVDF membrane (Bio-Rad, Cat#1620264) is performed by placing a piece of PVDF membrane in methanol to become activated. Additionally, sponges, filter papers and transfer cassettes were presoaked in transfer buffer then assembled in the following order starting the assembly on the black side of the transfer cassette: the soaked sponge, two soaked filter papers, the gel, the activated PVDF membrane, two more soaked filter papers and finally, the other sponge. The transfer buffer was made by first creating a 10X transfer buffer solution by mixing 288 g of glycine (Sigma-Aldrich, Cat#410225) and 60.4 g of tris base (Fisher BioReagents, Cat#BP1521) with 1.8 L of Milli-Q water. Then, a 1X transfer buffer was made by combining 100 mL of 10X transfer buffer with 200 mL of 99.9% methanol (Fisher BioReagents, Cat#FLBP11051) and 700 mL of Milli-Q water. Once the assembly was completed, the cassette was closed and placed in the module of the tank that was filled halfway with 1X transfer buffer and that also contained an ice pack and a stir bead. The tank was also placed in an ice bucket on top of a stir plate to ensure that the transfer buffer stayed cold throughout the transfer. The stir plate was turned on and the transfer was run by setting the voltage at 100 V for 70 minutes.

Once the transfer was complete, the PVDF membranes were observed under UV transillumination on the ChemiDoc to ensure successful transfer without any bubbles. Next, the membranes were blocked in blocking buffer (Bio-Rad, Cat#1706404) for 1 hour at room

temperature or overnight at 4 °C with gentle shaking. The membranes were then stained with primary antibodies by diluting the antibodies to their desired concentration (Table 2) in blocking buffer and placing this solution and the membranes in separate sealed plastic bags overnight at 4 °C with gentle shaking.

The next day, 1X tris-buffered saline (TBS)and 1X tris-buffered saline containing Tween 20 (TBST) were prepared before moving on to the next steps. The 1X TBS was made by diluting the 10X TBS (Fisher BioReagents, BP2471) to a 1X concentration using Milli-Q water and the TBST was prepared by adding 1 mL of Tween (Fisher BioReagents, Cat#BP337) per 1000 mL of 1X TBS. The membranes were washed three times in 1X TBST for 10 min followed by one 10-minute 1X TBS wash. Thereafter, the membranes were incubated in a 1/30,000 goat anti-rabbit IgG H&L (HRP) secondary antibody (abcam, Cat#ab97051) diluted in blocking buffer at room temperature for one hour with gentle shaking.

After one hour, the membranes were washed again three time in 1X TBST for 10 min followed by one 10-minute 1X TBS wash. Equal portions of the Stable Peroxide Solution and the Luminol/Enhancer solution from each enhanced chemiluminescence (ECL) reagents (Thermo Scientific, Cat#34094) were mixed in an Eppendorf tube and few drops were added to sealed plastic wraps. The membranes were gently blotted on a Kim Wipe to remove excess buffer, inserted in the sealed plastic wraps containing the ECL mix and then placed in the Chemidoc Imaging System. The membranes were visualized using chemiluminescence.

Table 2. Concentration and Description of Primary Antibodies used in Western Blots

Gene	Concentration of Primary Antibody	Description	Manufacturer	Catalog #	Theoretical Molecular Weight
AChE	1 / 3,000 dilution	Rabbit polyclonal antibody	Abcam	ab97299	68 kDa
BChE	1 / 3,000 dilution	Rabbit polyclonal antibody	Abcam	ab154763	68 kDa
ChAT #1	1 / 2,000 dilution	Rabbit polyclonal antibody	Abcam	ab223346	83 kDa
ChAT #2	1 / 1,000 dilution	Rabbit polyclonal antibody	Abcam	ab137349	83 kDa
VAChT	1 / 1,000 dilution	Rabbit polyclonal antibody	Synaptic Systems	139103	75 kDa
ChT	1 / 500 dilution	Rabbit polyclonal antibody	Abcam	ab56074	63 kDa

2.6 RNA extraction

RNA for the adherent cells was extracted using the Purelink® RNA Mini Kit (ThermoFisher, Cat#12183025). Briefly, the cells were lysed and homogenized in 500 µL of the manufacturer's lysis buffer containing 2-mercaptoethanol using a 5 mL syringe attached to a 21-gauge needle then transferred to a microcentrifuge tube. An equivalent volume of 70% ethanol was added to each tube and the samples were added to different spin columns, followed by various washing steps as described in the manufacturer's protocol. DNA contaminants in the samples was removed by inserting an on-column DNAse treatment into the protocol before eluting the RNA. This was accomplished by using the Purelink® DNAse (ThermoFisher, Cat#12185010). Afterwards, the RNA was eluted into a recovery tube and the RNA concentration was immediately assessed with the Nanodrop One (ThermoScientific, serial# AZY1708333). RNAse free water was used as the blank solution and the samples were then stored at -80 ℃ until further processing.

2.7 RNA integrity

To verify the RNA integrity, the RNA samples were run on a 1% agarose gel. First, the agarose gel was prepared by dissolving 1.6 g of agarose (Froggabio, Cat#A87-500G) in 160 ml of 1X Tris/Borate/EDTA (TBE) (BioBasic, Cat#A0014) and heating the mixture in the microwave for 1-3 minutes. The solution was left to cool down for approximately 10 min before adding 4 µL of ethidium bromide and pouring the solution into a gel tray with the well comb in place. Once solidified (approximately 30 min), the tray was placed in an electrophoresis chamber filled with 1X TBE and the comb was carefully removed from the gel. The RNA was prepared to be loaded onto the gel by diluting the RNA samples in 6X Ficoll based agarose gel loading buffer (Alfa Aesar, Cat#J62800). Thereafter, 10 µL of the samples was added to the wells. The lid for the chamber was placed and the gel was run at 120 V for 1 hour. Once completed, the gel was visualized in the Chemi Doc (BioRad, serial# 76S/03422) under UV transillumination.

2.8 cDNA Synthesis

The synthesis of cDNA was performed using the SensiFAST^{TM} cDNA Synthesis Kit (Bioline, Cat#BIO-65054). The synthesis was performed by following the manufacturer's protocol. Various controls were prepared for each sample and primer including a no reverse transcriptase (NRTC) control sample and a no template control (NTC). The NRTC was prepared by mixing all components of the reaction except for the reverse transcriptase, which is replaced for water. The NTC was prepared by mixing all components of the reaction in exception to the RNA which is once again replaced with water. Once the samples were prepared, the 8-strip PCR tubes were inserted in the Mini Thermal Cyclers (BioRad, serial# MM004240 and MM001660).

2.9 Reverse transcription polymerase chain reaction

The generated cDNA (see section 3.9) was then either used in RT-PCR or in SYBR Green qPCR (section 3.11). For RT-PCR, the Platinum^{TM} SuperFi II PCR Master Mix 2X (ThermoFisher, Cat#12368010) was used. The manufacturer's protocol for a 50 µL reaction was followed. The samples were then incubated in the thermal cyclers at the manufacturer's recommended thermal cycling conditions. The annealing temperature for each primer differed (Table 3). Afterwards, the products were analyzed by mixing each sample with the 6X Ficoll based agarose gel loading buffer and 10-15 µL of this mixture was added into the agarose gel (see section 3.8) wells. A DNA ladder (ThermoFisher, Cat#10787018) was also loaded to separate wells to verify the molecular weights of the bands. The agarose gel was run at 90 V for 1 hour (9-12 well gel) or 120 V for 1 hour (24 well gel). The gels were then visualized on the ChemiDoc under UV transillumination.

Table 3. Primers used in RT-PCR

Gene	Primer 1	Primer 2	Reference Sequence Number	Annealing Temp.	Predicted Band Size
α7 nAChR	5'-AGATGGCCAGATTTGGAAACC-3'	5'-GCAGGAACTCTTGAATATGCCT-3'	NM_000746.6	62 °C	142 bp
α9 nAChR	5'-TGGCACGATGCCTATCTCAC-3'	5'-TGATCAGCCCATCATACCGC-3'	NM_017581.4	61 °C	172 bp
α10 nAChR	5'-AGATCATCGACATGGATGAACGGA-3'	5'-ACGGGAAGGCTGCTACATC-3'	NM_020402.4	60 °C	294 bp
CHRFAM7A	5'-CCCGGCAAGAGGAGTGAAAGGT-3'	5'-TGCAGATGATGGTGAAGACC-3'	NM_139320.2	60° C	844 bp
AChE	5'-TGCGATACTGGGCCAACTT-3'	5'-TGGAACTCGGCCTTCCACT-3'	NM_015831.2	60 °C	997 bp and 244 bp

ChAT	5'-GCTTTTGTGAGAGCCGTGAC-3'	5'-CCGGTTGCTCATCAGGTAGG-3'	NM_020984.4	60 °C	222 bp
BChE	5'-ATCCTCCAAACTTCCGTGGC-3'	5'-GAATCCTGCTTTCCACTCCCA-3'	NM_000055.4	56 °C	370 bp
VAChT (SLC18A3)	5'-CTCACTATGCGGCCTCTGTT-3'	5'-ACCGCATCGTACAGACCTTG-3'	NM_003055.3	60 °C	336 bp
ChT (SLC5A7)	5'-GCCATACTCATTGGGGCCAT-3'	5'-AACTGAGGTACCAGAGCCCA-3'	NM_001305005.3	N/A	**367** bp

2.10 SYBR Green qPCR

To determine the mRNA expression of cell markers, the SensiFAST^{TM} SYBR Lo-ROX Kit (Bioline, Cat#BIO-94020) was used and the manufacturer's 3-step cycling protocol was followed. Different primers targeting various surface markers were purchased from IDT (Table 4). Primers were used at a 500 nM concentration. To ensure the specificity of each primer and determine the predicted bp size, the Primer-BLAST designing tool was used. The primer's optimal annealing temperatures were assessed by testing a range of annealing temperatures using the gradient feature. Since SYBR Green binds to all dsDNA, the specificity of the qPCR primers was further verified by running the qPCR products on an agarose gel and confirming that the single band observed was at the correct bp size. This agarose gel is shown in Figure 7.

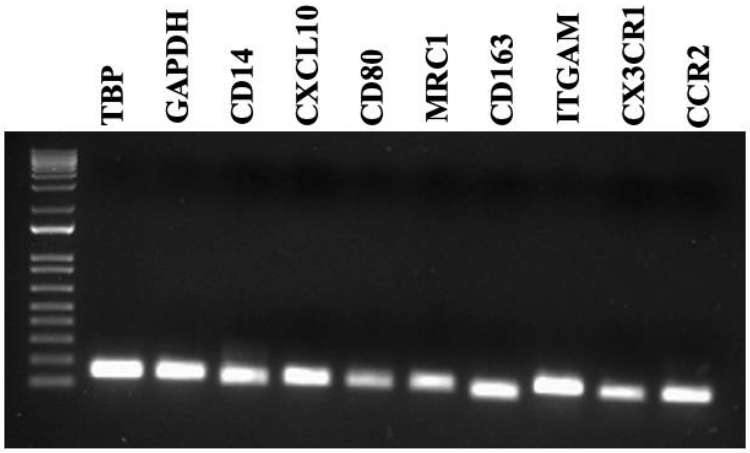

Figure 7. Agarose Gel of qPCR products

The products were run on the agarose gel once, and for subsequent reactions, a melt curve was included in the protocol to ensure only one product was being amplified. The efficiency of each primer was also determined by constructing a standard curve. Each primer had efficiencies of 89-105%, and the R^2 value of the standard curves were >0.980. The relative normalized expression was determined by the CFX Maestro Software where TBP and GAPDH served as reference genes.

Table 4. Primers used in SYBR Green qPCR

Gene	Primer 1	Primer 2	Reference Sequence Number	Annealing Temp.	Predicted Band Size
TBP	5'-GATAAGAGAGCCACGAACCAC-3'	5'-CAAGAACTTAGCTGGAAAACCC-3'	NM_003194	63.6 ºC	145 bp
GAPDH	5'-ACATCGCTCAGACACCATG-3'	5'-TGTAGTTGAGGTCAATGAAGGG-3'	NM_002046	63.6 ºC	143 bp
CXCL10	5'-GACATATTCTGAGCCTACAGCA-3'	5'-CAGTTCTAGAGAGAGGTACTCCT-3'	NM_001565	60.5 ºC	127 bp
CD80	5'-TCCTGATAACCTGCTCCCAT-3'	5'-ATCTCTCATTCCTCCTTCTCTCT-3'	NM_005191	60.5 ºC	122 bp
MRC1 (CD206)	5'-GGTTTTGGAGTAA	5'-TCCATCTTCCTTGTGTCAGC-3'	NM_002438	60.5 ºC	121 bp

	TATTCACTGTTCT-3’				
CD163	5’-GCATAGTAACTGTACTCACCAACA-3’	5’-CCAGAACACATATTCCCTCCAC-3’	NM_203416	60.5 ºC	99 bp
CD14	5’-CAGAGGTTCGGAAGACTTATCG-3’	5’-AATCTTCATCGTCCAGCTCAC-3’	NM_001174105	63.6 ºC	119 bp
ITGAM (CD11b)	5’-AGTCTGCCTCCATGTCCA-3’	5’-GTGTGCTGTTCTTTGTCTCATTG-3’	NM_001145808	61.8 ºC	140 bp
CX3CR1	5’-GGCAGACTTGGATTTCAGGA-3’	5’-GCCTCAGCCAAATCATCGTA-3’	NM_001171174	63.6 ºC	126 bp
CCR2	5’-CTGAGAAGCCTGACATACCAG-3’	5’-CTGATAAACCGAGAACGAGATGT-3’	NM_001123396	63.6 ºC	**367** bp

2.11 Cytokine Measurements

To prepare the human cytokine standard curves, known concentrations of lyophilized standards were obtain for each cytokine and a serial dilution was performed. The cytokine kits used included: Human IL-6 Flex Set (BD Biosciences, Cat#558276), Human IL-10 Flex Set (BD Biosciences, Cat#558274), Human IL-1β Flex Set (BD Biosciences, Cat#558279) and Human TNF-α Flex Set (BD Biosciences, Cat#560112). The manufacturer’s “Preparing Human Flex Set Standards” protocol was followed where cytokine concentrations ranging from 2,500 pg/mL to 10 pg/mL were prepared. To determine the cytokine concentrations in the cell supernatants, the manufacturer’s protocol found in the “BD CBA Human Soluble Protein Master Buffer Kit – Instruction Manual” was followed. Briefly, the cytokine bead master mix was prepared using the 50X capture bead stock vials from each flex kit and 1X PBS. The capture bead stocks were diluted with 1X PBS ensuring a total volume of 25 µL of Cytokine Beads Master Mix in each well (0.5

µL of each cytokine + 24.5 µL 1X PBS). Then, 25 µL of each sample was added to their respective wells on the 96-well plate and one well was reserved for the negative control where 25 µL of 1X PBS was added. 25 µL of capture bead master mix was then added to each sample. Each well was properly mixed by pipetting and incubated at room temperature, in the dark for one hour. After the incubation, the same steps used to prepare the cytokine beads master mix was performed to prepare the detection antibodies master mix. Similarly, 25 µL of the detection antibodies master mix was added to each and mixed by pipetting. The samples were once again incubated in the dark for one hour at room temperature. Afterwards, 100 µL of PBS was added to each well followed by a centrifugation at 230 x g and 4 °C for 5 minutes. The well supernatant was removed by inverting the plate and discarded. 100 µL of 1X PBS was added to each well, properly mixed by pipetting and transferred to their respective falcon tubes (Falcon, Cat#C352008). The samples in the falcon tubes were then analyzed via flow cytometry (described in section 3.13).

2.12 Flow Cytometry

Flow cytometry was performed on a FACSCanto II flow cytometer (BD Biosciences, serial# V96100029) and the BD FACSDiva Software (v6.1.3). The flow cytometer was regularly calibrated and verified to ensure accurate readings. The parameters were as follows, FSC: Voltage 400, SSC: Voltage 385, PE: Voltage 475, APC: Voltage 490, APC-Cy7: Voltage 470. For each sample, 2000 events were acquired. The data obtained were later interpreted using the FCAP Array Software (v3.0).

2.13 Mycoplasma

Cell culture supernatants were routinely tested for mycoplasma contamination using the Mycoplasma PCR Detection Kit (abm, Cat#G238). 2.5 µL of cells that were remained in culture for a minimum of 48 hours undisturbed and had a confluency of at least 80% were collected and placed in an Eppendorf on ice. The reaction mix was prepared following the manufacturer's protocol and loaded into 8-strip PCR tubes. Aside from our test samples, a positive control and NTC were also included as controls. Then, the tubes were placed in the thermal cycler where the manufacturer's recommended thermocycling conditions were used. After the PCR, the amplification products were visualized via agarose gel electrophoresis and ethidium bromide staining. The expected mycoplasma band size is at approximately 500 bp. The cell cultures were tested monthly to ensure they were free of mycoplasma. Mycoplasma was never detected in any of the samples analyzed.

2.14 LDH Measurements

The lactate dehydrogenase (LDH) measurements for the samples were analyzed using the CyQUANT LDH Cytotoxicity Assay – Fluorescence Kit (Invitrogen, Cat#C20303). The manufacturer's protocol was followed with some modifications. Briefly, 50 µL of each sample supernatant was added to a 96-well flat bottom plate. The Reagent Stock Solution was prepared by diluting 12 mL of Reporter Mix to the entire bottle of the Reagent Mix and mixed by vortex. Then, 50 µL of Reagent Stock Solution was added to each sample well and mixed by gentle tapping. Any visual bubbles were removed with a 10 µL pipet tip. The plate was then incubated at room temperature for 10 minutes, protected from light. After the incubation, 50 µL of Stop

Solution was added to each sample well. As a blank, a well containing only media was added to account for any background fluorescence. The positive control (100% cytotoxicity) consisted of THP-1 or U937 macrophages that were set aside as an extra well and left untreated. These cells were purposely lysed through a freeze/thaw cycle. The LDH from each sample's supernatant post-treatment were measured using the LDH assay kit and the Cytation 5 imaging reader. To determine LDH activity, the background fluorescence signal (media only) was subtracted from the sample's LDH activities. Afterwards, % cytotoxicity was calculated using the manufacturer's formula. The fluorescence was then immediately measured using the Cytation 5 imaging reader (BioTek, serial# 190509A).

2.15 Imaging Cell Count (Viability)

Adherent cells were washed twice with 1X PBS and 1mL of 1X PBS was added to each T25 flask. Then, 2 drops of NucBlue™ Fixed Cell ReadyProbes™ Reagent (DAPI) (Invitrogen, Cat#R37606) were added to each flask and incubated for 15 minutes. The cells were then imaged and counted using the Cytation 5 imaging reader.

2.16 Statistical Analysis

The cytokine concentration data was normalized by setting the concentration of each cytokine from the LPS or the LPS + DMSO to 100% and calculating all other values accordingly. Means were obtained by calculating the average of the normalized values for each treatment groups. The standard error mean (SEM) represents the standard error between the various values of the same treatment groups. Results are presented as means ± SEM. Data was analyzed by repeated measures one-way ANOVA multiple comparisons with Dunnett's

correction. Treatments were compared to either the LPS or the LPS + DMSO control groups and statistical significance was determined (*: $P \leq 0.0332$; **: $P \leq 0.0021$; ***: $P \leq 0.0002$; ****: $P \leq 0.0001$). All data analysis were calculated using the GraphPad Prism 9.0.1 software.

Results

3.0 Expression of Cholinergic Gene mRNA in Human Macrophages

PCR experiments assessing the expression of cholinergic genes in human macrophages were first performed to determine the presence of these genes within Mo, M1 and M2 macrophages of the two different cell lines (THP-1 and U937). RNA was extracted from the cells, whereby further transcribed into cDNA. These PCR experiments were performed to determine the presence of the genes and not used for quantification purposes. As for controls, a NRTC and NTC were included in each run to identify any potential genomic and/or environmental DNA contaminations, respectively.

According to the PCR results (Figure 8 and Figure 9), each set of primers generated distinct bands near the predicted band sizes, suggesting that these primers are highly specific and only amplifying the gene of interest. In THP-1 macrophages (Figure 8), AChE, BChE and VAChT were expressed by the cells. Within our RNA samples, AChE (Figure 8A) was expressed at two band sizes, the first at approximately 800 bp and the second at approximately 250 bp, suggesting the presence of AChE in THP-1 macrophages. BChE (Figure 8B) primers generated two bands in THP-1 samples, close to 400bp and 500bp suggesting the presence of BChE in THP-1 macrophages. No bands were detected with ChAT primers (Figure 8C), suggesting that this transcript is not expressed in THP-1 macrophages. To rule out the possibility that the PCR did not work, the THP-1 samples were run simultaneously with the U937 samples, which were positive for ChAT. Finally, VAChT (Figure 8D) seemed to be expressed in THP-1 macrophages since a PCR product was detected near the predicted band size.

Since THP-1 macrophages did not seem to express ChAT, we wanted to confirm the presence of ChAT in a different macrophage cell line, therefore we assessed the presence of cholinergic markers in the U937 cells. Similar results for AChE and VAChT were observed in U937 macrophages, however unlike THP-1, U937 seemed to also express ChAT (Figure 9). AChE (Figure 9A) was again expressed at two different band sizes. Additionally, ChAT (Figure 9C) and VAChT (Figure 9D) also seemed to be expressed by U937 macrophages by the bright bands seen on the gels. On the other hand, BChE (Figure 9B) seemed to be expressed in U937 Mo macrophages but did not seem to be or was only very slightly expressed in M1 and M2 macrophages.

Other than the cholinergic genes described above, the presence of various nAChR subunits (α7, α9, α10 and CHRFAM7A) were also assessed by PCR. In THP-1 differentiated macrophages, the α7 nAChR (Figure 10A) seemed to only be expressed in M2 macrophages while the α9 nAChR (Figure 10B) did not seem to be expressed in any of the THP-1 macrophages. On the other hand, the α10 nAChR (Figure 10C) and CHRFAM7A (Figure 10D) seemed to be expressed in all the THP-1 differentiated macrophages as seen by the amplification bands present.

Lastly, in the U937 differentiated macrophages, the α7 nAChR (Figure 11A) did not seem to be present in any of the U937 macrophages by the lack of amplification shown in the gel. On contrary, the α9, α10 and CHRFAM7A all seemed to be expressed in U937 Mo, M1 and M2 macrophages.

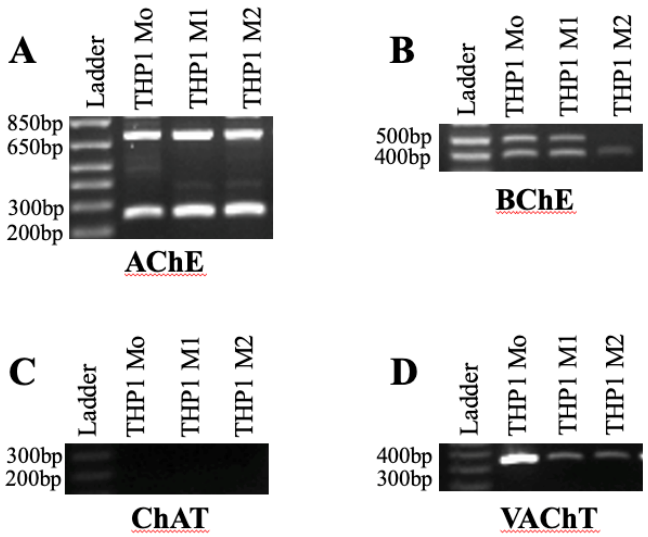

Gene	Predicted Band Size
AChE	997 bp and 244 bp
BChE	370 bp
ChAT	222 bp
VAChT	336 bp

Figure 8. PCR of Cholinergic Genes in THP-1 Differentiated Macrophages

Expression of cholinergic genes in THP-1 differentiated macrophages were first assessed by PCR. PCRs were repeated 3 times with different extracted RNA samples (n = 3). A NRTC and NTC were used as controls to identify any potential genomic DNA and/or environmental DNA contaminations, respectively. No amplification was seen in the controls. Based on these results, THP-1 Mo, M1 and M2 macrophages seemed to expressed AChE (A), BChE (B) and VAChT (D) by the bands present at the theoretical band sizes. No amplification was seen with the ChAT (C) primer.

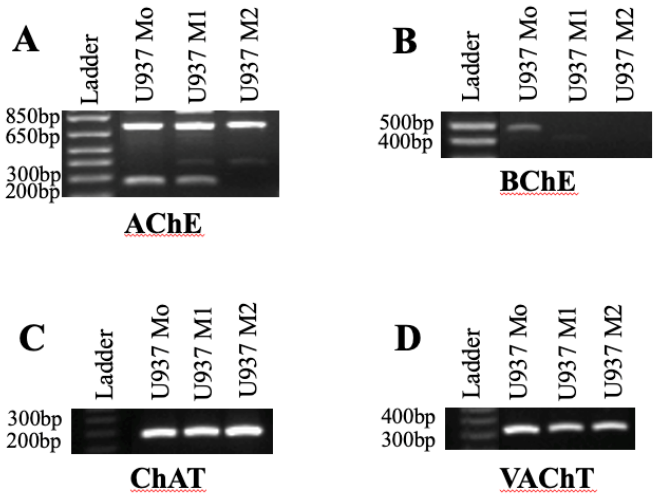

Gene	Predicted Band Size
AChE	997 bp and 244 bp
BChE	370 bp
ChAT	222 bp
VAChT	336 bp

Figure 9. PCR of Cholinergic Genes in U937 Differentiated Macrophages

Expression of cholinergic genes in U937 differentiated macrophages were determined by PCR. PCRs were repeated 3 times with different extracted RNA samples (n = 3). A NRTC and NTC were used as controls to identify any potential genomic DNA and/or environmental DNA contaminations, respectively. No amplification was seen in the controls. Based on these results, U937 Mo, M1 and M2 macrophages seemed to expressed AChE (A), ChAT (C) and VAChT (D)

by the bands present at the theoretical base pair sizes. As for BChE (B), some amplification was seen in the U937 Mo but not in M1 and M2 macrophages.

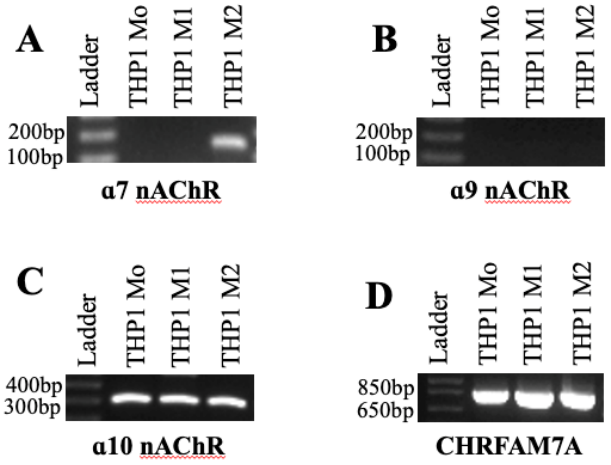

Gene	Predicted Band Size
α7 nAChR	142 bp
α9 nAChR	172 bp
α10 nAChR	294 bp
CHRFAM7A	844 bp

Figure 10. PCR of nAChRs in THP-1 Differentiated Macrophages

Expression of nAChRs in THP-1 differentiated macrophages were assessed by PCR. The PCRs were repeated 3 times with different extracted RNA samples (n = 3). A NRTC and NTC were used as controls to identify any potential genomic DNA and/or environmental DNA contaminations, respectively. No amplification was seen in the controls. Based on these results, THP-1 M2 macrophages seemed to express α7 nAChR (A) while Mo, M1 and M2 THP-1 macrophages did not seem to express α9 nAChR (B). Furthermore, THP-1 Mo, M1 and M2 macrophages seemed to express α9 nAChR (C) as well as CHRFAM7A (D).

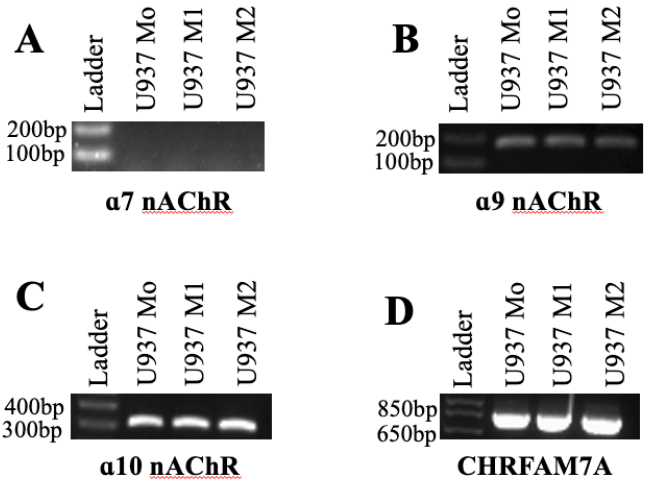

Gene	Predicted Band Size
α7 nAChR	142 bp
α9 nAChR	172 bp
α10 nAChR	294 bp
CHRFAM7A	844 bp

Figure 11. PCR of nAChRs in U937 Differentiated Macrophages

Expression of nAChRs in U937 differentiated macrophages were assessed by PCR. The PCRs were repeated 3 times with different extracted RNA samples (n = 3). A NRTC and NTC were used as controls to identify any potential genomic DNA and/or environmental DNA

contaminations, respectively. No amplification was seen in the controls. Based on these results, U937 differentiated macrophages did not seem to express α7 nAChR (A), while Mo, M1 and M2 U937 macrophages seemed to express α9 nAChR (B), α10 nAChR (C) and CHRFAM7A (D).

3.1 Expression of Cholinergic Proteins in Human Macrophages

Western blots were carried out afterwards to further verify the expression of cholinergic proteins in macrophages. The cholinergic proteins assessed by Western Blot include AChE, ChAT, BChE, ChT and VAChT. The expression of such proteins is shown in Figure 12 and 13 from THP-1 and U937 differentiated macrophages, respectively. Different positive control lysates were used for cholinergic proteins. First, IMR-32, a human neuroblastoma whole cell lysate was used as a positive control for AChE, ChAT and VAChT while 293T, a human kidney whole cell lysate was used as a positive control for BChE. The red arrows on Figures 12 and 13 indicate the protein's predicted molecular weight.

AChE has a theoretical molecular weight of 68 kDa, as determined by its protein sequence (UniProt accession #: P22303). However, the theoretical molecular weight of 68 kDa does not take into account any protein modifications post-translational modifications, which can influence the overall weight of the protein and its behaviour in a PAGE-SDS gel. As seen in Figure 12A and 13A, THP-1 differentiated macrophages did not seem to express AChE, while U937 macrophages seemed to slightly express AChE. However, the expression of AChE in both the positive control and the U937 macrophages seemed to be at a lower molecular weight, suggesting the presence of AChE of a different isoform. Further validation would be required to verify the expression of AChE in U937 macrophages.

Furthermore, the expression of ChAT was also assessed in the macrophages. Figure 12B,C and 13B,C show the expression of ChAT in THP-1 and U937 macrophages. The

expression of ChAT in the positive control and both THP-1 and U937 macrophages were at a lower molecular weight than that of ChAT's theoretical molecular weights. These lower bands were present in both ChAT blots (Figure 12B,C and 13B,C), which were generated using two different primary antibodies for ChAT. The ChAT #1 antibody targeted the human ChAT at the N-terminal to the mid-protein, while the ChAT #2 antibody targeted the human ChAT at a region within amino acids 102-351 (UniProt accession #: 28329). Consequently, there is evidence suggesting the presence of ChAT at a lower molecular weight than predicted in THP-1 and U937 differentiated macrophages.

Figure 12D and 13D demonstrate the expression of BChE in THP-1 and U937 differentiated macrophages, respectively. According to its protein sequence, BChE has a theoretical molecular weight of 68 kDa (UniProt accession #: P06276). Although a band size similar to that of the theoretical molecular weight was seen in the positive control, bands of much lower sizes were expressed in the THP-1 and U937 macrophages. Thus, BChE seemed to be expressed at the theoretical molecular weight in the positive control while it seemed to be expressed at a lower molecular weight in the differentiated THP-1 and U937 macrophages. This band may be due to nonspecific binding or may represent a different isoform of BChE.

ChT expression within the cells is shown in Figure 12E and 13E for THP-1 and U937 differentiated macrophages, respectively. ChT has a theoretical molecular weight of 63 kDa (UniProt accession #: Q9GZV3). As shown in Figure 12E and 13E, the positive control seemed to highly express ChT by the thick band near the theoretical molecular weight. While the band was detected in the positive control, no band appeared in the THP-1 samples (Figure 12E) and in the U937 samples (Figure 13E). Thus, this suggests that THP-1 and U937 differentiated macrophages do not express ChT.

Finally, Figure 12F and 13F demonstrate the expression of VAChT within THP-1 and U937 differentiated macrophages. As shown in these figures, VAChT seemed to be expressed at two different molecular weights in both the positive control and the THP-1 and U937 macrophages, suggesting the presence of VAChT within these cells.

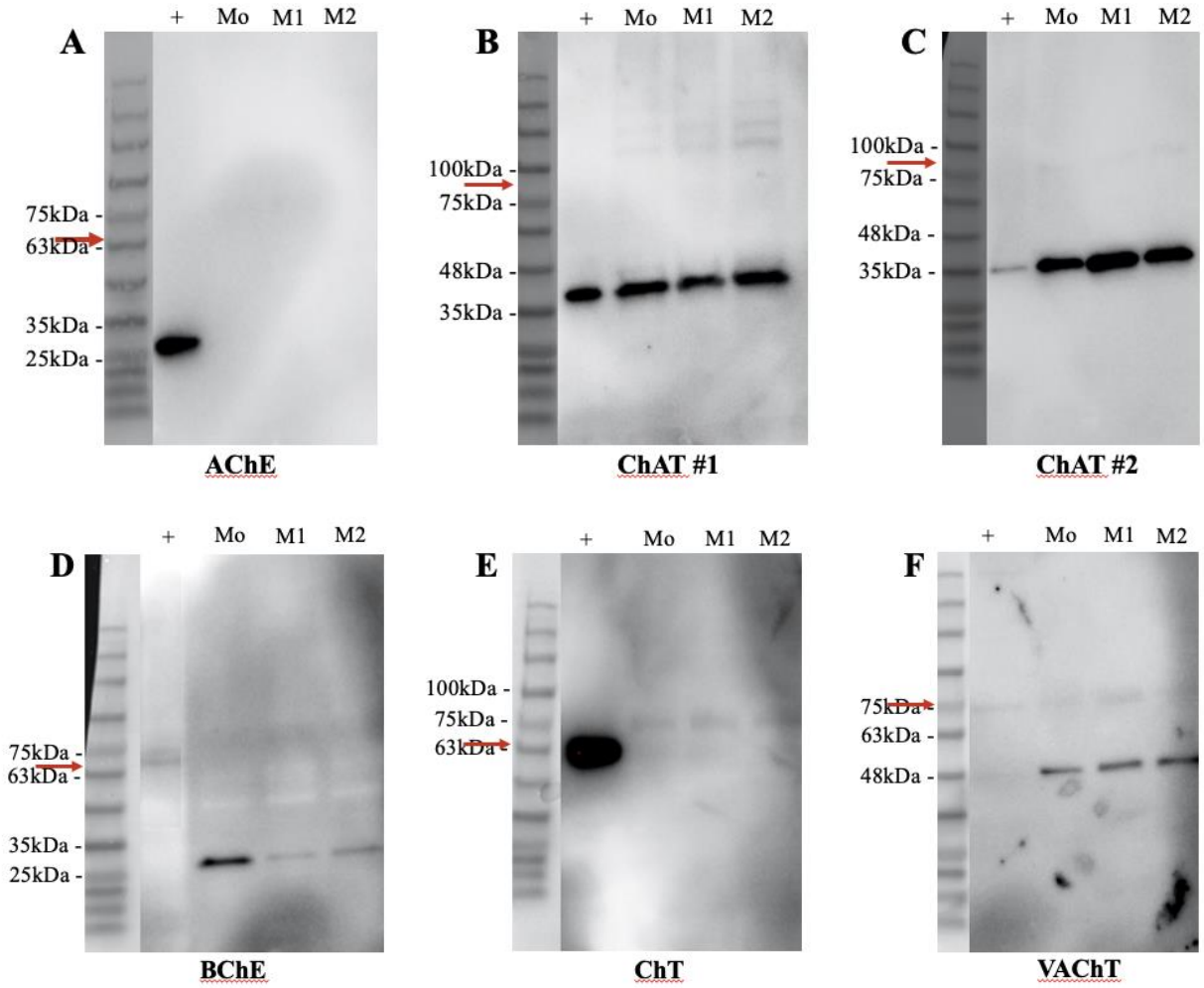

Figure 12. Cholinergic Protein Expression in THP-1 Differentiated Macrophages
The expression of cholinergic protein lysates from THP-1 differentiated Mo, M1 and M2 macrophages was assessed via western blots. The protein lysates in each well are indicated above each well, with the "+" symbol, signifying the positive control for that gene. IMR32, a human neuronal cell line, was used as a positive control for AChE, ChAT and VAChT while 293T, a human embryonic kidney cell line, was used as a positive control for BChE. Western Blots were repeated 3 times with different protein sample lysates (n = 3). Moreover, the red arrow indicates the antibody's predicted molecular weight. All protein samples including the positive controls

were loaded at identical concentrations of 10 mg into the wells. The Western Blots were auto exposed on the ChemiDoc Imaging System using Chemiluminescence. The protein AChE (A) was expressed in the positive control but does not seem to be expressed in any differentiated THP-1 macrophages. The protein ChAT (B and C) appeared to be expressed in the positive control as well as in each Mo, M1 and M2 macrophages, although at a different molecular weight than that of the predicted weight. BChE seemed to be expressed in the positive control at the theoretical molecular weight whereas in each Mo, M1 and M2 protein lysates, BChE was expressed at a much lower molecular weight. Additionally, the ChT protein was expressed in the positive control at the correct predicted molecular weight but did not seem to be expressed by the THP-1 samples. Finally, VAChT seemed to be expressed at two different molecular weights in all wells, including at around 75kDa and 48 kDa.

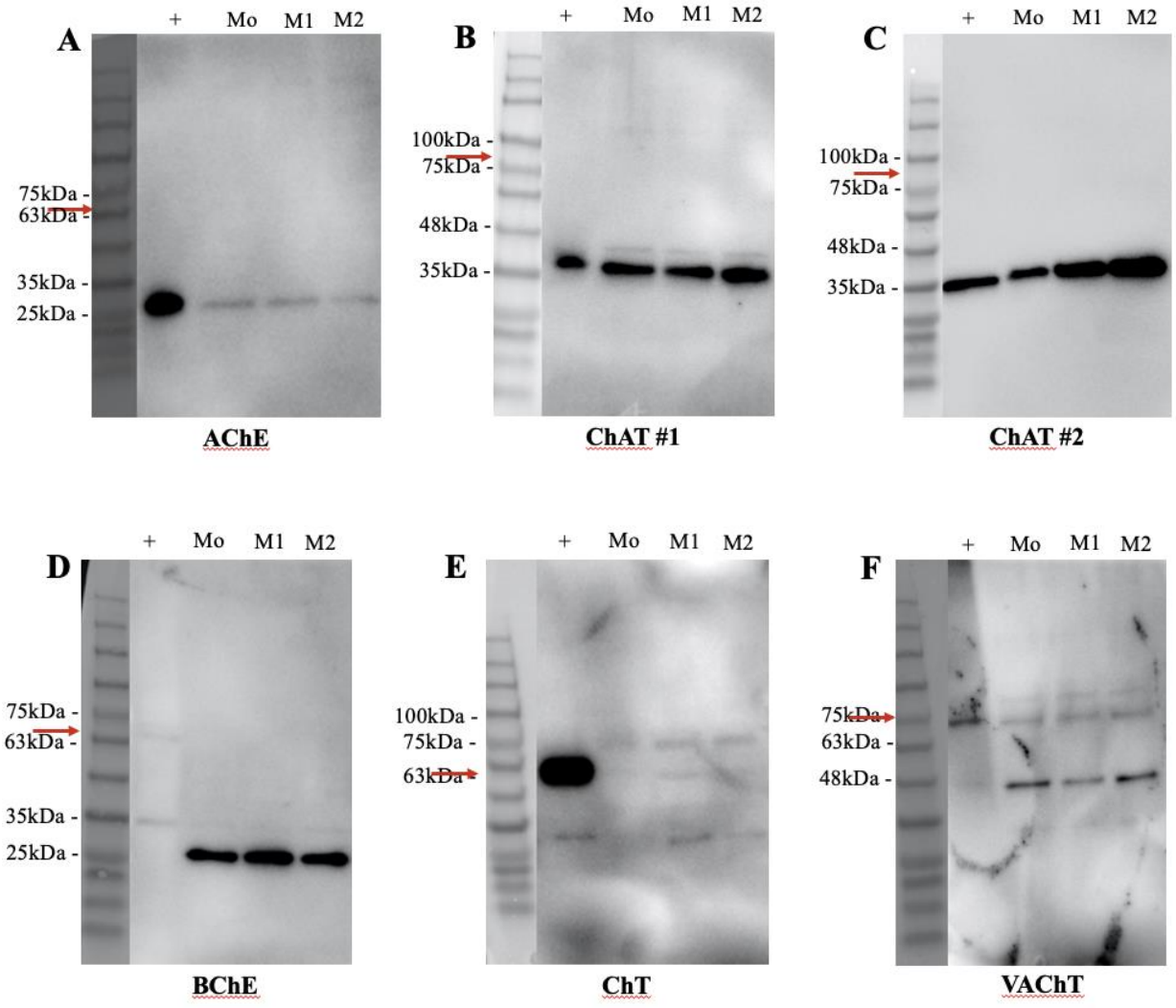

Figure 13. Cholinergic Protein Expression in U937 Differentiated Macrophages
The expression of cholinergic protein lysates from U937 differentiated Mo, M1 and M2 macrophages was assessed via Western Blots. The protein lysates are indicated above each well, with the "+" symbol, signifying the positive control for that gene. IMR32, a human neuronal cell line, was used as a positive control for AChE, ChAT and VAChT while 293T, a human

embryonic kidney cell line, was used as a positive control for BchE. Western Blots were repeated 3 times with different protein sample lysates (n = 3). The red arrow indicates the antibody's predicted molecular weight. All protein samples including the positive controls were loaded at identical concentrations of 10 mg into the wells. The Western Blots were auto exposed on the ChemiDoc Imaging System using Chemiluminescence. The protein AChE (A) was highly expressed in the positive control and seemed to be slightly expressed in the differentiated U937 macrophages. The protein ChAT (B and C) appeared to be expressed in each protein lysate, but at a different molecular weight than that of the predicted weight. BChE seemed to be expressed slightly at the theoretical molecular weight in the positive control whereas in each Mo, M1 and M2 protein lysates, BChE was expressed at a much lower molecular weight. Moreover, the ChT protein was expressed in the positive control at the correct predicted molecular weight but did not seem to be expressed in the U937 samples. Finally, VAChT seemed to be expressed at two different molecular weights in the protein lysates, at approximately 75kDa and 48 kDa.

3.2 Cytokine Profiles of Stimulated THP-1 and U937 Macrophages with 3 Different Silent Agonists and LPS

From our Western Blots and PCR results, we were able to determine that THP-1 and U937 differentiated macrophages expressed some cholinergic genes and proteins. Thus, we next assessed whether different nAChR silent agonist (p-CF_3 diEPP, m-bromo PEP and CONH2 diEPP Iodide) influenced immune functions and viability within these cells. Our lab previously showed that p-CF_3 diEPP and CONH2 diEPP Iodide successfully inhibited some pro-inflammatory cytokines in human peripheral blood mononuclear cells (PBMCs)[181], that m-bromo PEP delayed the onset and reduced the severity of EAE in mouse models, and had an anti-inflammatory effect in murine bone marrow derived macrophages (BMDM)[180]. Hence, these molecules were chosen to be assessed for their anti-inflammatory properties in THP-1 and U937 macrophages. Cultured THP-1 and U937 cells were differentiated into Mo or M1 macrophages as described in section 2.2. The supernatants were then collected upon stimulation with 100 mM of silent agonist for 1 hour followed by an 8-hour stimulation with 100 ng/mL of LPS. A vehicle control group (0.1% DMSO) was included in each analysis, since the silent agonists were diluted in DMSO prior to the stimulations. Cytokine concentrations were determined via CBAs using the

BD FACSCanto II flow cytometer. Outliers were determined by the GraphPad Prism 9 software using the ROUT outlier test (Q = 1%) and removed from the data set. A power analysis revealed that a sample size of 10 was necessary for statistical analysis and therefore, this is our sample size. Sample size represents independent experiments done on different days with different passages of cells. Data was normalized to the LPS + DMSO control and error bars indicate the SEM. One-way ANOVAs (multiple comparisons) with Dunnett's correction were performed to determine statistical significance (*: $P \leq 0.0332$; **: $P \leq 0.0021$; ***: $P \leq 0.0002$; ****: $P \leq 0.0001$). The raw cytokine data without normalization are shown in Appendix A.

3.2.1 THP-1 Macrophages

Cytokine profiles of THP-1 Mo macrophages upon treatment with the vehicle or the silent agonists (p-CF_3 diEPP, m-bromo PEP and CONH2 diEPP Iodide) in the presence of LPS were assessed (Figure 14). When comparing to the LPS + DMSO control group, p-CF_3 diEPP was the only silent agonist to influence the release of cytokines in THP-1 Mo macrophages. Although no significant differences were observed in IL-1β (Figure 14A) and TNF-α (Figure 14D) release, p-CF_3 diEPP statistically increased IL-6 secretion (Figure 14B) while inhibiting the release of IL-10 (Figure 14C). Overall, the silent agonist p-CF_3 diEPP had the most effect on cytokine release in THP-1 Mo cells under such conditions.

Figure 15 demonstrates the effects of silent agonists on LPS-induced cytokine release in THP-1 M1 macrophages. When comparing with the LPS + DMSO condition, m-bromo PEP slightly inhibited the release of IL-1β (Figure 15A) while no other silent agonist had any significant effects on its release. The 3 silent agonists did not influence on IL-6 release (Figure 15B) and IL-10 release (Figure 15C). However, p-CF_3 diEPP significantly inhibited the release of TNF-α (Figure 15D), inhibiting its release by approximately 50%. Taken together, the silent

agonist p-CF_3 diEPP had a great effect on the inhibition of TNF-α release while m-bromo PEP also slightly inhibited IL-1β release in THP-1 M1 macrophages.

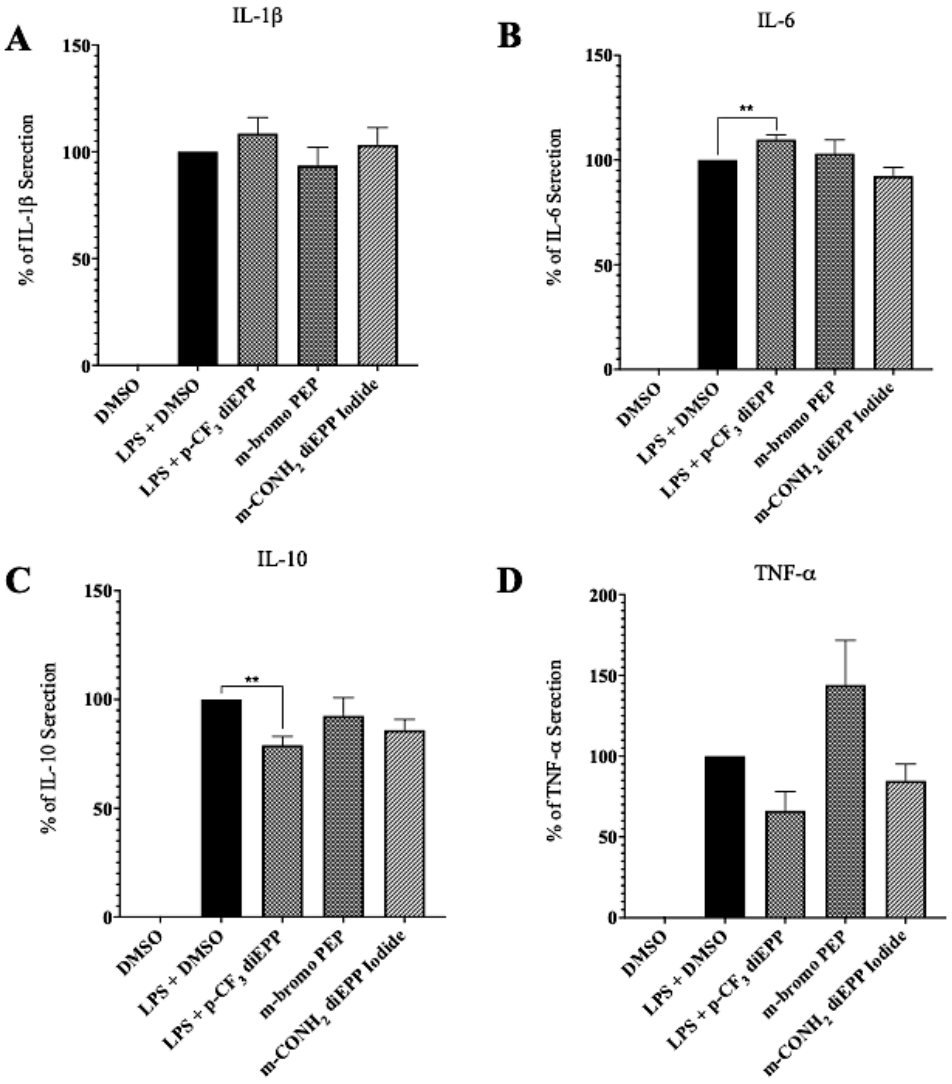

Figure 14. Cytokine Profiles of THP-1 Mo Macrophages Upon Stimulation with LPS and Various Silent Agonists (N = 10)

THP-1 cells were seeded into 5 different T25 flasks and differentiated into Mo macrophages by stimulation with 100 ng/mL of PMA for 48 hours. The media was then replaced with PMA-free media for 24 hours, to allow the cells to rest. Following this incubation, the media was replaced once more with fresh media for an additional 48 hours. Afterwards, the macrophages were given fresh media and pre-treated with 100 mM of silent agonists (p-CF_3 diEPP, m-bromo PEP, CONH2 diEPP Iodide) for 1 hour followed by an 8-hour stimulation with 100 ng/mL of LPS. A Vehicle control group (0.1 % DMSO only) was also included. Culture supernatants was then collected, and cytokine concentrations were analyzed via CBAs on the BD FACSCanto II flow cytometer. Data was normalized to the LPS + DMSO control and error bars indicate the SEM. One-way ANOVA statistical tests (multiple comparisons) with Dunnett's correction were performed to determine statistical significance (*: $P \leq 0.0332$; **: $P \leq 0.0021$; ***: $P \leq 0.0002$;

****: P ≤ 0.0001). No significant differences were observed in IL-1β (A) and TNF-α (D) release after treatment with the different silent agonists. However, p-CF_3 diEPP statistically increased IL-6 secretion (B) while inhibiting the release of IL-10 (C).

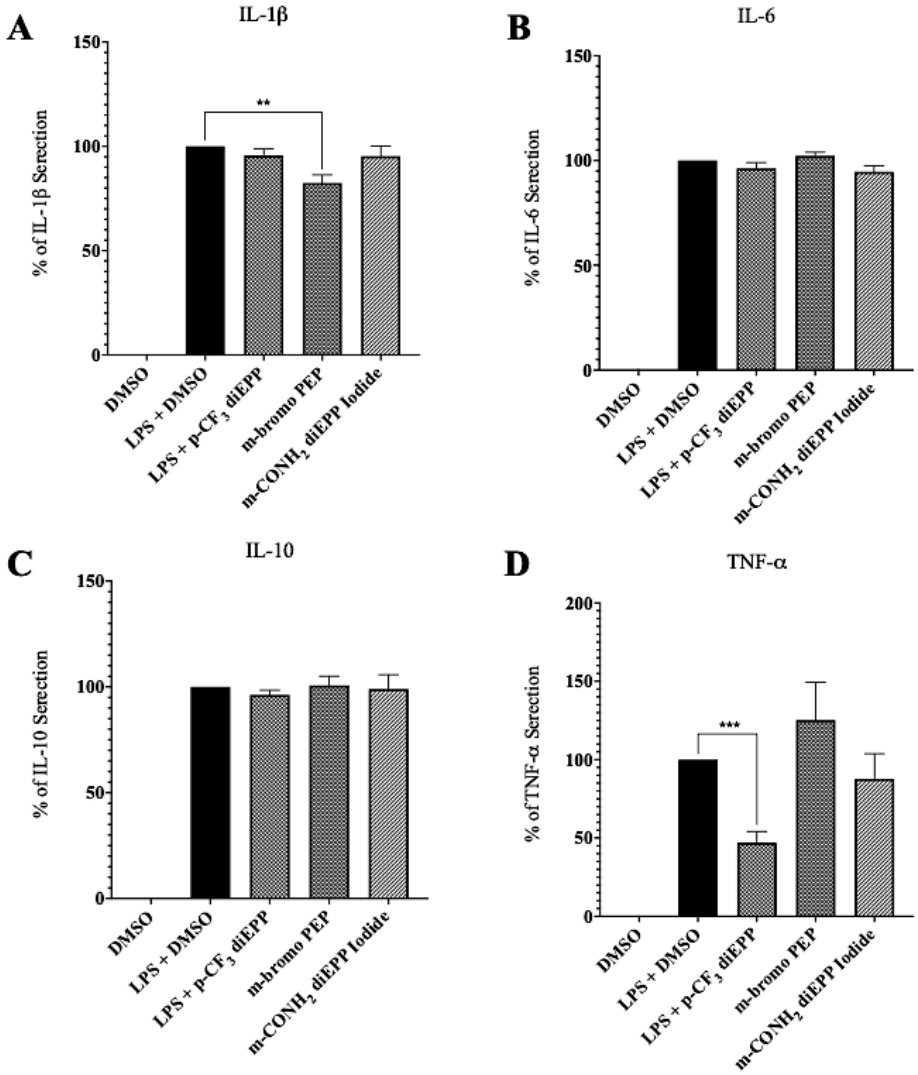

Figure 15. Cytokine Profiles of THP-1 M1 Macrophages Upon Stimulation with LPS and Various Silent Agonists (N=10)

THP-1 cells were seeded into 5 different T25 flasks and differentiated first into Mo macrophages by stimulation with 100 ng/mL of PMA for 48 hours. The media was then replaced with PMA-free media for 24 hours, to allow the cells to rest. Following this incubation, media was replaced with fresh media containing 10 ng/mL of INF-ɣ and 10 pg/mL of LPS for 48 hours, to further polarize macrophages into M1 macrophages. Afterwards, the M1 macrophages were given fresh media and pre-treated with 100mM of silent agonists (p-CF_3 diEPP, m-bromo PEP, CONH2 diEPP Iodide) for 1 hour followed by an 8-hour stimulation with 100 ng/mL of LPS. A Vehicle control group (0.1% DMSO only) was also included. Culture supernatants was then collected, and cytokine concentrations were analyzed via CBAs on the BD FACSCanto II flow cytometer. Data was normalized to the LPS + DMSO control and error bars indicate the SEM. One-way ANOVAs (multiple comparisons) with Dunnett's correction were performed to determine

statistical significance (*: $P \leq 0.0332$; **: $P \leq 0.0021$; ***: $P \leq 0.0002$; ****: $P \leq 0.0001$). IL-1β secretion (A) is inhibited by m-bromo PEP but remains unaffected upon treatment with the other silent agonists. IL-6 secretion (B) and IL-10 secretion (C) do not seem to be affected by any of the silent agonists. Lastly, TNF-α secretion is greatly inhibited by p-CF_3 diEPP.

3.2.2 U937 Macrophages

Cytokine profiles of U937 Mo macrophages were measured in the conditions previously described (Figure 16). It is important to note that U937 Mo macrophages did not release detectable amounts of IL-1β, therefore, this cytokine is not shown in this analysis. The release of IL-6 (Figure 16A), IL-10 (Figure 16B) and TNF-α (Figure 16C) were not significantly affected by any of the treatment groups.

Lastly, Figure 17 demonstrates the release of cytokines upon stimulation with the various silent agonists in the presence of LPS in U937 M1 macrophages. As seen in Mo U937, M1 macrophages did not release detectable amounts of IL-1β. Treatment with m-bromo PEP or CONH2 diEPP Iodide showed significant inhibition in IL-6 release (Figure 17A). The release of IL-10 (Figure 17B) was shown to be decreased by treatment with p-CF_3 diEPP. Finally, TNF-α release (Figure 17C) was shown to be very significantly inhibited by p-CF_3 diEPP, reducing its secretion by approximately 50%. Likewise, m-bromo PEP also displayed slight inhibitory effects in the release of TNF-α. Overall, each silent agonist had inhibitory capabilities for selected cytokines.

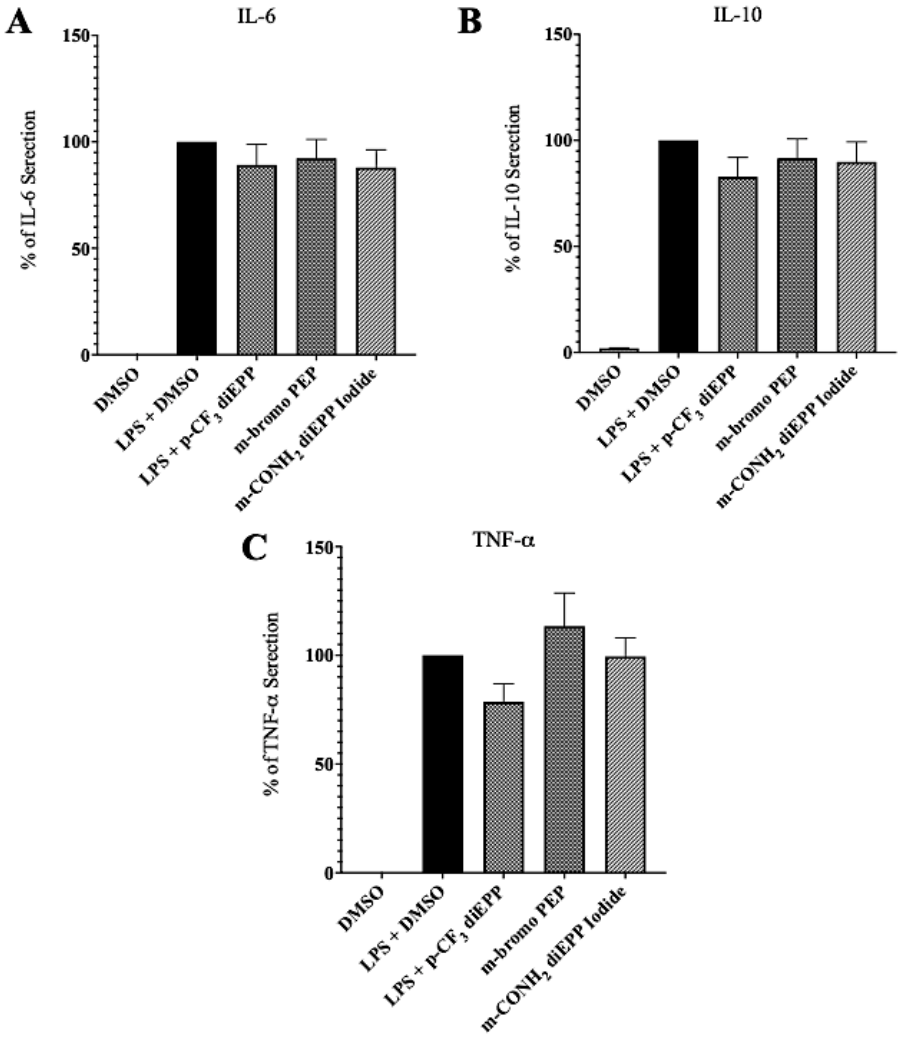

Figure 16. Cytokine Profiles of U937 Mo Macrophages Upon Stimulation with LPS and Various Silent Agonists (N = 10)

U937 cells were seeded into 5 different T25 flasks and differentiated into Mo macrophages by stimulation with 100 ng/mL of PMA for 48 hours. The media was then replaced with PMA-free media for 24 hours, to allow the cells to rest. Following this incubation, the media was replaced once more with fresh media for an additional 48 hours. Afterwards, the macrophages were given fresh media and pre-treated with 100mM of silent agonists (p-CF_3 diEPP, m-bromo PEP, CONH2 diEPP Iodide) for 1 hour followed by an 8-hour stimulation with 100 ng/mL of LPS. A Vehicle control group (0.1% DMSO only) was also included. Culture supernatants was then collected, and cytokine concentrations were analyzed via CBAs on the BD FACSCanto II flow cytometer. Data was normalized to the LPS + DMSO control and error bars indicate the SEM. One-way ANOVA statistical tests (multiple comparisons) with Dunnett's correction were performed to determine statistical significance (*: $P \leq 0.0332$; **: $P \leq 0.0021$; ***: $P \leq 0.0002$; ****: $P \leq 0.0001$). Overall, IL-6 (A), IL-10 (B) and TNF-α secretion (C) is not affected by any of the silent agonists.

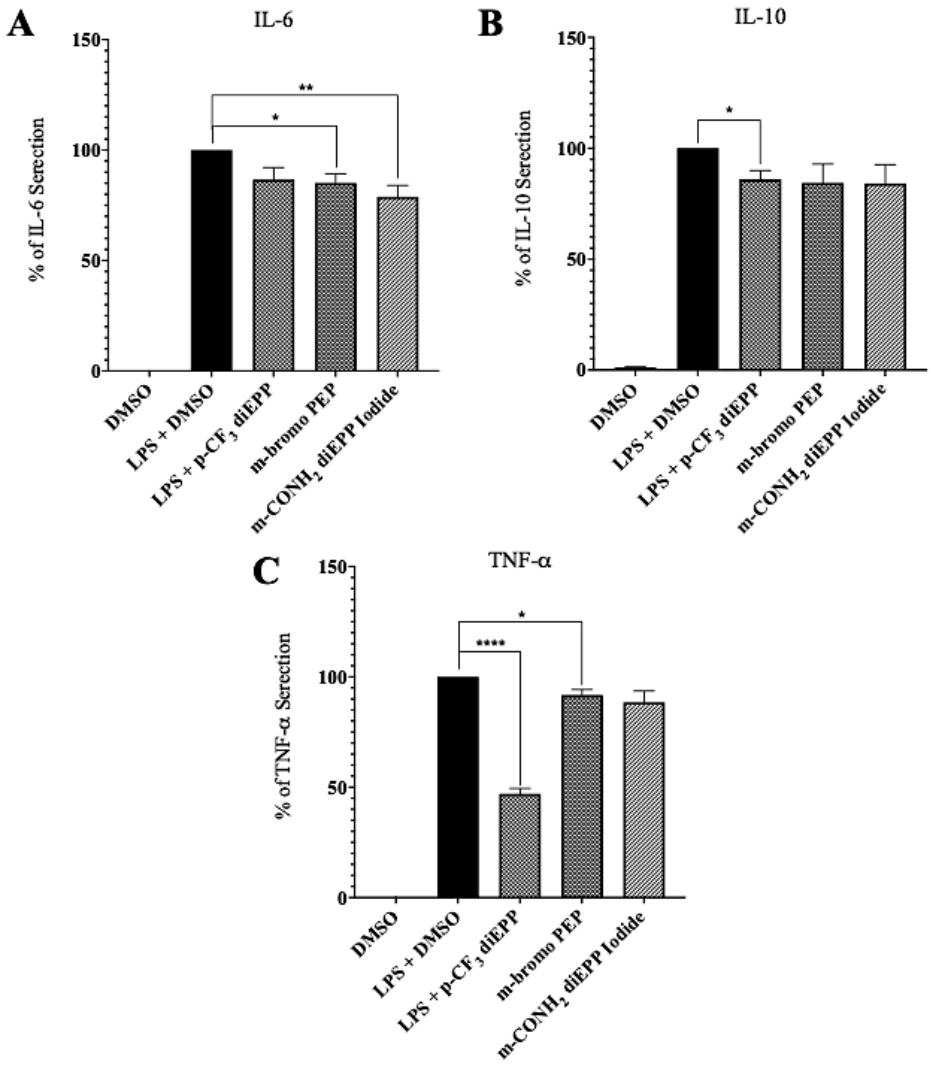

Figure 17. Cytokine Profiles of U937 M1 Macrophages Upon Stimulation with LPS and Various Silent Agonists (N=10)

U937 cells were seeded into 5 different T25 flasks and differentiated first into Mo macrophages by stimulation with 100 ng/mL of PMA for 48 hours. The media was then replaced with PMA-free media for 24 hours, to allow the cells to rest. Following this incubation, media was replaced with fresh media containing 10 ng/mL of INF-ɣ and 10 pg/mL of LPS for 48 hours, to further polarize macrophages into M1 macrophages. Afterwards, the M1 macrophages were given fresh media and pre-treated with 100mM of silent agonists (p-CF_3 diEPP, m-bromo PEP, CONH2 diEPP Iodide) for 1 hour followed by an 8-hour stimulation with 100 ng/mL of LPS. A Vehicle control group (0.1% DMSO only) was also included. Culture supernatants was then collected, and cytokine concentrations were analyzed via CBAs on the BD FACSCanto II flow cytometer. Data was normalized to the LPS + DMSO control and error bars indicate the SEM. One-way ANOVAs (multiple comparisons) with Dunnett's correction were performed to determine statistical significance (*: $P \leq 0.0332$; **: $P \leq 0.0021$; ***: $P \leq 0.0002$; ****: $P \leq 0.0001$). The treatments with m-bromo PEP and CONH2 diEPP Iodide showed significant inhibition in IL-6 release (Figure 17A). The release of IL-10 (Figure 17B) was shown to be decreased by treatment with p-CF_3 diEPP. Finally, TNF-α release (Figure 17C) was shown to be very significantly

inhibited by p-CF_3 diEPP, reducing its secretion by approximately 50%. Likewise, m-bromo PEP also displayed slight inhibitory effects in the release of TNF-α.

3.3 Cell Counts of THP-1 and U937 Macrophages Treated with 3 Different Silent Agonist in the Presence of LPS

Cell counts were assessed to determine overall viability within the different treatment groups. Viable macrophages tightly adhere to the flasks or cell plates during culture while dead macrophages or macrophages undergoing apoptosis typically float in the media. Dividing macrophages can also detach from their cell culture flasks or plates but the frequency of cell division in macrophages is low[198]. Hence, the cells counted using DAPI is a good representation of overall live cells. In this experiment, the adhered macrophages were stained with NucBlue™ Fixed Cell ReadyProbes™ Reagent (DAPI) and counted using the Cytation 5 imaging reader. The cell counts were normalized to the LPS + DMSO control group and error bars indicate the SEM.

Normalized cell counts of THP-1 and U937 differentiated macrophages after treatment with the silent agonists in the presence of LPS was assessed (Figure 18). Due to technical issues in the initial stages of these experiments, sample sizes of <10 were obtained for the cell counts of THP-1 Mo (Figure 18A), THP-1 M1 (Figure 18B) and U937 Mo (Figure 18C) macrophages, but a sample size of 10 was achieved for U937 M1 macrophages (Figure 18D). Multiple comparison one-way ANOVA's with Dunnett's corrections were performed to determine statistical significance (*: $P \leq 0.0332$; **: $P \leq 0.0021$; ***: $P \leq 0.0002$; ****: $P \leq 0.0001$). The results shown in Figure 18 suggest that the silent agonist stimulations did not result in significant cell death. However, it is important to note that a very small sample size was obtained for the cell

counts of U937 Mo macrophages (N = 3), therefore, it is difficult to make concrete conclusions based on these results.

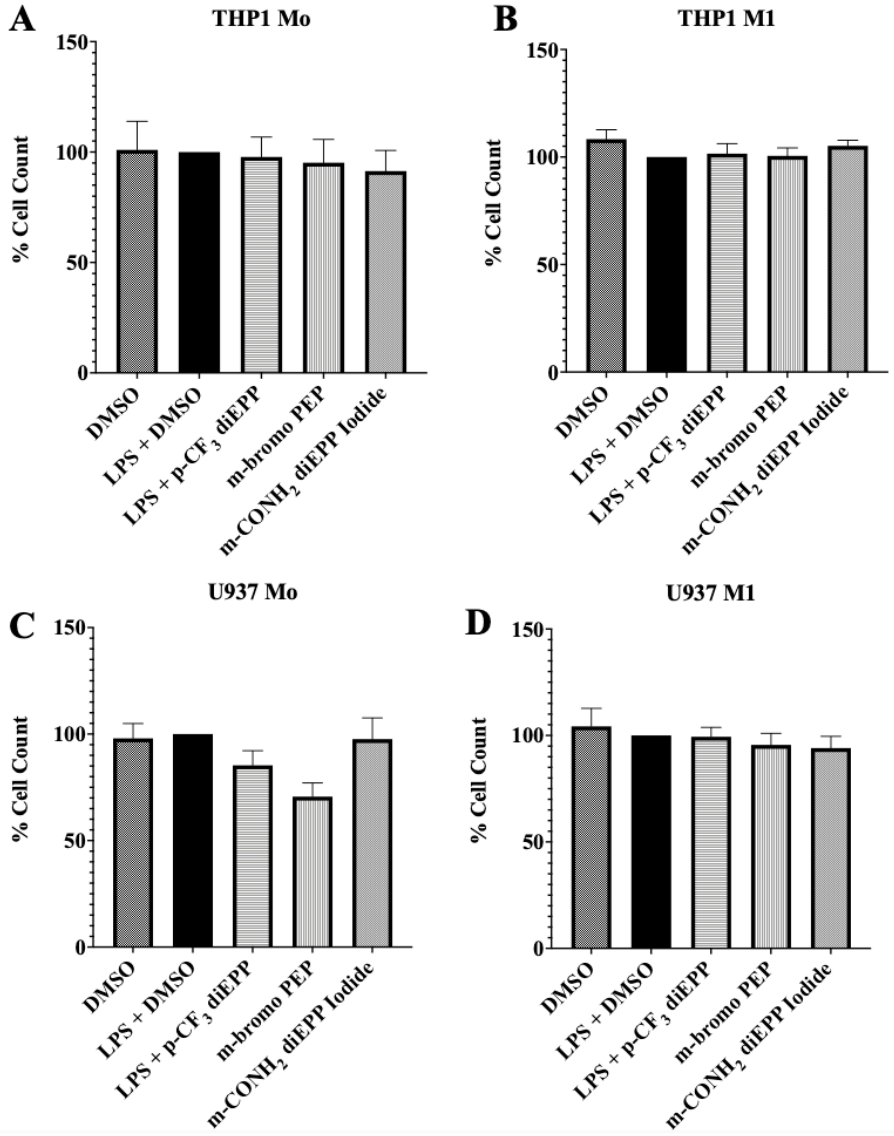

Figure 18. Normalized Cell Counts (%) of THP-1 and U937 Macrophages Treated with Various Silent Agonists and Stimulated with LPS (N = 5 – 10)

THP-1 Mo macrophage (A; N = 5), THP-1 M1 macrophage (B; N = 9), U937 Mo macrophage (C, N = 3) and U937 M1 macrophage (D, N = 10) treated with silent agonists and stimulated with LPS were counted using NucBlue™ Fixed Cell ReadyProbes™ Reagent (DAPI) and the Cytation 5 imaging reader. Cell counts were normalized to the LPS + DMSO control and error bars indicate the SEM. One-way ANOVAs (multiple comparisons) with Dunnett's correction were performed to determine statistical significance (*: $P \leq 0.0332$; **: $P \leq 0.0021$; ***: $P \leq 0.0002$; ****: $P \leq 0.0001$). This figure suggests that the silent agonist stimulations did not result in significant cell death.

3.4 Cytokine Profiles of THP-1 and U937 Macrophages Treated Acutely with Agonists and Cholinergic Inhibitors in the Presence of LPS

Our Western Blots and PCR results suggest the presence of various cholinergic genes within THP-1 and U937 differentiated macrophages. Thus, we further assessed the effect of acute pharmacological inhibition of cholinergic inhibitors and agonist on cytokine release in THP-1 and U937 differentiated macrophages. Considering the effectiveness of p-CF_3 diEPP in inhibiting the release of pro-inflammatory cytokines (Section 3.2), this silent agonist was also included in these experiments. Cultured THP-1 and U937 cells were differentiated into Mo or M1 macrophages as described in section 2.2. Cells were then treated with various conditions described in section 2.2.2 and table 1 for 5 hours. Cell supernatants were collected, and cytokine concentrations were determined via CBAs using the BD FACSCanto II flow cytometer. It is important to note that U937 Mo macrophages did not release detectable amounts of IL-1β, therefore, this cytokine is not shown in this analysis. Outliers were determined by the GraphPad Prism 9 software outlier test and removed from the data set. The cytokine data was normalized by setting the concentration of each cytokine from the LPS or the LPS + DMSO to 100% and calculating all other values accordingly. One-way ANOVAs (multiple comparisons) with Dunnett's correction were performed to determine statistical significance (*: $P \leq 0.0332$; **: $P \leq 0.0021$; ***: $P \leq 0.0002$; ****: $P \leq 0.0001$). The raw cytokine data without normalization are shown in Appendix B.

3.4.1 THP-1 Macrophages

Cytokine profiles of THP-1 Mo macrophages upon acute treatment with agonists (Ach, Ch, Nic and p-CF_3 diEPP) and cholinergic inhibitors (Gal, ML352 and α-NETA) followed by

stimulation with LPS were assessed (Figure 19). The release of IL-1β (Figure 19A) was significantly reduced by inhibition of ChT (ML352), inhibition of ChAT (α-NETA) and nAChR silent agonism (p-CF_3 diEPP) while IL-6 secretion (Figure 19B) significantly decreased by inhibition of ChT (ML352). Moreover, IL-10 release (Figure 19C) was significantly reduced by ChT inhibition (ML352) and ChAT inhibition (α-NETA). Finally, inhibiting ChT (ML352) significantly reduced TNF-α release (Figure 19D) by approximately 50%. Overall, inhibiting ChT resulted in successful inhibition of all 4 cytokines (IL-1β, IL-6, IL-10 and TNF-α) and showed the most significant inhibition of TNF-α release.

The cytokine profiles of THP-1 M1 macrophages upon acute treatment of agonists (Ach, Ch, Nic and p-CF_3 diEPP) and cholinergic inhibitors (Gal, ML352 and α-NETA) in the presence of LPS were additionally assessed (Figure 20). In the presence of LPS, IL-1β secretion (Figure 20A) was significantly inhibited by nAChR silent agonism (p-CF_3 diEPP) and by inhibiting ChAT (α-NETA). On the other hand, IL-6 secretion (Figure 20B) was not significantly influenced by any of the treatments. Furthermore, IL-10 release (Figure 20C) was reduced by inhibiting ChT (ML352) and TNF-α secretion (Figure 20D) was significantly inhibited via treatment with a nAChR silent agonist (p-CF_3 diEPP). Conclusively, nAChR silent agonism treatment successfully inhibited the release of 2 pro-inflammatory cytokines (IL-1β and TNF-α) while treatments with ChAT and ChT inhibitors resulted in a decrease in IL-1β and IL-10 release, respectively.

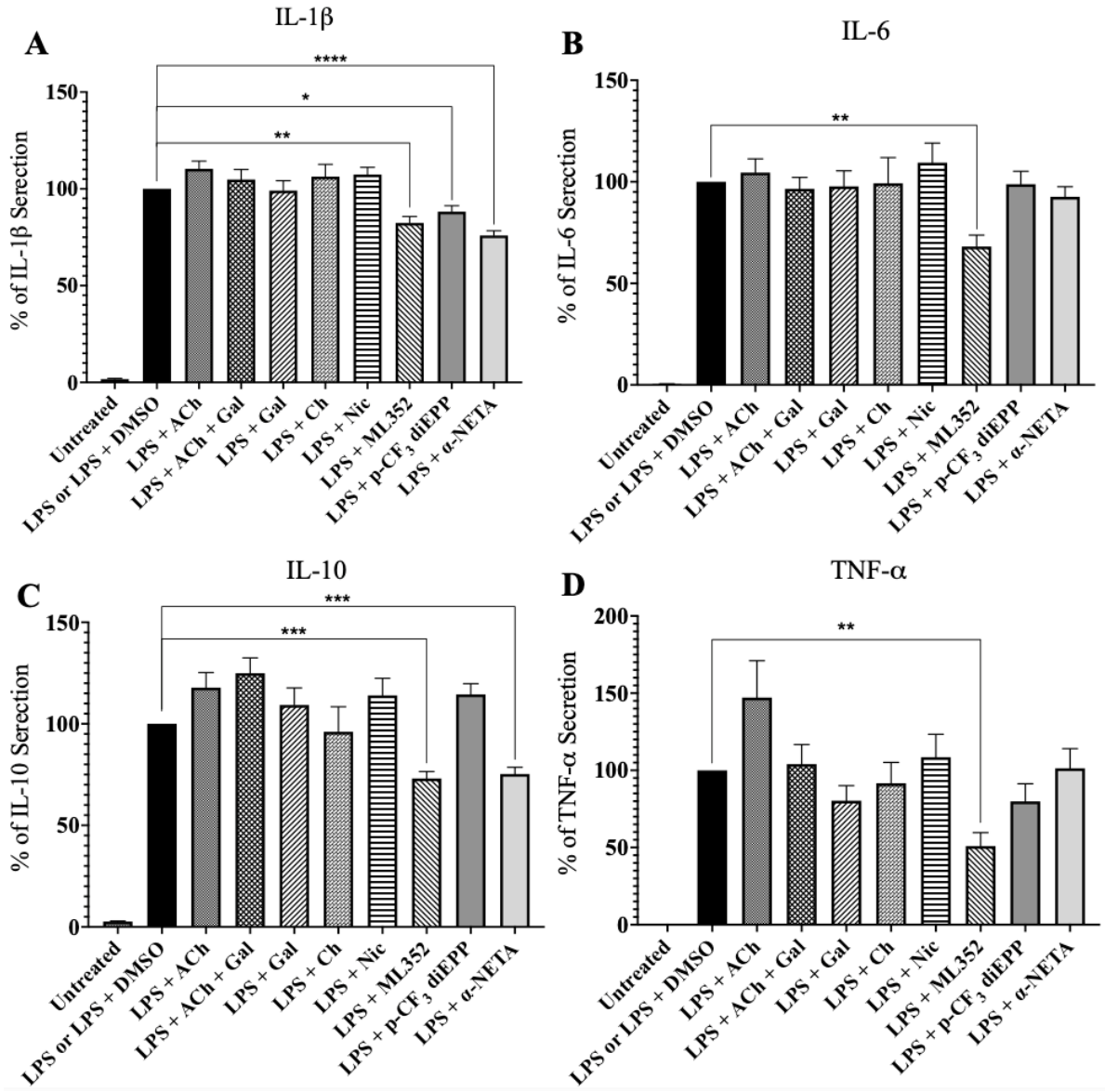

Figure 19. Cytokine Release of THP-1 Mo Macrophages Upon Acute Cholinergic Inhibitor and Agonist Treatments in the Presence of LPS (N=10)

THP-1 cells were seeded into 6 well plates and differentiated into Mo macrophages by stimulation with 100 ng/mL of PMA for 48 hours. The media was then replaced with PMA-free media for 24 hours, allowing the cells to rest. Then, media was replaced with fresh media for an additional 48 hours. Afterwards, the cell culture media was replaced, and the macrophages were treated with DMSO (vehicle control), LPS, agonists and/or cholinergic inhibitors (shown in Table 1) for 5 hours. Culture supernatants were collected, and cytokine concentrations were analyzed via CBAs on the BD FACSCanto II flow cytometer. Data was normalized to either the LPS treated group (columns with different patterns) or the LPS + DMSO treated group (columns with solid colors). Errors bars indicate the SEM. One-way ANOVAs (multiple comparisons) with Dunnett's correction were performed to determine statistical significance (*: $P \leq 0.0332$; **: $P \leq 0.0021$; ***: $P \leq 0.0002$; ****: $P \leq 0.0001$). IL-1β secretion (A) was significantly reduced by inhibition of ChT (ML352), inhibition of ChAT (α-NETA) and nAChR silent agonism (p-CF_3 diEPP) while IL-6 release (B) was only shown to be significantly reduced by

inhibition of ChT (ML352). Furthermore, IL-10 release (C) was significantly inhibited by ChT inhibition (ML352) and ChAT inhibition (α-NETA). Finally, TNF-α release was significantly reduced by approximately 50% by inhibiting ChT (ML352).

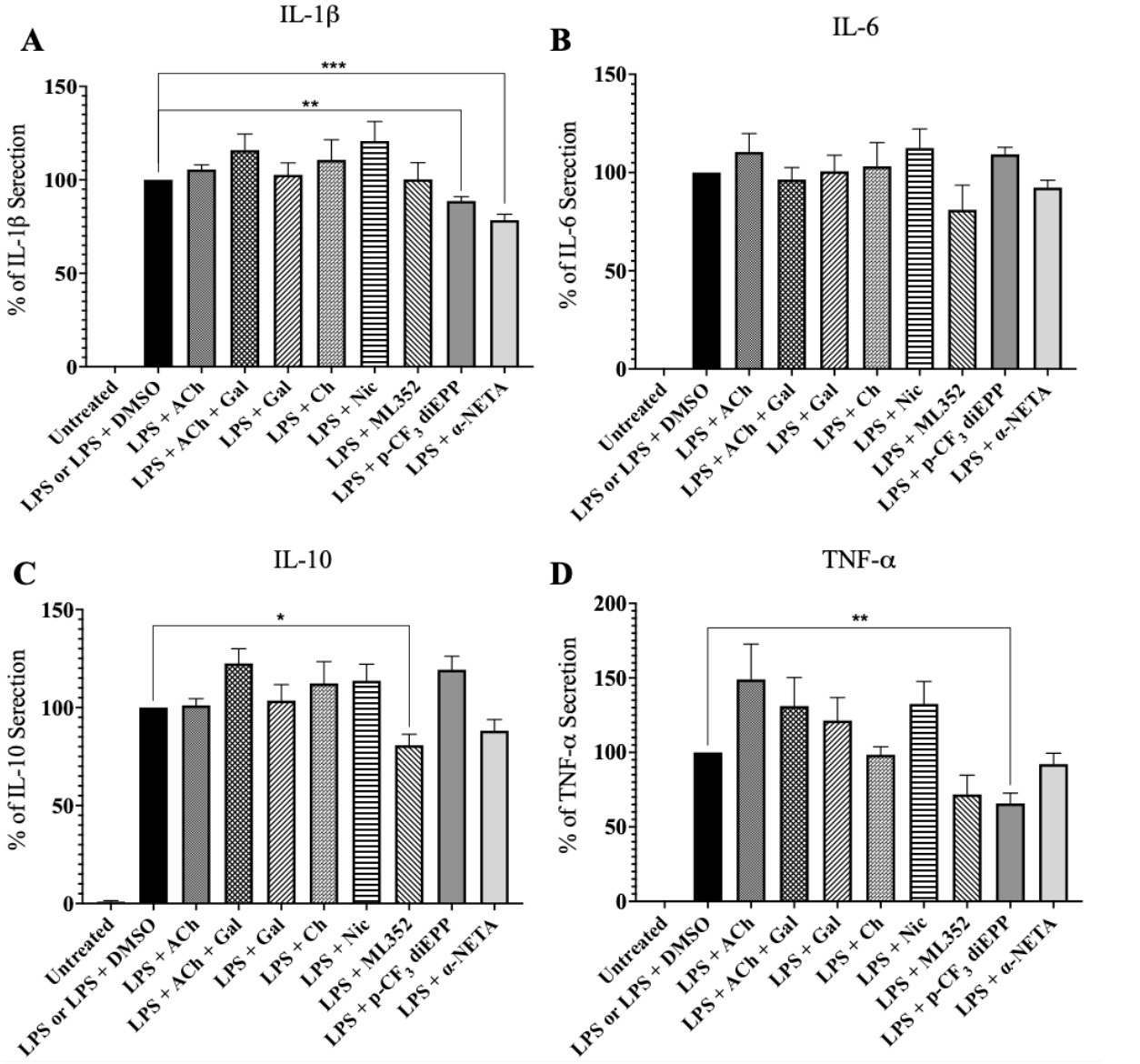

Figure 20. Cytokine Release of THP-1 M1 Macrophages Upon Acute Cholinergic Inhibitor and Agonist Treatments in the Presence of LPS (N=10)

THP-1 cells were seeded into 6 well plates and differentiated into macrophages by stimulation with 100 ng/mL of PMA for 48 hours. The media was then replaced with PMA-free media for 24 hours, allowing the cells to rest. Then, the media was removed, and fresh media supplemented with 10 ng/mL of INF-ɣ and 10 pg/mL of LPS was added, to polarize the macrophages into M1 macrophages. Afterwards, the cell culture media was replaced, and the macrophages were treated with DMSO (vehicle control), LPS, agonists and/or cholinergic inhibitors (shown in Table 1) for 5 hours. Culture supernatants were collected, and cytokine concentrations were analyzed via CBAs on the BD FACSCanto II flow cytometer. Data was normalized to either the LPS treated group (columns with different patterns) or the LPS + DMSO treated group (columns with solid

colors). Errors bars indicate the SEM. One-way ANOVAs (multiple comparisons) with Dunnett's correction were performed to determine statistical significance (*: $P \leq 0.0332$; **: $P \leq 0.0021$; ***: $P \leq 0.0002$; ****: $P \leq 0.0001$). In the presence of LPS, IL-1β secretion (A) was significantly inhibited by nAChR silent agonism (p-CF_3 diEPP) and by inhibiting ChAT (α-NETA). IL-6 secretion (B) was not significantly influenced by any of the treatments whereas inhibiting ChT (ML352) successfully inhibited IL-10 release (C). Finally, only treatment with the nAChR silent agonist (p-CF_3 diEPP) resulted in a significant inhibition of TNF-α release from the cells.

3.4.2 U937 Macrophages

Cytokine profiles of U937 Mo macrophages upon acute treatment of agonists (Ach, Ch, Nic and p-CF_3 diEPP) and cholinergic inhibitors (Gal, ML352 and α-NETA) followed by stimulation with LPS were assessed (Figure 21). First, the release of IL-6 (Figure 21A) in the presence of LPS was significantly reduced after treatment with a nAChR agonist (ACh), a nAChR agonist (ACh) in the presence of an AChE inhibitor (Gal) and finally, upon treatment with a ChT inhibitor (ML352). Moreover, IL-10 secretion (Figure 21B) was shown to be significantly reduced by inhibiting ChT (ML352). Finally, the release of TNF-α (Figure 21C) was not significantly affected by any of the treatments. Altogether, inhibiting ChT successfully inhibited the release of a pro-inflammatory cytokine (IL-6) and an anti-inflammatory cytokine (IL-10) but inhibiting AChE and treatment with an nAChR agonist only resulted in the inhibition of IL-6.

The cytokine profiles of U937 M1 macrophages upon acute treatment of agonists (Ach, Ch, Nic and p-CF_3 diEPP) and cholinergic inhibitors (Gal, ML352 and α-NETA) in the presence of LPS were additionally assessed (Figure 22). The release of IL-6 (Figure 22A) was not significantly influenced by any of the treatments. IL-10 secretion (Figure 22B) was inhibited following treatment with a nAChR agonist (Ch) and by inhibiting ChT (ML352). Finally, TNF-α release (Figure 22C) was reduced by approximately 50% after inhibiting ChT (ML352). Overall, ChT inhibition was the most successful treatment in inhibiting cytokine release (IL-10 and TNF-α) in acutely treated U937 M1 macrophages.

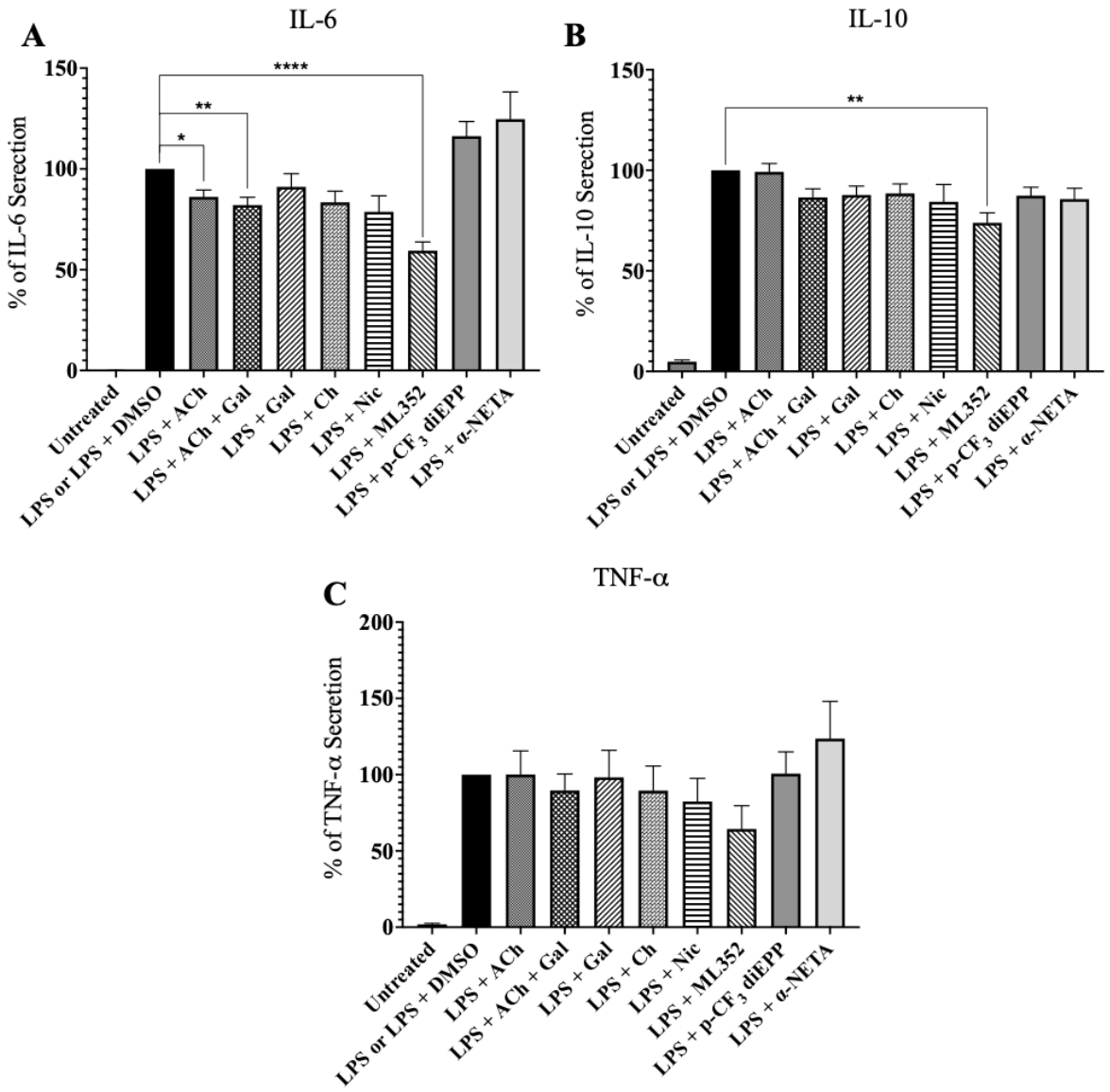

Figure 21. Cytokine Release of U937 Mo Macrophages Upon Acute Cholinergic Inhibitor and Agonist Treatments in the Presence of LPS (N=10)

U937 cells were seeded into 6 well plates and differentiated into Mo macrophages by stimulation with 100 ng/mL of PMA for 48 hours. The media was then replaced with PMA-free media for 24 hours, allowing the cells to rest. Then, media was replaced with fresh media for an additional 48 hours. Afterwards, the cell culture media was replaced, and the macrophages were treated with DMSO (vehicle control), LPS, agonists and/or cholinergic inhibitors (shown in Table 1) for 5 hours. Culture supernatants were collected, and cytokine concentrations were analyzed via CBAs on the BD FACSCanto II flow cytometer. Data was normalized to either the LPS treated group (columns with different patterns) or the LPS + DMSO treated group (columns with solid colors). Errors bars indicate the SEM. One-way ANOVAs (multiple comparisons) with Dunnett's correction were performed to determine statistical significance (*: $P \leq 0.0332$; **: $P \leq 0.0021$; ***: $P \leq 0.0002$; ****: $P \leq 0.0001$). The release of IL-6 (A) in the presence of LPS was significantly reduced after treatment with an nAChR agonist (ACh), with an nAChR agonist (ACh) in the presence of an AChE inhibitor (Gal) and upon treatment with a ChT inhibitor

(ML352). IL-10 secretion (B) was significantly reduced by inhibiting ChT (ML352). Finally, the release of TNF-α (Figure 21C) was not significantly affected by any of the treatments.

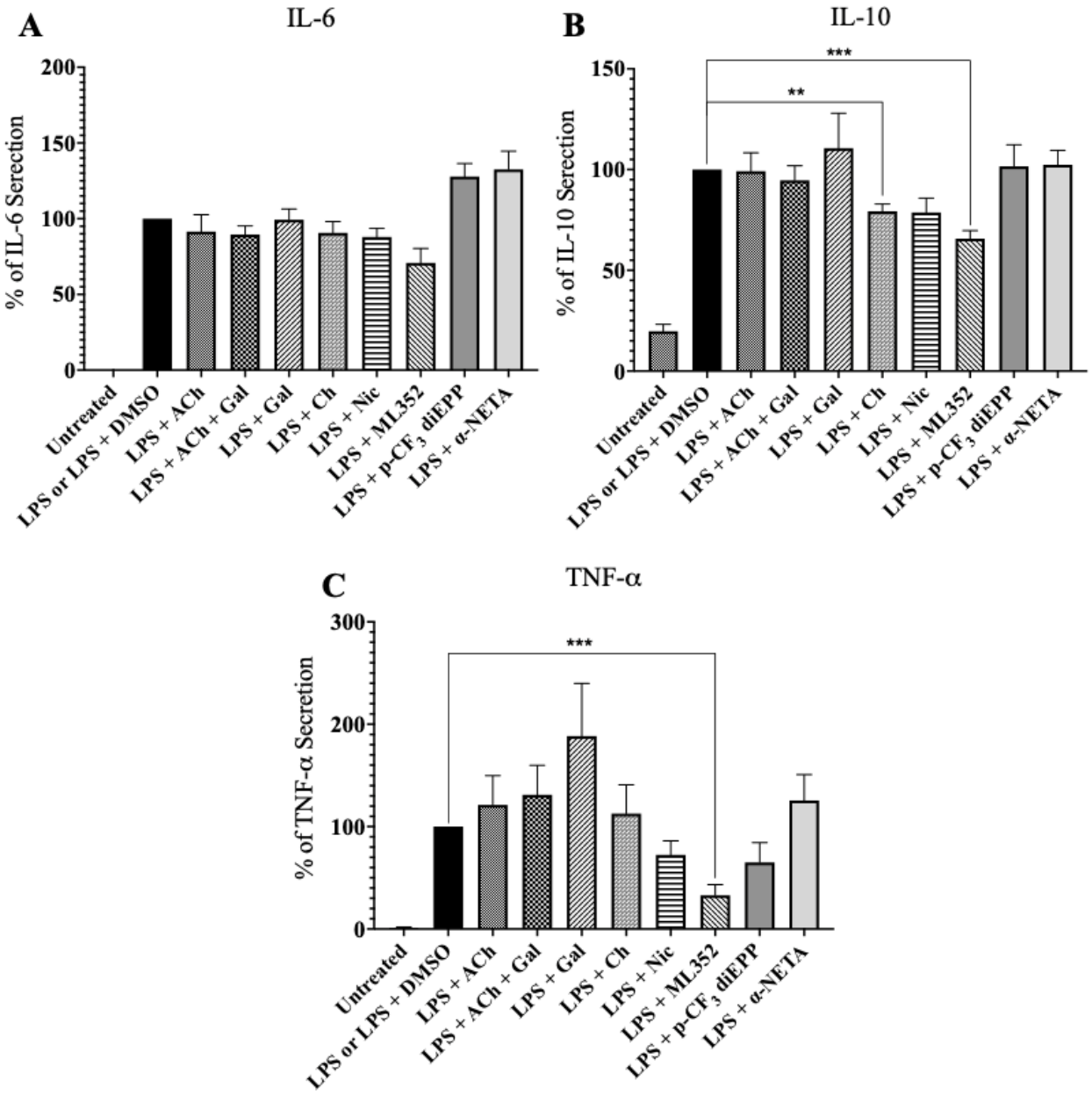

Figure 22. Cytokine Release of U937 M1 Macrophages Upon Acute Cholinergic Inhibitor and Agonist Treatments in the Presence of LPS (N=10)

U937 cells were seeded into 6 well plates and differentiated into macrophages by stimulation with 100 ng/mL of PMA for 48 hours. The media was then replaced with PMA-free media for 24 hours, allowing the cells to rest. Then, the media was removed, and fresh media supplemented with 10 ng/mL of INF-ɣ and10 pg/mL of LPS was added, to polarize the macrophages into M1 macrophages. Afterwards, the cell culture media was replaced, and the macrophages were treated with DMSO (vehicle control), LPS, agonists and/or cholinergic inhibitors (shown in Table 1) for 5 hours. Culture supernatants were collected, and cytokine concentrations were analyzed via

CBAs on the BD FACSCanto II flow cytometer. Data was normalized to either the LPS treated group (columns with different patterns) or the LPS + DMSO treated group (columns with solid colors). Errors bars indicate the SEM. One-way ANOVAs (multiple comparisons) with Dunnett's correction were performed to determine statistical significance (*: $P \leq 0.0332$; **: $P \leq 0.0021$; ***: $P \leq 0.0002$; ****: $P \leq 0.0001$). The release of IL-6 (A) was not significantly influenced by any of the treatments. IL-10 secretion (B) was inhibited following treatment with an nAChR agonist (Ch) and by inhibiting ChT (ML352). Finally, TNF-αα release (C) was reduced by approximately 50% after inhibition of ChT (ML352).

3.5 Cytotoxicity of THP-1 and U937 Macrophages Treated Acutely with Agonists and Cholinergic Inhibitors in the Presence of LPS

Our data indicate that some agonists and cholinergic inhibitors can modulate the release of some pro-inflammatory and anti-inflammatory cytokines in the presence of an immune stimulant like LPS. Thus, we next wanted to confirm that the effects seen from these treatments on the cytokine profiles was not due to cell death. Therefore, a cytotoxicity test was carried out, in which LDH released from the treated cells was quantified using a Fluorescent LDH kit. LDH is an enzyme that is released from the cytosol upon cell death and is a well-established and reliable assay to detect toxicity. The cells were not stained with DAPI and counted as performed for the silent agonists experiment because the RNA from the pharmacological-treated macrophages was isolated to evaluate changes in cell surface markers (discussed below), therefore we were unable to stain the cells. Figure 23 displays the % cytotoxicity values in THP-1 and U937-treated Mo and M1 macrophages. Repeated measures one-way ANOVAs (multiple comparisons) with Dunnett's correction were performed to determine statistical significance (*: $P \leq 0.0332$; **: $P \leq 0.0021$; ***: $P \leq 0.0002$; ****: $P \leq 0.0001$).

The cytotoxicity levels of THP-1 Mo, THP-1 M1, U937 Mo and U937 M1-treated macrophages (Figure 23) were shown to be none significant in comparison to the LPS or LPS +

DMSO treated groups. These results therefore suggest that the inhibitory effects and increase in cytokine release seen by some treatment groups is likely not due to cell death.

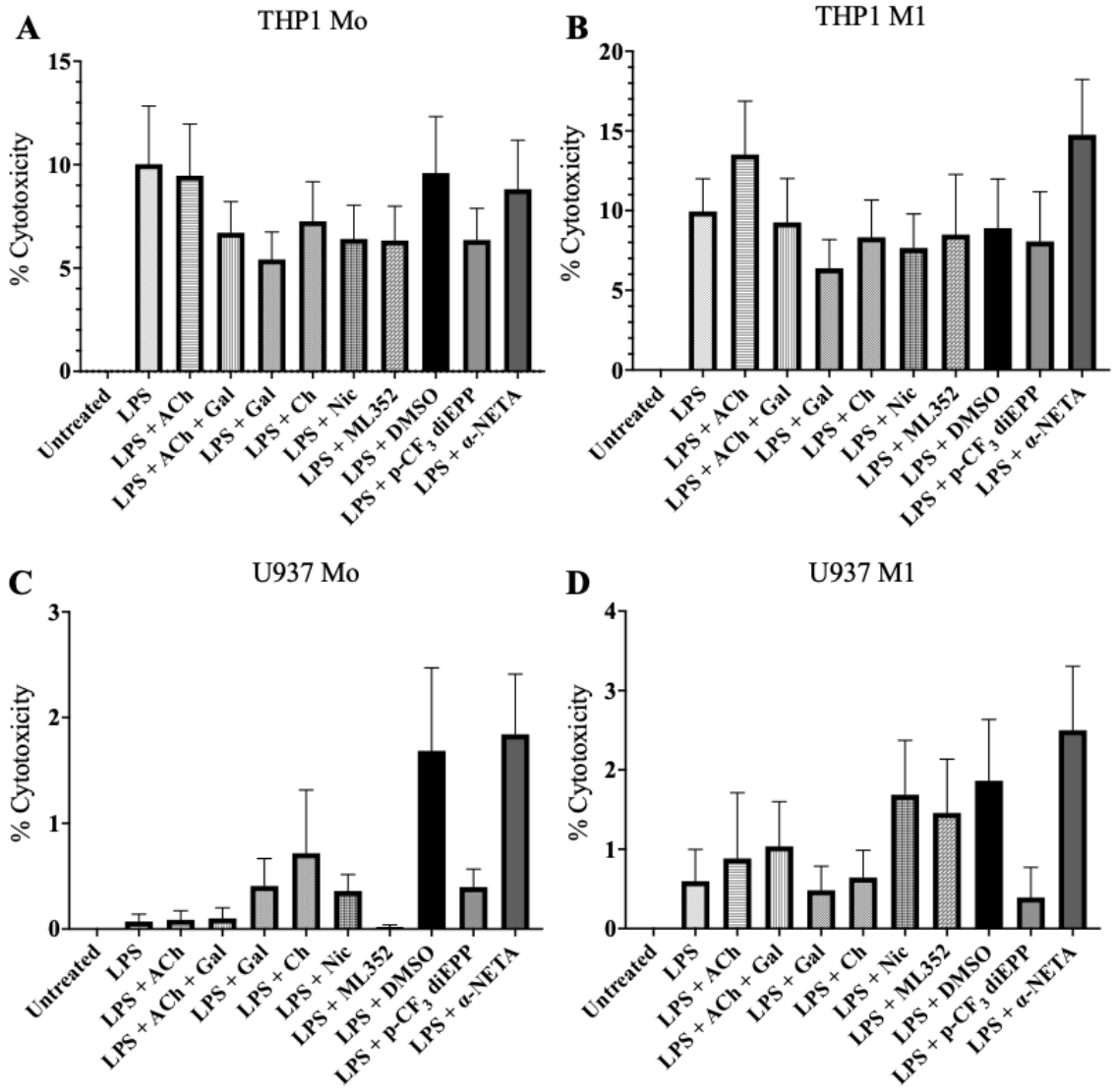

Figure 23. Normalized Cytotoxicity (%) of THP-1 and U937 Macrophages Upon Acute Cholinergic Inhibitor and Agonist Treatments in the Presence of LPS (N=10)

Upon acute treatments of the THP-1 Mo (A), THP-1 M1 (B), U937 Mo (C) and U937 Mo (D) differentiated macrophages in the presence of LPS, the supernatants were collected to assess cytotoxicity of each treatment group. This was completed using a fluorescent LDH assay. The percent cytotoxicity was calculated by using the fluorescent signals acquired from the Cytation 5. Cell culture media was used as a negative (blank) control and a total release control (cells left untreated and lysed through a freeze/thaw cycle) was used as a positive control (100% cell death). The data was normalized to the untreated control group, which represents 0% cytotoxicity. The error bars represent the SEM and one-way ANOVAs (multiple comparisons) with Dunnett's correction were performed to determine statistical significance (*: $P \leq 0.0332$; **: $P \leq 0.0021$; ***: $P \leq 0.0002$; ****: $P \leq 0.0001$). Data was compared to either the LPS

treated group (columns with different patterns) or the LPS + DMSO treated group (columns with solid colors). Altogether, in the presence of LPS, the treatment groups do not result in significant difference in cytotoxicity levels in comparison to the LPS or LPS + DMSO treated groups.

3.6 Cytokine Profiles of THP-1 and U937 Macrophages Treated Chronically with Agonists and Cholinergic Inhibitors in the Presence of LPS

Since our acute treatments were successful in inhibiting some cytokines, we further wanted to assess the effect of chronic pharmacological inhibition on cytokine release in macrophages and compare these results with those obtained in the acute treatment groups. The treatment groups included in chronic stimulations are the same as the ones included and previously described in acute stimulations (see section 3.4). Briefly, cultured THP-1 and U937 cells were differentiated into Mo or M1 macrophages as described in section 2.2. Cells were additionally treated with DMSO, various agonists or cholinergic inhibitors during the 48-hour polarization step. Then, the cell culture media was replaced, and cells were treated once again with the various conditions, in the presence of 10 ng/mL of LPS (described in table 1) for 5 hours. Afterwards, cell supernatants were collected, and cytokine concentrations were determined via CBAs using the BD FACSCanto II flow cytometer. It is important to note that U937 Mo macrophages did not release detectable amounts of IL-1β, therefore, this cytokine is not shown in this analysis. Outliers were determined by the GraphPad Prism 9 software outlier test and removed from the data set. The cytokine data was normalized by setting the concentration of each cytokine from the LPS or the LPS + DMSO to 100% and calculating all other values accordingly. One-way ANOVAs (multiple comparisons) with Dunnett's correction were performed to determine statistical significance (*: $P \leq 0.0332$; **: $P \leq 0.0021$; ***: $P \leq$

0.0002; ****: $P \leq 0.0001$). The raw cytokine data without normalization are shown in Appendix C.

3.6.1 THP-1 Macrophages

Cytokine profiles of THP-1 Mo macrophages upon chronic treatment of agonists (Ach, Ch, Nic and p-CF_3 diEPP) and cholinergic inhibitors (Gal, ML352 and α-NETA) followed by stimulation with LPS were assessed (Figure 24). First, the secretion of IL-1β (Figure 24A) was reduced by various treatment groups, including treatments inhibiting AChE (Gal), ChT (ML352) and ChAT (α-NETA) as well as treatment with a nAChR silent agonist (p-CF_3 diEPP). IL-6 secretion (Figure 24B) was not shown to be significantly inhibited by any of the treatment groups. Moreover, IL-10 release (Figure 24C) was significantly reduced upon ChAT (α-NETA) inhibition. Finally, TNF-α secretion (Figure 24D) was decreased by inhibiting AChE (Gal) and after treatment with a nAChR agonist (Nic). Overall, the release of cytokines in chronically treated THP-1 Mo macrophages, more specifically IL-1β, seems to be mostly controlled by inhibitors of cholinergic proteins and nAChR agonists like p-CF_3 diEPP and Nic.

The cytokine profiles of THP-1 M1 macrophages upon chronic treatment of agonists (Ach, Ch, Nic and p-CF_3 diEPP) and cholinergic inhibitors (Gal, ML352 and α-NETA) in the presence of LPS were additionally assessed (Figure 22). First, IL-1β release (Figure 25A) was significantly reduced upon treatment with a ChAT (α-NETA) inhibitor and a nAChR silent agonist (p-CF_3 diEPP), in the presence of LPS. Treatment with a nAChR agonist (Nic) also showed to increase IL-1β release from the cells. Moreover, the different treatments did not have significant effects on the release of IL-6 (Figure 25B) and TNF-α (Figure 25D). Finally, IL-10 secretion (Figure 25C) was significantly reduced by inhibiting ChAT (α-NETA) and significantly increased by treating with a nAChR agonist (ACh). Altogether, while nAChR

silent agonism and ChAT inhibition reduced the release of IL-1β, the opposite effect is seen when treating with a nAChR agonist. Similarly, ChAT inhibition reduced the release of IL-10 whereas treatments with a nAChR agonist resulted in an increase in cytokine release.

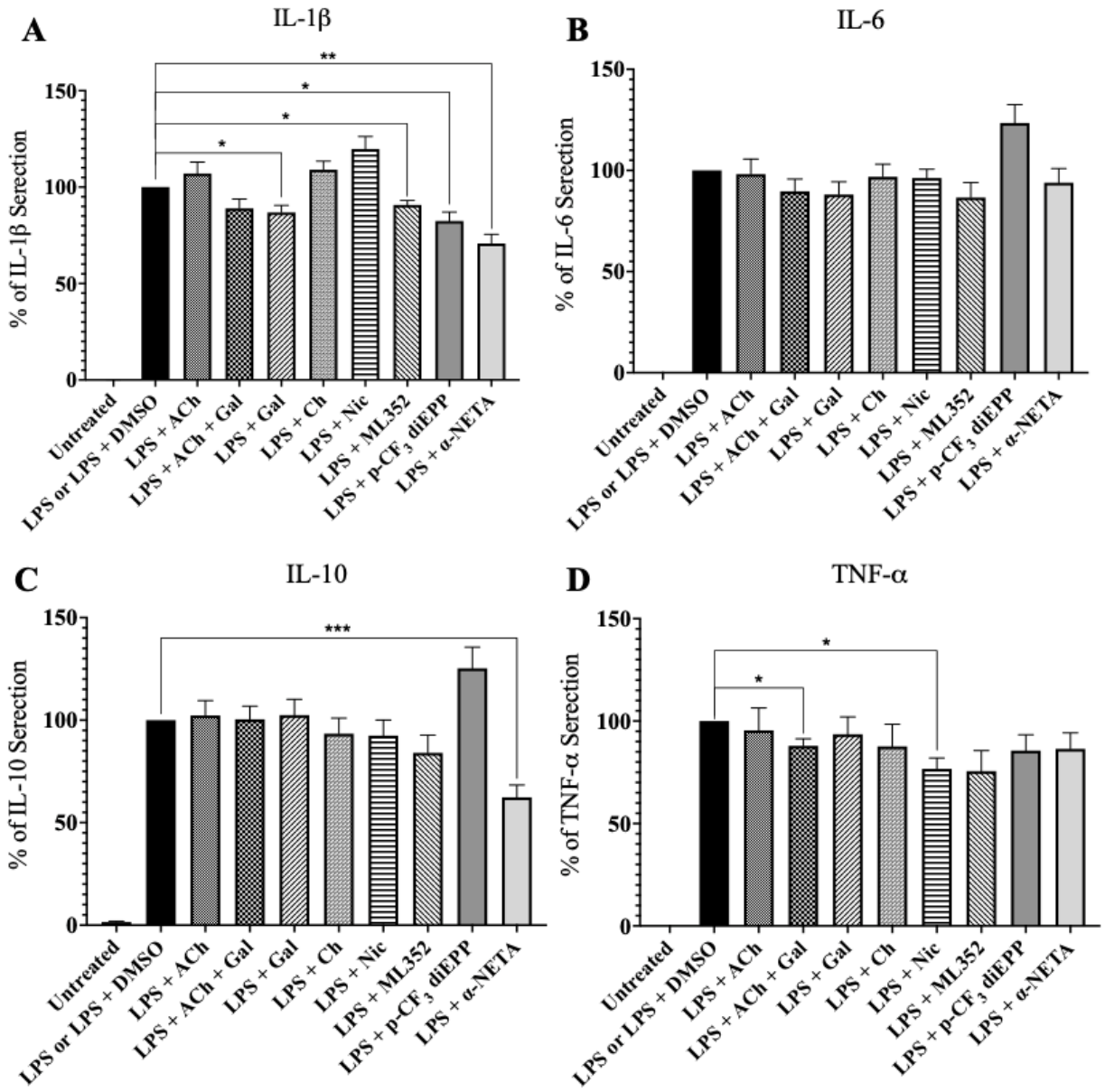

Figure 24. Cytokine Release of THP-1 Mo Macrophages Upon Chronic Cholinergic Inhibitor and Agonist Treatments in the Presence of LPS (N=10)

THP-1 cells were seeded into 6 well plates and differentiated into macrophages by stimulation with 100 ng/mL of PMA for 48 hours. The media was then replaced with PMA-free media for 24 hours, allowing the cells to rest. Then, the macrophages were given fresh media and treated with DMSO, various agonists and/or cholinergic inhibitors for 48 hours. Afterwards, the cell culture

media was replaced, and the macrophages were treated with DMSO (vehicle control), LPS, agonists and/or cholinergic inhibitors (shown in Table 1) for 5 hours. Culture supernatants were collected, and cytokine concentrations were analyzed via CBAs on the BD FACSCanto II flow cytometer. Data was normalized to either the LPS treated group (columns with different patterns) or the LPS + DMSO treated group (columns with solid colors). Errors bars indicate the SEM. One-way ANOVAs (multiple comparisons) with Dunnett's correction were performed to determine statistical significance (*: $P \leq 0.0332$; **: $P \leq 0.0021$; ***: $P \leq 0.0002$; ****: $P \leq 0.0001$). The secretion of IL-1β (A) was reduced by various treatment groups, including treatments inhibiting AChE (Gal), ChT (ML352) and ChAT (α-NETA) as well as treatments with an nAChR silent agonist (p-CF_3 diEPP). IL-6 secretion (B) was not shown to be significantly inhibited by any of the treatment groups. Moreover, IL-10 release (C) was significantly reduced upon ChAT (α-NETA) inhibition. Finally, TNF-α secretion (D) was decreased by inhibiting AChE (Gal) and treated with a nAChR agonist (Nic).

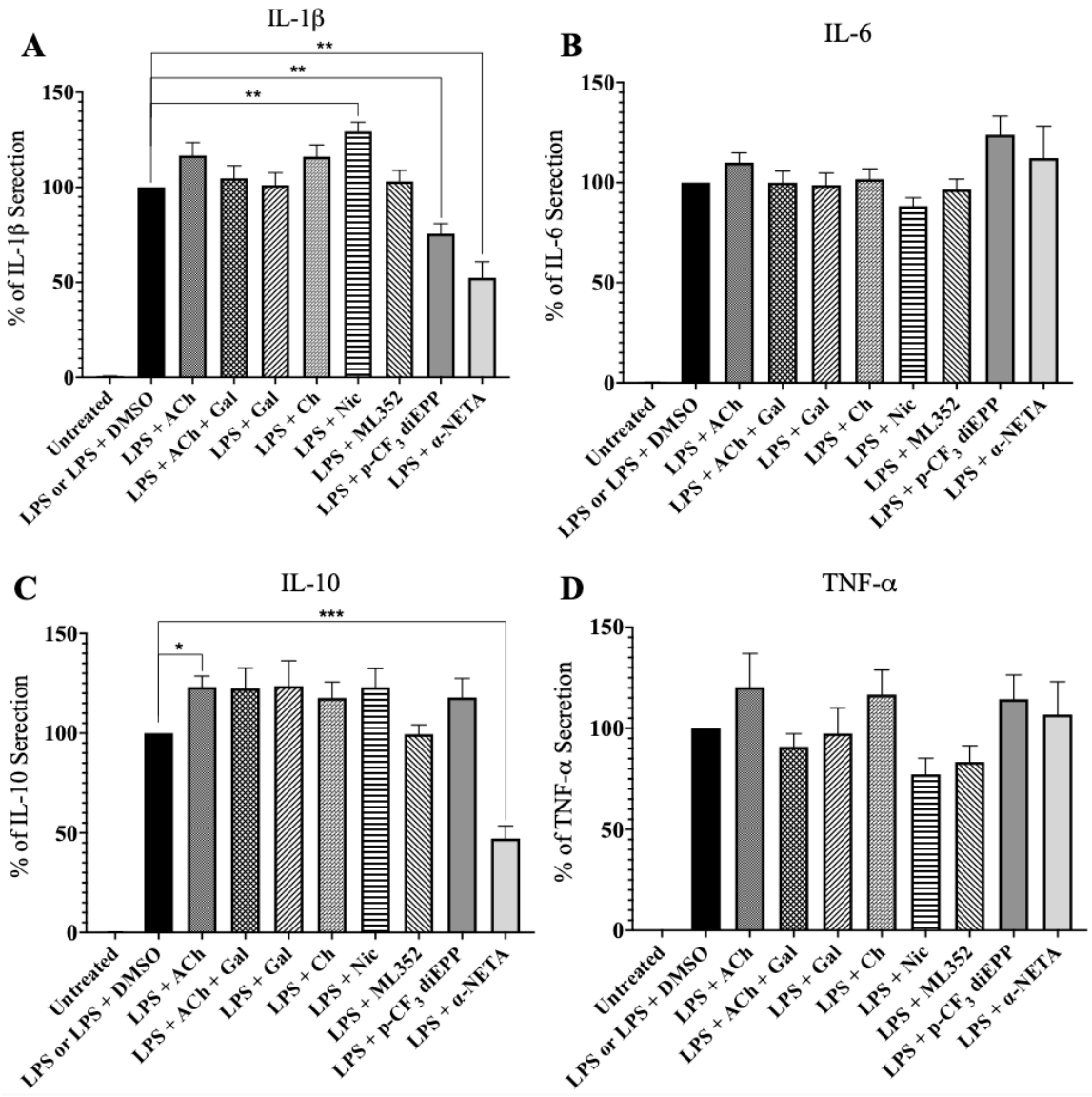

Figure 25. Cytokine Release of THP-1 M1 Macrophages Upon Chronic Cholinergic Inhibitor and Agonist Treatments in the Presence of LPS (N=10)

THP-1 cells were seeded into 6 well plates and differentiated into macrophages by stimulation with 100 ng/mL of PMA for 48 hours. The media was then replaced with PMA-free media for 24 hours, allowing the cells to rest. To further polarize into M1 macrophages, the cell culture media was replaced with fresh media containing 10 ng/mL of INF-ɣ and 10 pg/mL of LPS for 48 hours. The macrophages were additionally treated with DMSO, various agonists and/or cholinergic inhibitors during this polarization step. Afterwards, the cell culture media was replaced, and the macrophages were treated with DMSO (vehicle control), LPS, agonists and/or cholinergic inhibitors (shown in Table 1) for 5 hours. Culture supernatants were collected, and cytokine concentrations were analyzed via CBAs on the BD FACSCanto II flow cytometer. Data was normalized to either the LPS treated group (columns with different patterns) or the LPS + DMSO treated group (columns with solid colors). Errors bars indicate the SEM. One-way ANOVAs (multiple comparisons) with Dunnett's correction were performed to determine statistical significance (*: $P \leq 0.0332$; **: $P \leq 0.0021$; ***: $P \leq 0.0002$; ****: $P \leq 0.0001$). IL-1β release

(A) was significantly reduced by treating with a ChAT (α-NETA) inhibitor and a nAChR silent agonist (p-CF_3 diEPP), in the presence of LPS. Treatments with a nAChR agonist (Nic) also showed to increase IL-1β release from the cells. The different treatments did not have significant effects on the release of IL-6 (B) and TNF-α (D). Finally, IL-10 secretion (C) was significantly reduced by inhibiting ChAT (α-NETA) and significantly increased by treating with a nAChR agonist (ACh).

3.6.2 U937 Macrophages

Cytokine profiles of U937 Mo macrophages upon chronic treatment of agonists or cholinergic inhibitors followed by stimulation with LPS were assessed (Figure 26). First, the release of IL-6 (Figure 26A) and IL-10 (Figure 26B) were reduced by different treatment groups in the presence of LPS, including nAChR agonist (Nic) and silent agonist (p-CF_3 diEPP) as well as by inhibiting ChT (ML352). The release of IL-10 was also additionally inhibited by ChAT inhibition (α-NETA). Finally, TNF-α secretion (Figure 26C) was significantly reduced by nAChR agonism (Nic) and silent agonism (p-CF_3 diEPP). Overall, the release of all 3 cytokines were significantly reduced by treatment with a nAChR agonist (Nic) and a silent agonist (p-CF_3 diEPP).

The cytokine profiles of U937 M1 macrophages upon chronic treatment of agonists or cholinergic inhibitors in the presence of LPS were additionally assessed (Figure 27). This Figure demonstrates that IL-6 release (Figure 27A) was significantly decreased by ChT inhibition (ML352) and silent agonism (p-CF_3 diEPP). Moreover, IL-10 secretion (figure 27B) was inhibited by nAChR agonist (Nic) and silent agonism (p-CF_3 diEPP) as well as by inhibiting ChAT (α-NETA). The release of TNF-α (Figure 27C) on the other hand, was not shown to be significantly influenced by any of the treatment groups. Taken together, silent agonism (p-CF_3 diEPP) demonstrated the most significant effects in the release of IL-10 and IL-6.

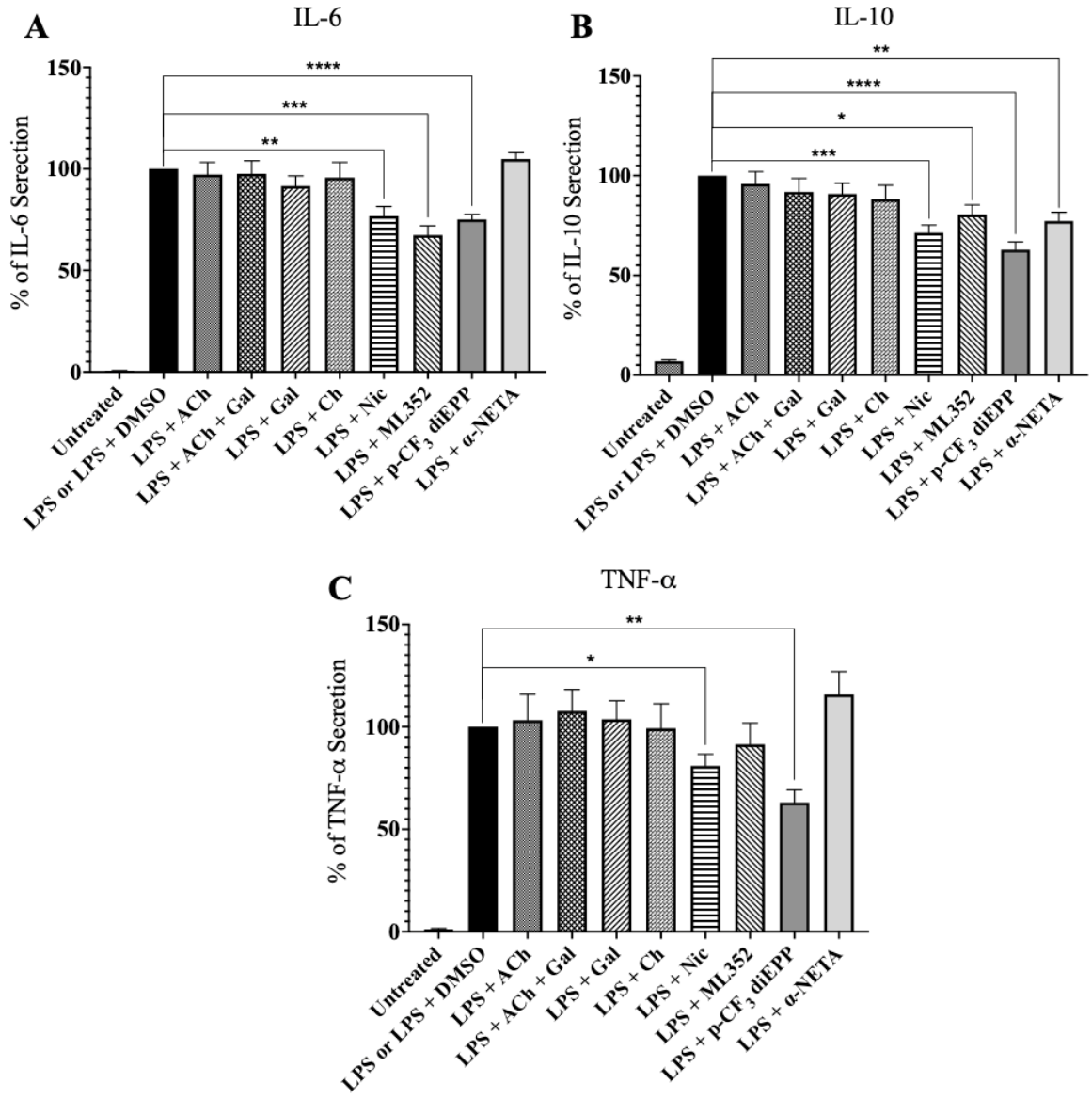

Figure 26. Cytokine Release of U937 Mo Macrophages Upon Chronic Cholinergic Inhibitor and Agonist Treatments in the Presence of LPS (N=10)

U937 cells were seeded into 6 well plates and differentiated into macrophages by stimulation with 100 ng/mL of PMA for 48 hours. The media was then replaced with PMA-free media for 24 hours, allowing the cells to rest. Then, the macrophages were given fresh media and treated with DMSO, various agonists and/or cholinergic inhibitors for 48 hours. Afterwards, the cell culture media was replaced, and the macrophages were treated with DMSO (vehicle control), LPS, agonists and/or cholinergic inhibitors (shown in Table 1) for 5 hours. Culture supernatants were collected, and cytokine concentrations were analyzed via CBAs on the BD FACSCanto II flow cytometer. Data was normalized to either the LPS treated group (columns with different patterns) or the LPS + DMSO treated group (columns with solid colors). Errors bars indicate the SEM. One-way ANOVAs (multiple comparisons) with Dunnett's correction were performed to determine statistical significance (*: $P \leq 0.0332$; **: $P \leq 0.0021$; ***: $P \leq 0.0002$; ****: $P \leq$

0.0001). The release of IL-6 (A) and IL-10 (B) was reduced by different treatment groups in the presence of LPS, including nAChR agonist (Nic) and silent agonist (p-CF3 diEPP) as well as by inhibiting ChT (ML352). The release of IL-10 was also additionally inhibited by ChAT inhibition (α-NETA). Finally, TNF-α secretion (C) was significantly reduced by nAChR agonism (Nic) and silent agonism (p-CF3 diEPP).

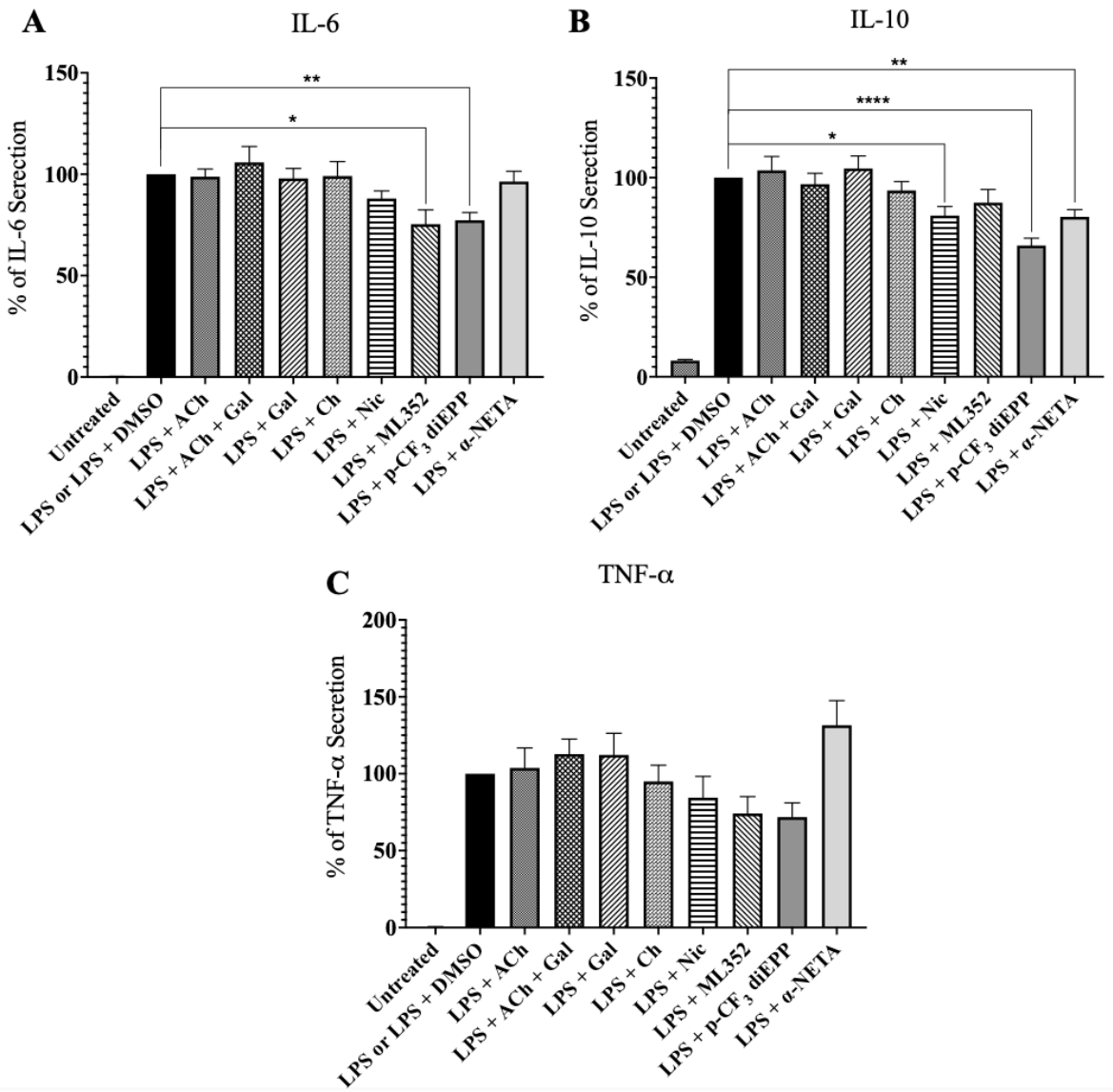

Figure 27. Cytokine Release of U937 M1 Macrophages Upon Chronic Cholinergic Inhibitor and Agonist Treatments in the Presence of LPS (N=10)

U937 cells were seeded into 6 well plates and differentiated into macrophages by stimulation with 100 ng/mL of PMA for 48 hours. The media was then replaced with PMA-free media for 24 hours, allowing the cells to rest. To further polarize into M1 macrophages, the cell culture media was replaced with fresh media containing 10 ng/mL of INF-ɣ and 10 pg/mL of LPS for 48 hours. The macrophages were additionally treated with DMSO, various agonists and/or cholinergic

inhibitors during this polarization step. Afterwards, the cell culture media was replaced, and the macrophages were treated with DMSO (vehicle control), LPS, agonists and/or cholinergic inhibitors (shown in Table 1) for 5 hours. Culture supernatants were collected, and cytokine concentrations were analyzed via CBAs on the BD FACSCanto II flow cytometer. Data was normalized to either the LPS treated group (columns with different patterns) or the LPS + DMSO treated group (columns with solid colors). Errors bars indicate the SEM. One-way ANOVAs (multiple comparisons) with Dunnett's correction were performed to determine statistical significance (*: $P \leq 0.0332$; **: $P \leq 0.0021$; ***: $P \leq 0.0002$; ****: $P \leq 0.0001$). IL-6 release (A) was significantly decreased by ChT inhibition (ChT) and silent agonism (p-CF_3 diEPP). Moreover, IL-10 secretion (B) was inhibited by nAChR agonist (Nic) and silent agonism (p-CF_3 diEPP) as well as by inhibiting ChAT (α-NETA). The release of TNF-α (C) was not shown to be significantly influenced by any of the treatment groups.

3.7 Cytotoxicity of Chronic Stimulations of THP-1 and U937 Macrophages with LPS, Agonists and Cholinergic Inhibitors

Similar to the analysis of cytotoxicity in acute stimulations of THP-1 and U937 macrophages, the cytotoxicity of chronic agonist and cholinergic inhibitor stimulations in THP-1 and U937 macrophages were also carried out. This cytotoxicity test was performed to confirm that the effects seen from these chronic treatments on the cytokine profiles was not due to cell death. Thus, LDH release was once again analyzed in these cells using a Fluorescent LDH kit. Figure 28 demonstrate the % cytotoxicity of chronically-treated THP-1 and U937 macrophages (Mo and M1). Repeated measures one-way ANOVAs (multiple comparisons) with Dunnett's correction were performed to determine statistical significance (*: $P \leq 0.0332$; **: $P \leq 0.0021$; ***: $P \leq 0.0002$; ****: $P \leq 0.0001$).

After statistical analysis, the cytotoxicity levels of chronically treated THP-1 Mo macrophages (Figure 28A) were significantly lower in the p-CF_3 diEPP-treated group in comparison to the LPS + DMSO group. On the contrary, in THP-1 M1 (Figure 28B), U937 Mo (Figure 28C) and U937 M1 (Figure 28D) differentiated macrophages, the treatment groups did not have significant differences in cytotoxicity levels in comparison to the LPS or LPS + DMSO

treated groups. Overall, in all differentiated THP-1 and U937 macrophages (Mo and M1), p-CF_3 diEPP was the only treatment to have significantly lower cytotoxicity in THP-1 Mo macrophages.

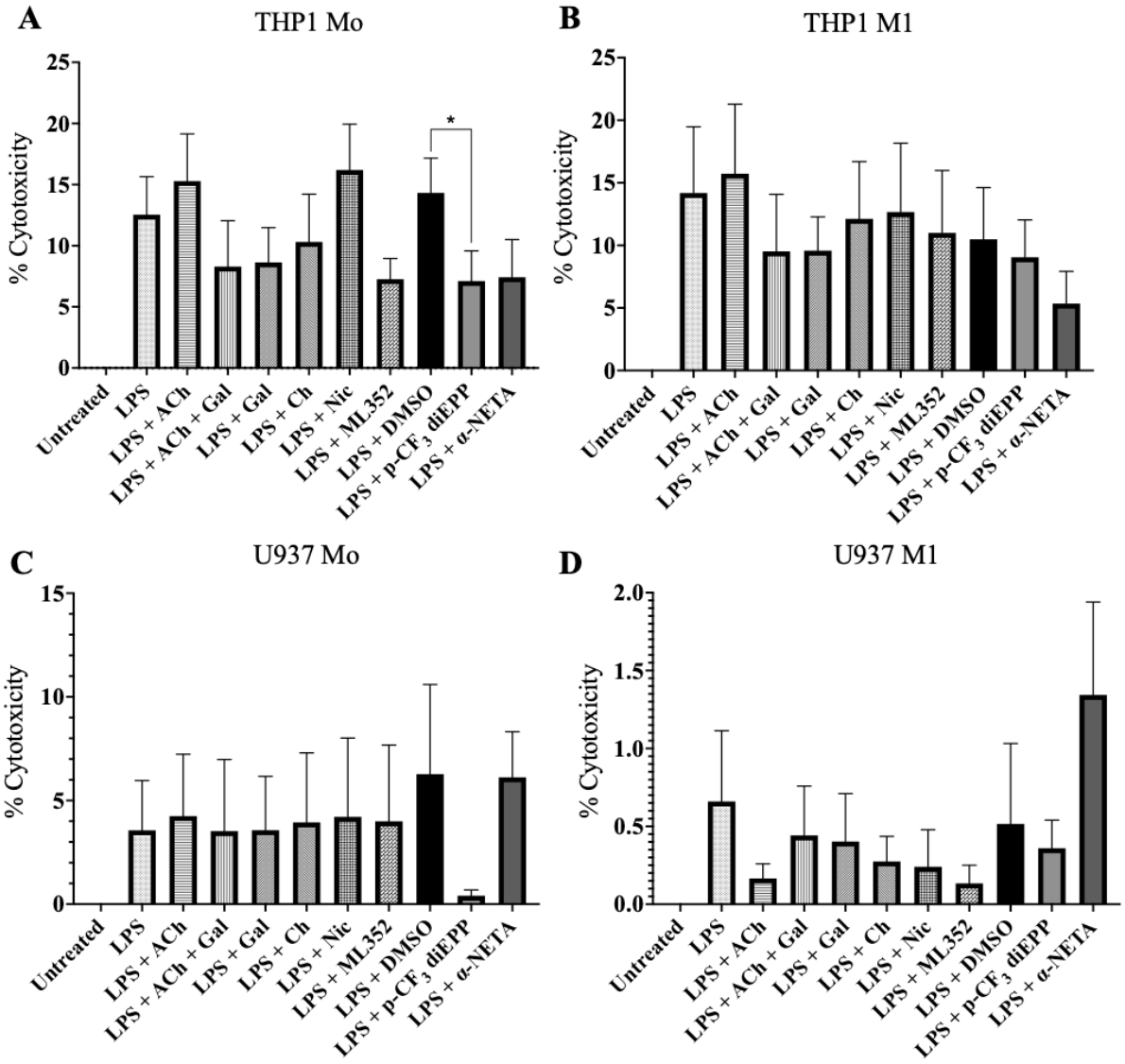

Figure 28. Normalized Cytotoxicity (%) of THP-1 and U937 Macrophages Upon Chronic Cholinergic Inhibitor and Agonist Treatments in the Presence of LPS (N=10)

Upon chronic treatments of THP-1 and U937 Mo and M1 differentiated macrophages in the presence of LPS, the supernatants were collected to assess cytotoxicity of each treatment group. This was completed using a fluorescent LDH assay. The percent cytotoxicity was calculated by using the fluorescent signals acquired from the Cytation 5. Cell culture media was used as a negative (blank) control and a total release control (cells left untreated and lysed through a freeze/thaw cycle) was used as a positive control (100% cell death). The data was normalized to

the untreated control group, which represents 0% cytotoxicity. The error bars represent the SEM and one-way ANOVAs (multiple comparisons) with Dunnett's correction were performed to determine statistical significance (*: $P \leq 0.0332$; **: $P \leq 0.0021$; ***: $P \leq 0.0002$; ****: $P \leq 0.0001$). Data was compared to either the LPS treated group (columns with different patterns) or the LPS + DMSO treated group (columns with solid colors). The % cytotoxicity in THP-1 Mo macrophages (A) was shown to be significantly lower in silent agonist-treated (p-CF_3 diEPP) cells in comparison to the LPS + DMSO group. In THP-1 M1 (B), U937 Mo (C) and U937 M1 (D) differentiated macrophages, the treatment groups did not seem to have significant differences in cytotoxicity levels in comparison to the LPS or LPS + DMSO treated groups.

3.8 Cell Marker Expression of THP-1 and U937 Macrophages Treated Chronically with Agonists and Cholinergic Inhibitors in the Presence of LPS

M1 and M2 polarized macrophages have distinguishing features, as previously mentioned in Section 1.0.2; one of them being their expression of cell markers. It is important to remember that although some markers are more highly expressed in one phenotype than the other, extreme polarities are uncommon. M1 macrophages typically have a higher expression of CD80 and CXCL10. In contrast, M2 macrophages typically have higher expressions of MRC1 (CD206) and CD163. Other general macrophage / monocyte markers include CCR2, CD14, ITGAM (CD11b) and CX3CR1.

3.8.1 THP-1 Macrophages

Relative normalized expression of cell markers in THP-1 Mo macrophages upon chronic treatment of agonists (Ach, Ch, Nic and p-CF_3 diEPP) and cholinergic inhibitors (Gal, ML352 and α-NETA) followed by stimulation with LPS for 5 hours were assessed (Figure 29). This figure demonstrates two significant observations in cell marker expression. First, CCR2 (Figure 29A), expressed by most monocytes and macrophages, is highly expressed in the control sample not treated with LPS whereas it is significantly lower in the LPS-treated sample. Likewise, CX3CR1 (Figure 29E), a common macrophage gene, follows a similar

trend in which the LPS-treated sample had a lower expression of this gene in comparison to the control (untreated group). The other cell markers did not seem to have significant differences in expression when treated with the different conditions. Overall, CCR2 and CX3CR1 are more highly expressed in the untreated group when compared to the LPS-treated group.

The relative normalized expression of cell markers in THP-1 M1 macrophages upon chronic treatment of agonists (Ach, Ch, Nic and p-CF_3 diEPP) and cholinergic inhibitors (Gal, ML352 and α-NETA) in the presence of LPS for 5 hours were additionally assessed (Figure 30). Like THP-1 Mo macrophages, CCR2 (Figure 30A) and CX3CR1 (Figure 30E) are more significantly expressed in the untreated group in comparison to the LPS-treated group. Furthermore, CD80 (Figure 30C), a gene more commonly expressed by M1 macrophages, is more highly expressed in the LPS-treated group and hardly expressed in the untreated group. Overall, while CCR2 and CX3CR1 are more highly expressed in the untreated group, CD80 is more highly expressed in the LPS-treated group.

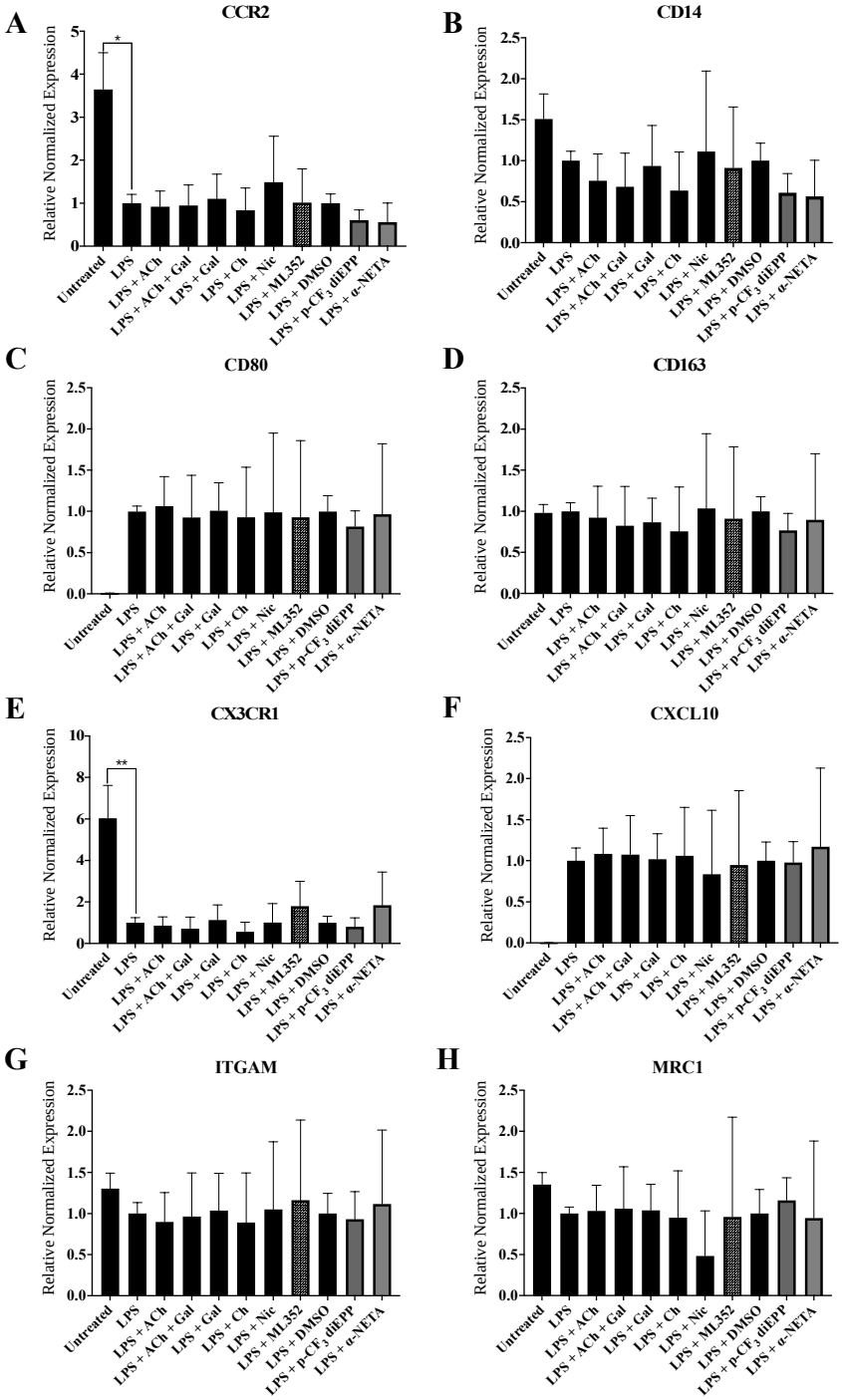

Figure 29. Normalized Expression of Cell Markers in THP-1 Mo Macrophages Upon Chronic Cholinergic Inhibitor and Agonist Treatments in the Presence of LPS (N=5)

Upon chronic treatments of THP-1 Mo macrophages in the presence of LPS, RNA was extracted from the cells, quantified using Nanodrop One and transcribed into cDNA. The mRNA expression of cell markers was determined using the SensiFAST SYBR Lo-ROX Kit and various primers specific to cell markers. The cell markers assessed include CCR2 (A), CD14 (B), CD80 (C), CD163 (D), CX3CR1 (E), CXCL10 (F), ITGAM (G) and MRC1 (H). All NTC and NRTC samples

had no signal, thus no contamination and genomic DNA was present within the samples. The relative normalized expression was calculated using the CFX Maestro Software where TBP and GAPDH expressions served as reference genes. The error bars represent the SEM and one-way ANOVAs (multiple comparisons) with Dunnett's correction were performed to determine statistical significance (*: $P \leq 0.0332$; **: $P \leq 0.0021$; ***: $P \leq 0.0002$; ****: $P \leq 0.0001$). Data was compared to either the LPS treated group (columns with different patterns) or the LPS + DMSO treated group (columns with solid colors). CCR2 (A) is highly expressed in the control sample not treated with LPS whereas it is significantly lower in the LPS-treated sample. CX3CR1 (E) follows similar trends in which the LPS-treated sample had a lower expression in comparison to the control (untreated group). The other cell markers do not seem to have significant differences in expression when treated with the different treatment groups.

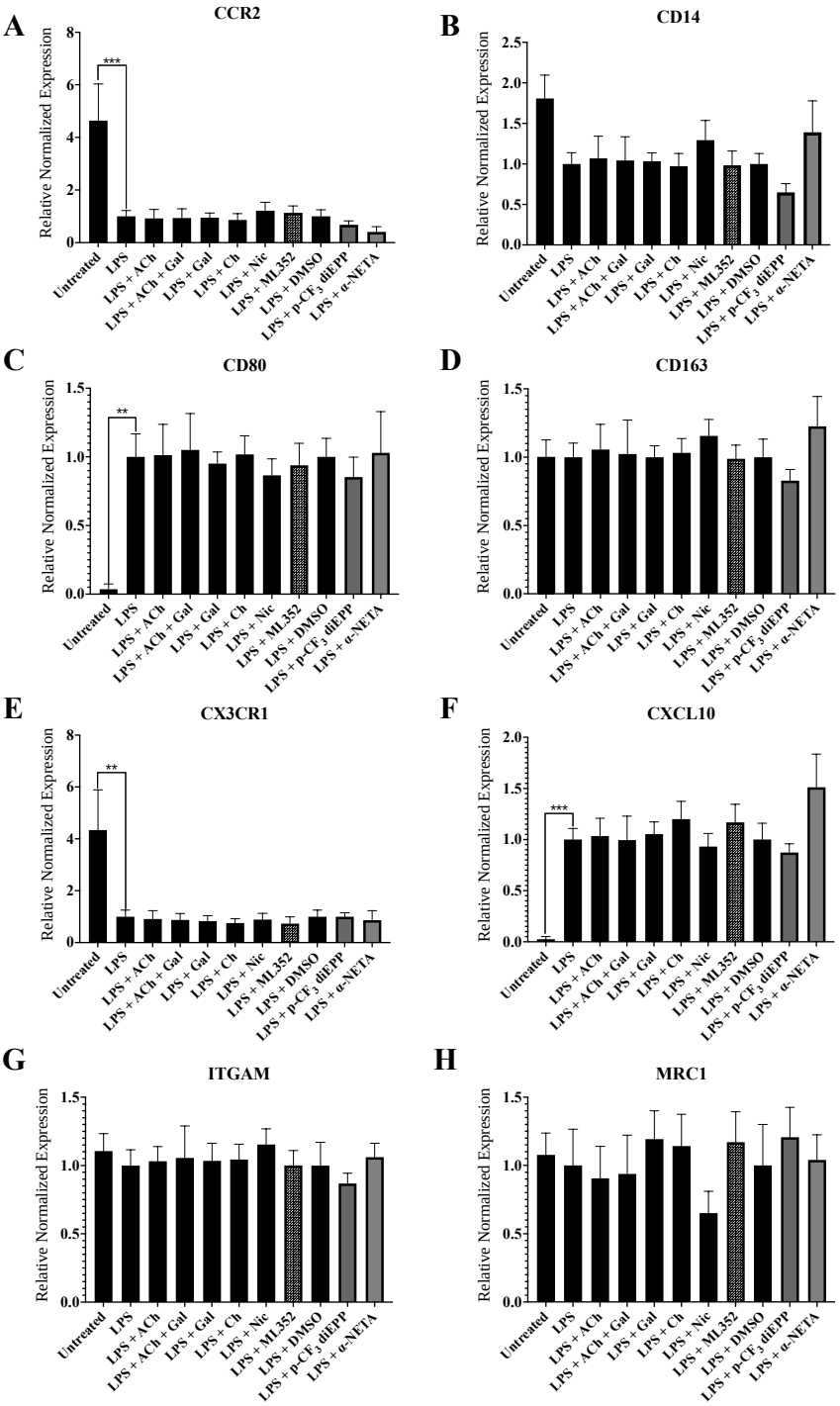

Figure 30. Normalized Expression of Cell Markers in THP-1 M1 Macrophages Upon Chronic Cholinergic Inhibitor and Agonist Treatments in the Presence of LPS (N=5)

Upon chronic treatments of THP-1 M1 macrophages in the presence of LPS, RNA was extracted from the cells, quantified using Nanodrop One and transcribed into cDNA. The mRNA expression of cell markers was determined using the SensiFAST SYBR Lo-ROX Kit and various primers specific to cell markers. The cell markers assessed include CCR2 (A), CD14 (B), CD80 (C), CD163 (D), CX3CR1 (E), CXCL10 (F), ITGAM (G) and MRC1 (H). All NTC and NRTC

samples had no signal, thus no contamination and genomic DNA was present within the samples. The relative normalized expression was calculated using the CFX Maestro Software where TBP and GAPDH expressions served as reference genes. The error bars represent the SEM and one-way ANOVAs (multiple comparisons) with Dunnett's correction were performed to determine statistical significance (*: $P \leq 0.0332$; **: $P \leq 0.0021$; ***: $P \leq 0.0002$; ****: $P \leq 0.0001$). Data was compared to either the LPS treated group (columns with different patterns) or the LPS + DMSO treated group (columns with solid colors). CCR2 (A) and CX3CR1 (E) are more significantly expressed in the untreated group in comparison to the LPS-treated group. CD80 (C), is more highly expressed in the LPS-treated group and hardly expressed in the untreated group.

3.8.2 U937 Macrophages

Relative normalized expression of cell markers in U937 Mo macrophages upon chronic treatment of agonists (Ach, Ch, Nic and p-CF_3 diEPP) and cholinergic inhibitors (Gal, ML352 and α-NETA) followed by stimulation with LPS for 5 hours were assessed (Figure 31). In terms of statistical significance, no significant changes in surface markers were determined after treatment with the various conditions. However, CXCL10 (Figure 31E) expression, a gene more highly expressed by M1 macrophages, seems to be lower in the untreated group in comparison to the LPS-treated group, but this was not shown to be statistically significant. Overall, no significant differences in surface marker expression were seen.

The relative normalized expression of cell markers in U937 M1 macrophages upon chronic treatments of agonists (Ach, Ch, Nic and p-CF_3 diEPP) and cholinergic inhibitors (Gal, ML352 and α-NETA) in the presence of LPS for 5 hours were additionally assessed (Figure 32). CXCL10 expression (Figure 32E) was shown to be significantly higher in the LPS-treated group in comparison to the untreated group. Moreover, a trend in CD80 expression (Figure 32C), a gene more highly expressed by M1 macrophages, seems to be present. CD80 expression seems to be lower in the untreated group in comparison to the LPS-treated groups, but this was not shown to be statistically significant. Taken together, the only statistically significant observation

is the increase of CXCL10 expression in the LPS-treated group in comparison to the untreated group.

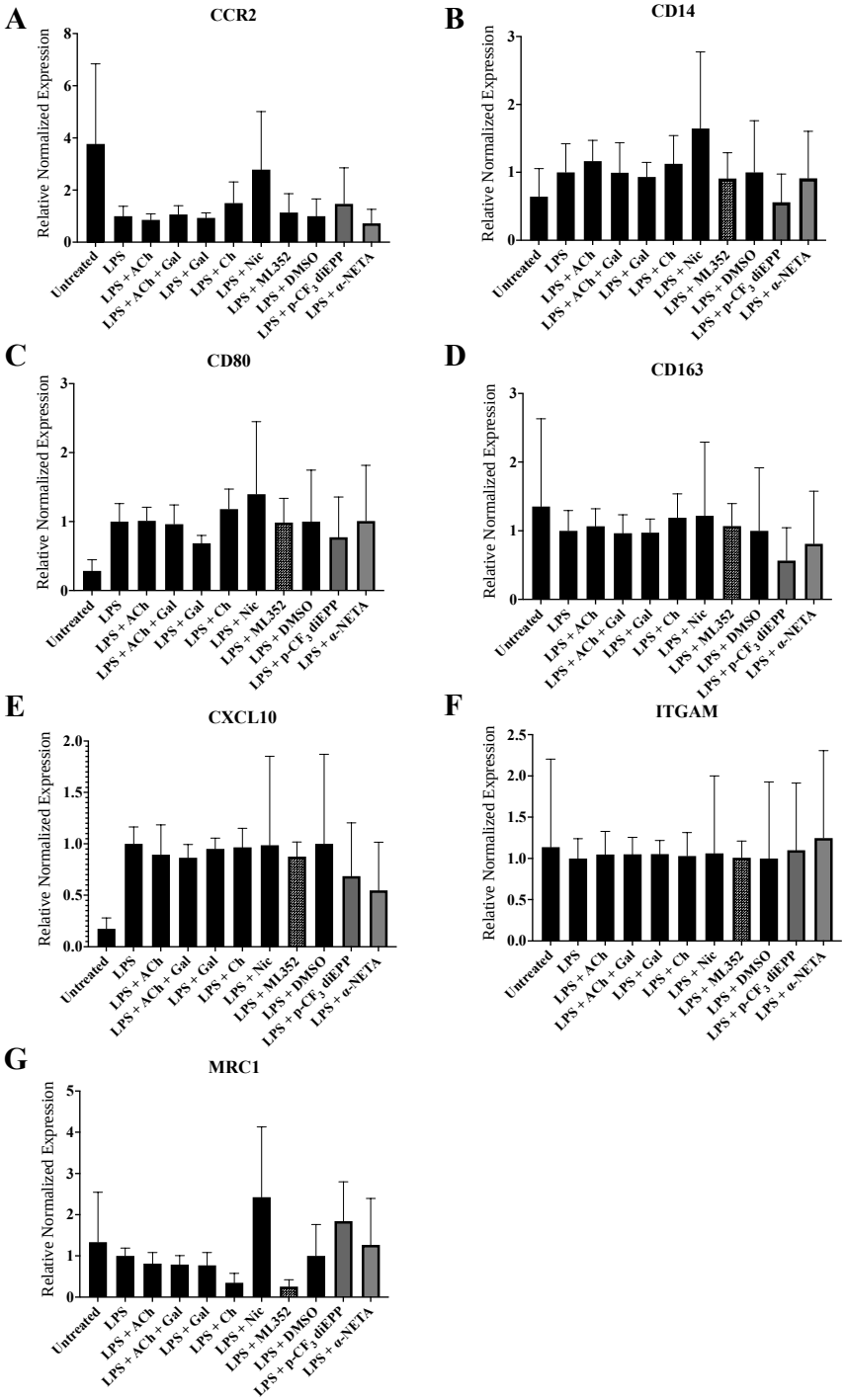

Figure 31. Normalized Expression of Cell Markers in U937 Mo Macrophages Upon Chronic Cholinergic Inhibitor and Agonist Treatments in the Presence of LPS (N=5)

Upon chronic treatments of U937 Mo macrophages in the presence of LPS, RNA was extracted from the cells, quantified using Nanodrop One and transcribed into cDNA. The mRNA expression of cell markers was determined using the SensiFAST SYBR Lo-ROX Kit and various primers specific to cell markers. The cell markers assessed include CCR2 (A), CD14 (B), CD80 (C), CD163 (D), CXCL10 (E), ITGAM (F), MRC1 (G). All NTC and NRTC samples had no signal, thus no contamination and genomic DNA was present within the samples. The relative normalized expression was calculated using the CFX Maestro Software where TBP and GAPDH expressions served as reference genes. The error bars represent the SEM and one-way ANOVAs (multiple comparisons) with Dunnett's correction were performed to determine statistical significance (*: $P \leq 0.0332$; **: $P \leq 0.0021$; ***: $P \leq 0.0002$; ****: $P \leq 0.0001$). Data was compared to either the LPS treated group (columns with different patterns) or the LPS + DMSO treated group (columns with solid colors). No statistically significant changes in cell marker expression were determined after treatment with the various conditions. However, CXCL10 expression (E), seems to be lower in the untreated group in comparison to the LPS-treated group, but this was not shown to be statistically significant.

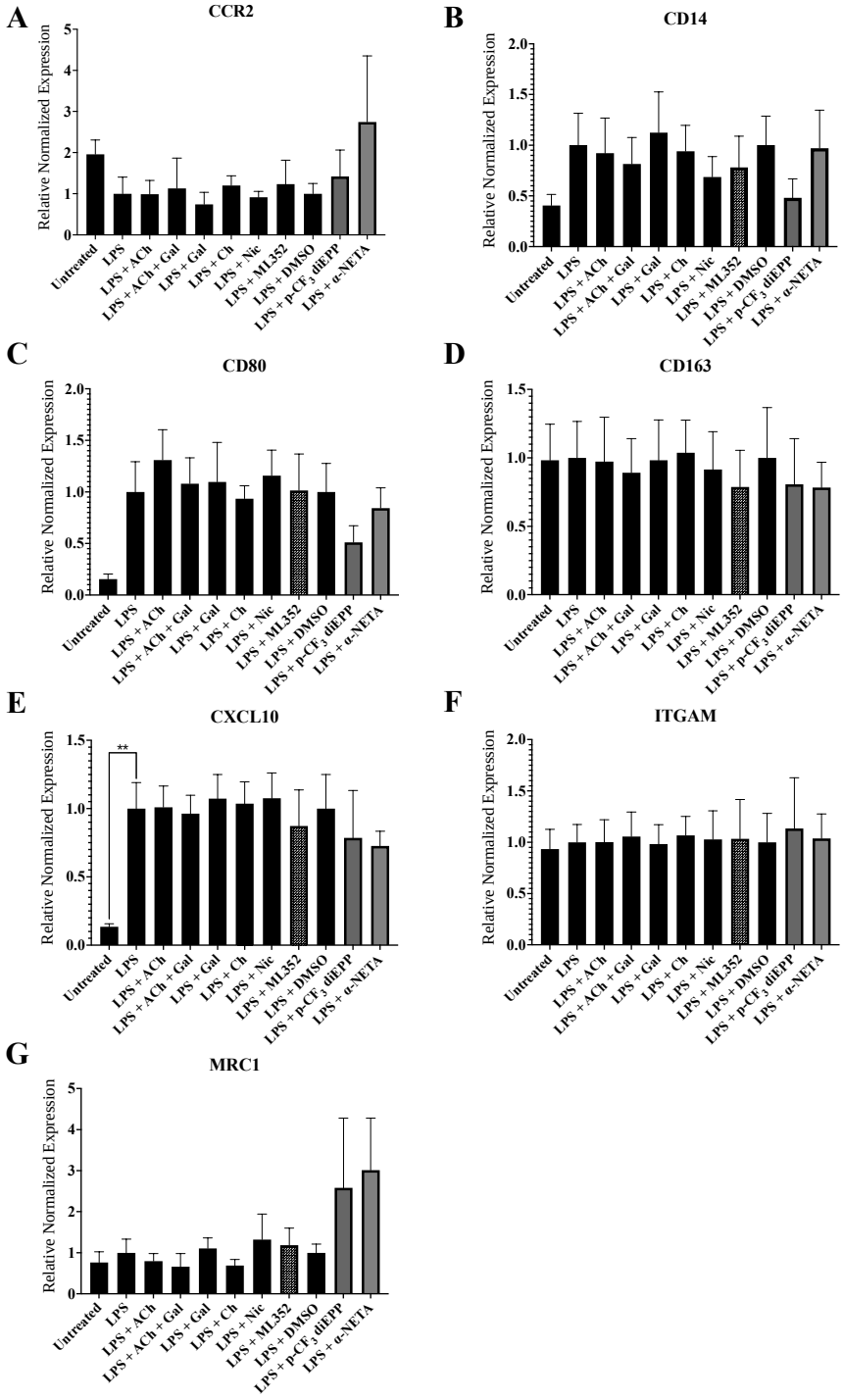

Figure 32. Normalized Expression of Cell Markers in U937 M1 Macrophages Upon Chronic Cholinergic Inhibitor and Agonist Treatments in the Presence of LPS (N=5)

Upon chronic treatments of U937 M1 macrophages in the presence of LPS, RNA was extracted from the cells, quantified using Nanodrop One and transcribed into cDNA. The mRNA expression of cell markers was determined using the SensiFAST SYBR Lo-ROX Kit and various primers specific to cell markers. The cell markers assessed include CCR2 (A), CD14 (B), CD80 (C), CD163 (D), CXCL10 (E), ITGAM (F), MRC1 (G). All NTC and NRTC samples had no signal,

thus no contamination and genomic DNA was present within the samples. The relative normalized expression was calculated using the CFX Maestro Software where TBP and GAPDH expressions served as reference genes. The error bars represent the SEM and one-way ANOVAs (multiple comparisons) with Dunnett's correction were performed to determine statistical significance (*: $P \leq 0.0332$; **: $P \leq 0.0021$; ***: $P \leq 0.0002$; ****: $P \leq 0.0001$). Data was compared to either the LPS treated group (columns with different patterns) or the LPS + DMSO treated group (columns with solid colors). CXCL10 expression (E) is significantly higher in the LPS-treated group in comparison to the untreated group. CD80 expression (C) seems to be lower in the untreated group in comparison to the LPS-treated group, but this was not shown to be statistically significant.

Discussion

This study set out to investigate the role of the cholinergic system as well as silent agonism in immune regulation. Our first objective was to determine the presence of cholinergic genes in human macrophages (THP-1 and U937 cell lines) at the transcript level by PCR and at the protein level by Western Blot. Both methods were utilized for qualitative analysis to determine the presence of cholinergic genes and not to quantitively compare expression levels of the genes. The second aim of this study was to investigate the anti-inflammatory properties of nAChR silent agonists and various other nAChR agonists and cholinergic inhibitors in human macrophages stimulated with LPS. The inflammatory responses were measured by assessing cytokine profiles and immune cell phenotype following stimulation with LPS and treatment with various conditions. Cytokine profiles were determined using CBAs whereas immune cell phenotype was studied by assessing cellular markers via qPCR. To ensure the various treatment groups did not promote significant cell death, viability and cytotoxicity tests were performed. It was hypothesized that some, if not most cholinergic proteins would be expressed by human macrophages and that the nAChR agonists/silent agonists would result in anti-inflammatory responses whereas cholinergic inhibitors would result in pro-inflammatory responses in LPS-stimulated human macrophages. Furthermore, it was also hypothesized that agonists that have anti-inflammatory effects would also decrease the expression of cellular markers more commonly expressed by pro-inflammatory cells while promoting the expression of cellular markers expressed by anti-inflammatory cells.

First, the expression of cholinergic gene mRNA in human macrophages was assessed through PCR experiments (Figures 8-11). Both THP-1 and U937 differentiated macrophages seemed to express most cholinergic genes. More specifically, U937 differentiated macrophages

seemed to express all cholinergic genes assessed (AChE, BChE, ChAT, VAChT) while THP-1 differentiated macrophages seemed to express most (AChE, BChE and VAChT), except for ChAT. Although not many studies have focused on the presence of BChE mRNA in human macrophages, its presence has been confirmed in human peripheral blood T lymphocytes[199]. Similarly, previous studies have demonstrated the presence of AChE mRNA in mouse lymphocytes, dendritic cells (DCs), and macrophages[113] as well as in human blood MNLs, human leukemic T cell lines and Daubi B cells[116]. These findings align with our PCR results where AChE and BChE mRNA seemed to be expressed in both THP-1 and U937 macrophages. Furthermore, while the presence of ChAT mRNA was not previously detected in murine peritoneal macrophages using an RT-PCR protocol of 40 amplification cycles[113], Koarai et al showed the presence of ChAT mRNA expression in human lung and alveolar macrophages using an RT-PCR protocol of 45 amplification cycles. Such findings suggest possible very low ChAT mRNA expression within macrophages[114]. Therefore, although negative results were obtained for ChAT in THP-1 macrophages, it is possible that these macrophages express very little ChAT which was not detected with our PCR protocol that was limited to 40 amplification cycles. Further experiments utilizing digital droplet PCR or targeted Next Generation Sequencing should be performed to further verify the presence of ChAT in THP-1 macrophages. Finally, according to a study performed by Fujii et al[200], human peripheral blood MNLs do not express VAChT mRNA. Yet, VAChT immunoreactivity in human peripheral blood T and B cells was previously detected, suggesting the expression of VAChT by at least some immune cells[117]. From our findings, it seems as though THP-1 and U937 differentiated macrophages also express VAChT mRNA.

AChE (Figure 8A and Figure 9A) was expressed at two band sizes within U937 and THP-1 macrophages. This is likely because the AChE primer used could amplify various AChE mRNA transcript variants according to Primer-BLAST[201]. The AChE transcript variant 4 was expected to generate a product of 997 bp whereas all other AChE transcript variants were expected to generate a product of 244 bp. The two bands seen within our gels were at approximately 800 bp and 250 bp, respectively. The 250 bp product seen in our gels was very close to the predicted product for the multiple variants (expected product of 244 bp). However, the 800 bp band seen in our gel was smaller than the predicted product for variant 4 (expected product of 997 bp). Without sequencing the amplified product, we were unable to confirm the presence of AChE within the macrophages nor determine the specificity of our AChE primer.

Moreover, similar to the AChE mRNA expression, BChE was expressed at two different band sizes in THP-1 differentiated macrophages (Figure 8B), one at approximately 400 bp and second at approximately 500 bp. The expression of BChE in U937 macrophages (Figure 9B) was however only expressed at one band size, close to 400 bp. The expected band size for BChE according to Primer-BLAST[201] is 370 bp. We can therefore conclude that the band seen in the gels close to the 400 bp length, is likely to be the expected product for BChE amplification. However, the band close to 500 bp seen in THP-1 macrophages remains unknown. It would be of interest to isolate the band and sequence it to determine the product. Considering it is very close to the expected product of 370 bp, it suggests that BChE is present in THP-1 and U937 macrophages.

Furthermore, as previously mentioned, the expression of ChAT mRNA was detected in U937 macrophages (Figure 9C) but not in THP-1 macrophages (Figure 8C). The predicted band size for the ChAT primer used was 222 bp. The band seen in the U937 macrophages was slightly

higher than 200 bp, thus suggesting its presence within U937 macrophages. Although no bands for THP-1 macrophages were detected by PCR, it is possible that these cells express such low levels of ChAT which was not detected with a 40-amplification cycle PCR protocol. Additionally, since the ChAT primer used is specific to one transcript variant, and that ChAT has multiple transcript variants, it is possible that a different ChAT transcript is present in THP-1α macrophages that is not detected with the primer used.

Finally, VAChT mRNA was detected in both THP-1 (Figure 8D) and U937 (Figure 9 D) macrophages. The band seen for VAChT was close to the predicted band size of 336 bp, once again suggesting the presence of VAChT in both THP-1 and U937 macrophages. It is important to remember that for these PCRs, it is not possible to confirm that the bands present within the gels are indeed ChAT and VAChT amplification without sequencing the product.

In terms of nAChR expression, α7, α9 and 10 nAChR subunit mRNA were assessed in both THP-1 (Figure 10) and U937 (Figure 11) macrophages. In THP-1 differentiated macrophages, the α7 nAChR (Figure 10A) seemed to only be expressed in M2 macrophages. These findings are interesting considering M2 macrophages are deemed anti-inflammatory, and many studies suggest the role of α7 in such anti-inflammatory processes. It is also possible that THP-1 Mo and M1 macrophages still express α7 nAChR subunits, but at much smaller concentrations than M2, lying below the limit of detection. In U937 differentiated macrophages, α7 nAChR subunit (Figure 11A) does not seem to be present in any of the macrophages as no amplification bands were detected. These results differ from previous studies demonstrating the expression of α7 nAChR in both THP-1 Mo macrophages[202] and U937 Mo macrophages[203] via Western Blots. As described in more detail below, it is possible that the articles previously published used primers that also amplified the partially duplicated α7 nAChR, called

CHRFAM7A whereas the primers used in our experiments were specific to the α7 only. It is also important to note that nAChR antibodies used in Western Blots are known to have poor specificity across the different receptor subtypes, which could result in false interpretations. On the other hand, the α9 nAChR subunit (Figure 10B and Figure 11B) did not seem to be expressed in any of the differentiated THP-1 macrophages whereas amplification bands of the right product size were detected in U937 differentiated macrophages. Thus, these results suggest that although U937 macrophages express the α9 nAChR, the THP-1 macrophages do not. These results support previous Western Blot findings demonstrating the lack of α9 nAChR in THP-1 Mo macrophages[202] but its presence in U937 Mo macrophages[203]. On the contrary, α10 nAChR (Figure 10C and Figure 11C) seemed to be expressed by both THP-1 and U937 differentiated macrophages as seen by the amplification bands present at the predicted band size of 294 bp. Previous studies assessing α10 nAChR via Western Blot in THP-1 macrophages have not been previously published to date, however, similar to our findings, the α10 nAChR expression has been previously reported in U937 Mo macrophages[203].

Lastly, the *CHRFAM7A* mRNA was additionally assessed unintentionally. During the initial stages of the PCR experiments, an α7 primer from a previously published paper was used. After entering the primer sequence into Primer-Blast[201], the primer was reported to amplify both *CHRFAM7A* and the normal α7 nAChR, both with expected amplification products of 844 bp. *CHRFAM7A* is a human-specific fusion gene comprising exons 5-10 of the α7 nAChR protein coding gene and 5 exons of the FAM7 fusion sequence resulting in a part-functional α7 nAChR[204]. In fact, previous studies on Xenopus oocytes have demonstrated that *CHRFAM7A* is a dominant-negative regulator of α7 nAChR[205,206]. Considering the lack of bands in the PCR gels when using the α7 nAChR-specific primer, the bands seen using the CHRFAM7A primer are

likely due to the presence of CHRFAM7A and not α7 nAChR. Thus, THP-1 and U937 differentiated macrophages seem to express CHRFAM7A. Moreover, since CHRFAM7A is a human specific fusion gene and considering its recent emergence in literature, its effect was likely not considered in preclinical studies. Perhaps most of the α7 data from previous publications are due to the presence of CHRFAM7A and not the real α7 nAChR.

To further validate the PCR results obtained, isolating the PCR products and sequencing them would be a good way to confirm our findings. These experiments would validate whether the observed band reflects the amplification of our gene of interest. Furthermore, sequencing the PCR product could allow us to differentiate between transcript variants whose bands are of similar sizes, like the transcript variants for AChE. We would be able to determine exactly which transcript variant our cells express and distinguish between the real α7 nAChR and CHRFAM7A. Therefore, sequencing the PCR product would be a great way to validate the PCR results obtained in these experiments. Another method to validate the PCR results obtained is to use a cell line which has the gene of interest knocked out and perform the same PCR experiments to verify the lack of amplification. This would confirm the specificity of the primers for the gene of interest.

The expression of cholinergic genes was additionally assessed via Western Blot (Figures 12-13) which, instead of determining mRNA expression, determines expression at the protein level. The first cholinergic gene assessed was AChE. AChE has multiple isoforms due to alternative splicing which includes AChE-S ("synaptic"), AChE-E ("erythrocytic"), and AChE-R ("readthrough")[187]. Although these isoforms have a similar catalytic domain, they differ in their C-terminal domain further influencing solubility and subcellular localization[207]. According to Figure 12A and 13A, THP-1 macrophages do not seem to express AChE whereas U937

macrophages do seem to express AChE. However, the AChE expression present in both the positive control and the U937 macrophages is at approximately 30 kDa which is much lower than the theoretical molecular weight of 68 kDa. Previous studies have reported bands for AChE to be anywhere from 55 kDa to 80 kDa[188,189]. Therefore, the band at 30 kDa may result from unspecific binding, and may not represent the presence of AChE, especially considering the bands do not fall within the range of AChE bands previously documented in the literature. To validate our results, cells with conditional knockouts and using another AChE primary antibody should be performed. These future steps would allow us to confidently determine whether or not THP-1 and U937 express AChE.

In addition, the expression of ChAT proteins was assessed via Western Blots in both THP-1 (Figure 12B,C) and U937 (Figure 13B,C) macrophages. Many splice variants for ChAT exist which includes R-, N- and M-type[190,191]. While the M-type mRNA can produce both a large (82 kDa) and a small (69 kDa) isoform, the R- and N-types can only produce the small isoform[191]. The major isoform of human ChAT is often referred to as the common type of ChAT (cChAT) distributed within the CNS[208,209]. An additional ChAT isoform also exists, referred to as the peripheral type of ChAT (pChAT) more commonly expressed by peripheral neurons and has an expected molecular weight of 50 kDa[192]. Moreover, evidence of a smaller mRNA splice variant of 27 kDa exists, which appears to be lacking catalytic activity but may be involved in regulating the full-length ChAT[193]. Hence, the various isoforms of ChAT results in differences in molecular weights and possibly function. From the Western Blot experiments performed, the expression of ChAT proteins seemed to be present in both THP-1 and U937 macrophages. Interestingly, the bands obtained using the first ChAT primary antibody (Figure 12B and Figure 13B) were at approximately 40 kDa. This band was further confirmed using a different ChAT

primary antibody (Figure 12C and Figure 13C), targeting a different epitope than the first ChAT antibody. Since the band detected using both ChAT antibodies is relatively close to the molecular weight of pChAT (50 kDa), the isoform present in THP-1 and U937 may be pChAT or a variant of pChAT with different post-translational modifications. It is also possible that THP-1 and U937 express the 27 kDa isoform of ChAT, but with added post-translational modifications that increase its molecular weight.

Furthermore, the expression of BChE protein in both THP-1 (Figure 12D) and U937 (Figure 13D) were assessed via Western Blot. Unlike AChE and ChAT, BChE does not have any known alternative splicing and has molecular weight of approximately 68 kDa[210]. Moreover, in addition to the usual BChE (BChE-U) form, more than 60 genetic variations of the BChE gene have been described to date, with the BChE-K being the most frequent genomic variant[210,211]. According to Figure 12D and 13D, the positive control (293T) seemed to slightly express BChE at the theoretical molecular weight of 68 kDa, whereas a smaller molecular weight BChE was detected in THP-1 and U937 macrophages, at approximately 30 kDa. Since no BChE isoform of 30 kDa have been described to date, the band seen is likely due to nonspecific binding. Thus, BChE expression in THP-1 and U937 macrophages remain inconclusive as further experimentation would need to be performed to validate these results.

In addition, the expression of ChT protein was also assessed in THP-1 (Figure 12E) and U937 macrophages (Figure 13E) via Western Blot. The primer used in the Western Blot experiments was specific to the high-affinity choline transporter (ChT1). Previous studies have shown the expression of ChT to be anywhere from 60 to 75 kDa, likely due to differences in post-translational modifications[194]. In terms of the Western Blot results obtained, ChT seemed to be expressed in the positive control (IMR-32) at the theoretical molecular weight of

approximately 63 kDa. However, no bands in the THP-1 and U937 macrophages were obtained suggesting the lack of ChT expression within these cells. Considering ChT is predominantly expressed in cholinergic neurons, it is not surprising that THP-1 and U937 macrophages do not express ChT. It is possible that these macrophages possess other choline transporters such as choline transporter-like proteins (CTLs) which have been shown to be expressed in tissues other than neuronal tissues. In fact, CTLs have been shown to be expressed in glial and endothelial cells as well as in various tissues including the tongue, muscle, kidney, heart, lung, testis, intestine and stomach[212,213]. Therefore, future experiments assessing the presence of various CTLs in THP-1 and U937 macrophages would be of great interest.

Finally, the expression of the VAChT protein was assessed in THP-1 (Figure 12F) and U937 macrophages (Figure 13F). VAChT is expressed at different molecular weights depending on whether or not it is glycosylated[195]. The glycosylated VAChT form has been shown to be expressed at approximately 70 kDa whereas the nonglycosylated form is expressed at 44-55 kDa[195–197]. The VAChT primer used in the Western Blot experiments detected both the glycosylated and unglycosylated forms of the VAChT proteins. According to Figure 12F and 13F, the positive control (IMR-32) seemed to express VAChT at a molecular weight of 75 kDa only. Thus, the positive control seemed to only express the glycosylated VAChT form. On the other hand, THP-1 and U937 macrophages seemed to express VAChT at two different molecular weights, one at 75 kDa and the other at 48 kDa. Hence, THP-1 and U937 macrophages seemed to express both glycosylated and nonglycosylated forms of VAChT. The VAChT antibody used for these experiments was previously validated in mouse KO experiments[196] as well as in mouse gene knockdown (KD) experiments[214]. We can therefore be fairly confident that the bands

detected were in fact VAChT expression and that THP-1 and U937 macrophages express both the glycosylated and nonglycosylated forms of VAChT.

In comparison to the cholinergic mRNA PCR results obtained, the cholinergic protein Western Blot results are relatively similar. The PCR experiments suggested the presence of BChE mRNA within THP-1 and U937 macrophages which was further supported by the presence of BChE protein obtained by Western Blot results, although the bands seen in the Western Blots are not at the predicted molecular weight. Similarly, VAChT mRNA and protein was detected in both THP-1 and U937 macrophages by PCR experiments and Western Blots, respectively. Differences in PCR results and Western Blot results were obtained for AChE and ChAT. AChE mRNA was detected in both THP-1 and U937 macrophages by PCR, but AChE protein was only detected in U937 in the Western Blot experiments. Likewise, although the ChAT protein was detected in THP-1 and U937 macrophages by Western Blot, ChAT mRNA was only detected in U937 macrophages. Such findings could be explained by low ChAT mRNA levels with the macrophages. In addition, ChT was not included in the PCR experiments as the primers obtained were not specific and resulted in multiple bands within the gel, therefore, ChT was omitted from the PCR experiments. Finally, nAChR subunits were not assessed by Western Blot because there are no specific antibodies capable of differentiating between the various nAChR subunits, especially the homomeric subunits.

In terms of validating the Western Blot results obtained, assessing the antibody specificity in cells with conditional knockouts could be performed, although available conditional knockout animals for cholinergic genes is very limited or may not exist. Within the antibodies used, only the VAChT antibody has been previously validated in knockouts whereas the antibodies for AChE, BChE, ChAT and ChT have not. Additionally, different antibodies than

the ones previously used to detect the genes of interest could be utilized to further confirm findings; ideally, antibodies targeting a different epitope of the protein of interest. Both validation methods would further confirm our findings and allow us to make concrete conclusions regarding which cholinergic proteins are present in THP-1 and U937 macrophages.

Next, to evaluate the anti-inflammatory role of silent agonists (p-CF_3 diEPP, m-bromo PEP and m-$CONH_2$ diEPP Iodide), cytokine profiles of stimulated THP-1 and U937 Mo and M1 macrophages were assessed (Figures 14-17). The cultured and differentiated cells were treated with the silent agonist (100 mM) one hour prior to the 8-hour LPS (100 ng/mL) stimulation. The 1-hour pre-treatment with the silent agonist was chosen based on a previous study in our laboratory demonstrating cytokine release after 1-hour and 24-hour silent agonist pretreatment[181]. Ultimately, after 24 hours the anti-inflammatory effect on the silent agonist seems to diminish[181]. The 8-hour stimulation with LPS was chosen based on preliminary data demonstrating the reduction of cytokine release after 9 hours of LPS stimulation. Thus, the 8-hour time point was chosen to study the maximal release of cytokines.

Regarding the THP-1 Mo macrophages (Figure 14), the various silent agonists did not have significant effects on IL-1β and TNF-α release. However, the release of IL-6 was significantly higher in the presence of p-CF_3 diEPP whereas the release of IL-10 was significantly lower in the presence of p-CF_3 diEPP. These results are surprising considering previous findings have demonstrated the anti-inflammatory effects of p-CF_3 diEPP whereby this silent agonist inhibited pro-inflammatory cytokines while having little to no effect on anti-inflammatory cytokines[181]. However, it is important to keep in mind that such findings were observed in human whole blood and that these are the first studies assessing silent agonism in THP-1 and U937 macrophages. Additionally, p-CF_3 diEPP, being α7 and α9 nAChR selective,

does not have anti-inflammatory effects in THP-1 Mo macrophages since our PCR results suggested the lack of α7 and α9 nAChR within these cells.

In THP-1 M1 macrophages (Figure 15), the release of IL-1β secretion was decreased by m-bromo PEP and TNF-α secretion was strongly inhibited by p-CF_3 diEPP. A study by Godin et *al.*, 2020, found that m-bromo PEP protects against autoimmune EAE**,** ultimately diminishing immune cell infiltration into the CNS[180]. Likewise, m-bromo PEP was shown to decrease cytokine release from murine bone marrow (BM) cells[180]. In addition, as previously mentioned, p-CF_3 diEPP was shown to significantly reduce pro-inflammatory cytokine release[181]. Thus, it is not surprising that m-bromo PEP and p-CF_3 diEPP successfully reduced pro-inflammatory cytokine release in THP-1 M1 macrophages. However, since the PCR results suggested the lack of α7 and α9 within these cells, m-bromo PEP and p-CF_3 diEPP may be acting on a different nAChR subunit such as a heteromeric nAChR comprising the α10 subunits. Considering the α7 nAChR subunit was detected in THP-1 M2 macrophages, it is also possible that THP-1 Mo and M1 macrophages do possess the α7 nAChR, but at a much lower concentration.

Regarding U937 Mo macrophages (Figure 16), the silent agonists did not have a significant effect on IL-6, IL-10 and TNF-α secretion. While this may imply a lack of drug efficacy, significant inhibitory effects were observed in U937 M1 macrophages (Figure 17). Being more pro-inflammatory and classically activated, it is possible that U937 M1 macrophages have different downstream signaling and display greater inhibitory effects in the presence of a silent agonist in comparison to Mo macrophages. Likewise, differences in cytokine release after treatment with the silent agonists in THP-1 Mo macrophages in comparison to the THP-1 M1 macrophages would further suggest that downstream signaling mechanisms may differ between the two polarized states. In U937 M1 macrophages, treatments with m-bromo PEP and CONH2

diEPP Iodide showed significant inhibition in IL-6 release. Furthermore, the release of IL-10 was decreased by treatment with p-CF_3 diEPP. Finally, TNF-α release was shown to be inhibited by m-bromo PEP and even more so by p-CF_3 diEPP, reducing its secretion by approximately 50%. As mentioned previously, m-bromo PEP and p-CF_3 diEPP have been reported in previous studies to have anti-inflammatory roles in mouse and human cells[180,181]. Thus, the results obtained in U937 M1 macrophages further confirm the anti-inflammatory effects of p-CF_3 diEPP and m-bromo PEP. In addition, to date, not much is known regarding the anti-inflammatory effects of CONH2 diEPP Iodide. Therefore, this study provides initial insights on its anti-inflammatory role in human macrophages.

Afterwards, to determine the overall viability of THP-1 and U937 macrophages treated with the various silent agonists, after the incubation with the treatments, the cells were stained with DAPI and counted using the Cytation 5 Imaging Reader (Figure 18). Viable macrophages tightly adhere to the surface of the culture plates whereas dead and apoptotic macrophages will typically float in the media. Thus, macrophage division should not have a significant effect on cell count during these experiments. To avoid biases, the Cytation 5 Imaging Reader captured 9 different collated pictures of the cells from each well (each treatment group) and counted the number of stained nuclei in each picture. The cell counts from each treatment group were normalized to the LPS + DMSO control group to determine any significant differences in cell count and ultimately cell viability within the treatment groups. According to Figure 18, no significant differences were observed in the various treatment groups in comparison to the LPS + DMSO control group in THP-1 and U937 macrophages. Hence, the anti-inflammatory effects of the silent agonists observed within THP-1 and U937 macrophages is likely not due to cell death.

Subsequently, to evaluate the effects of acute and chronic pharmacological inhibition on cytokine release, THP-1 and U937 macrophages were differentiated into Mo or M1 macrophages and treated with the various conditions described in section 2.2.2. In chronic conditions, the cells were treated with the various treatment groups during the 48-hour polarization step. The cells were treated with the various treatment groups first, then stimulated with LPS (10 ng/mL) for 5 hours. The 5-hour stimulation time point was chosen to be able to compare our data to similar experiments currently being carried out by our collaborators. Originally, 100 ng/mL of LPS instead of 10 ng/mL was used in the experiments, but in the chronic treatments, 100 ng/mL resulted in an increase in cell death and the concentration was therefore reduced to 10 ng/mL for both acute and chronic treatments. Cell supernatants were collected, and cytokine release was assessed via CBAs. Additionally, it is important to note that U937 macrophages did not release detectable amounts of IL-1β, thus, this cytokine was not assessed in these cells. Overall, under acute and chronic pharmacological conditions, ML352, Nic, p-CF_3 diEPP and α-NETA had the most significant effects on cytokine release.

First, under acute settings (Figures 19-22), ML352 significantly inhibited all 4 cytokines in THP-1 Mo macrophages, IL-10 in THP-1 M1 macrophages, IL-6 and IL-10 in U937 Mo macrophages and finally, IL-10 and TNF-α in U937 M1 macrophages. In contrast, under chronic treatments (Figures 24-27), ML352 only inhibited IL-1β in THP-1 Mo macrophages, IL-6 and IL-10 in U937 Mo macrophages and IL-6 in U937 M1 macrophages. ML352 is a noncompetitive inhibitor of ChT, therefore inhibiting the rate-limiting step in ACh synthesis[215]. Since ACh is known for its anti-inflammatory properties, mainly by binding to nAChRs[216], inhibiting its synthesis should theoretically increase inflammatory responses. However, our cytokine data suggest a more anti-inflammatory role. Based on our Western Blot results, ChT did not seem to

be expressed in THP-1 and U937 macrophages, thus, it is possible that ML352 may have some off target effects that, in the absence of ChT, promote an anti-inflammatory response. The potency and specificity of ML352 was studied by Ennis et *al.*[215], in which they demonstrated some off-target interactions of ML352 against 68 G-protein couple receptors, ion channels, and transporters. In fact, inhibitory effects (12 – 32 % inhibition) in nAChRs and muscarinic M1-M3 receptors were confirmed. The inhibition of nAChRs and muscarinic receptors (mAChRs) have previously been associated with anti-inflammatory effects in various cell types[217,218], which may account for the anti-inflammatory effect observed upon treatment with ML352. In addition, it is also possible that inhibiting ChT and preventing Ch uptake, increases Ch levels resulting in an anti-inflammatory effect via Ch binding to nAChRs.

Next, nicotine did not have any significant effects on cytokine release in acute settings, but under chronic conditions, inhibited TNF-α in THP-1 Mo macrophages, IL-6, IL-10 and TNF-α in U937 Mo macrophages and IL-10 in U937 M1 macrophages. Nicotine also significantly increased IL-1β in THP-1 M1 macrophages. Therefore, under chronic treatments, nicotine displayed both pro-inflammatory effects (by the increase of IL-1β release and inhibition of anti-inflammatory cytokine (IL-10)) and anti-inflammatory effects (by the inhibition pro-inflammatory cytokines). Nicotine is a major constituent of cigarette smoke, capable of suppressing inflammatory responses and attenuating the symptoms of EAE[172,219]. Likewise, many studies have shown the inhibitory effects of TNF-α release from mononuclear cells while also increasing secretion of IL-10[220]. The cytokine data obtained in THP-1 macrophages are similar to such findings in which TNF-α was significantly reduced in THP-1 Mo macrophages whereas IL-10 release seemed to be higher, although not statistically significant. Interestingly, AlQasrawi *et al.*[220] also showed that although nicotine has anti-inflammatory effects in nicotine

pre-treated cells, in LPS pre-stimulated cells, the administration of nicotine has opposite effects, heightening inflammatory cytokine release. Thus, such findings would explain why inhibitory effects are only seen in chronic treatments and not in acute treatments.

Moreover, treatments of p-CF_3 diEPP showed very significant inhibitory effects in cytokine release from acutely and chronically treated macrophages. More specifically, under acute conditions, p-CF_3 diEPP significantly inhibited the release of IL-1β in THP-1 Mo macrophages and IL-1β and TNF-α in THP-1 M1 macrophages. Similarly, under chronic conditions, p-CF_3 diEPP significantly inhibited IL-1β from both THP-1 Mo and M1 macrophages. In chronic treatments, p-CF_3 diEPP also inhibited IL-6, IL-10 and TNF-α in U937 Mo macrophages as well as IL-6 and IL-10 in U937 M1 macrophages. Hence, p-CF_3 diEPP displayed anti-inflammatory properties by inhibiting various pro-inflammatory cytokines, which seems to be more pronounced in cells treated chronically with p-CF_3 diEPP. As previously mentioned, studies have shown the anti-inflammatory effects of p-CF_3 diEPP[181], therefore its ability to inhibit various pro-inflammatory cytokines was not surprising. However, the inhibitory effects in IL-10 release in U937 macrophages was surprising considering previous studies have demonstrated that p-CF_3 diEPP, while able to inhibit pro-inflammatory cytokines, has little to no effect on anti-inflammatory cytokines[181]. Such findings were observed in human whole blood; thus, it is possible that p-CF_3 diEPP can inhibit most cytokines in U937 macrophages. In fact, human whole blood differs from U937 macrophages as it contains many other cells than simply macrophages, such as red blood cells, various other white blood cells (granulocytes, T and B cells, etc.) and platelets. Thus, it is possible that p-CF_3 diEPP inhibits IL-10 release in macrophages but its increase in whole blood, is likely due to the presence of other cell types such as T cells.

The effects of p-CF_3 diEPP treatment from acutely and chronically treated macrophages differ from the silent agonist experiments previously described where cells were pre-treated with p-CF_3 diEPP for 1-hour, followed by an 8-hour LPS stimulation. The differences in cytokine release observed could be due to many factors including LPS concentration, silent-agonist pretreatment, and treatment time. First, acutely and chronically treated macrophages were only stimulated with 10 ng/mL of LPS whereas in the silent agonist experiments, 100 ng/mL of LPS was used to stimulate the cells. This change in LPS concentration, as mentioned above, was due to increased cell death seen in chronically treated macrophages. The differences in LPS concentration can influence immune cell phenotype, as THP-1 and U937 cell lines polarize into M1 macrophages in the presence of LPS. It is possible that an increase in LPS concentration can lead to increased polarization and ultimately, differences in cytokine profiles. Second, during the silent agonist experiments, the macrophages were pre-treated for 1-hour with the silent agonists whereas in the acute and chronic treatments, the macrophages were not. Hence, the silent agonist pre-treatment may influence the release of cytokines from the cells. Finally, the treatment time of the silent agonist differed. In the silent agonists experiment, the macrophages were treated with p-CF_3 diEPP for a total of 9 hours, whereas in acute and chronic experiments, the cells were treated with p-CF_3 diEPP for 5 hours and 48 hours + 5 hours, respectively. Thus, the various treatment times of p-CF_3 diEPP could also have an influence on overall cytokine release.

The acute and chronic treatment of α-NETA in THP-1 and U937 was additionally assessed. α-NETA is a commercially available ChAT inhibitor, capable of inhibiting ChAT at 93% inhibition[221] while have little to no effect on AChE and BChE. ChAT is the enzyme responsible for ACh synthesis, thus its inhibition would result in a reduction of ACh production and overall, an increase in immune responses[191]. Therefore, a more pro-inflammatory effect is

expected in cells treated with α-NETA. Our cytokine data suggests both a pro-inflammatory and anti-inflammatory effect in THP-1 and U937 macrophages. In acute treatments, α-NETA inhibited the release of IL-1β and IL-10 in THP-1 Mo macrophages as well as IL-1β in THP-1 M1 macrophages. In chronic treatments, α-NETA inhibited the release of IL-1β in THP-1 Mo and M1 macrophages while also significantly inhibiting IL-10 release in all cells. Additionally, α-NETA also seemed to increase TNF-α in all macrophages, though this was not shown to be statistically significant. Therefore, although inhibition of ChAT resulted in anti-inflammatory effects by inhibiting IL-1β in THP-1 macrophages, it also had pro-inflammatory effects by increasing the release of TNF-α and by also inhibiting the release of IL-10. Thus, the net outcome of α-NETA treatments remains unclear.

Finally, all other acute and chronic treatment groups (ACh, Gal and Ch) did not have much of an effect on cytokine release in comparison to the other treatment groups described above. First, ACh was assessed to determine its effect as an agonist to AChRs, both in the presence and absence of an AChE inhibitor, Gal. ACh is known for its anti-inflammatory role, mainly by binding to the α7 nAChR and preventing the release of pro-inflammatory cytokines[216]. Gal was used to prevent the breakdown of ACh by AChE, further increasing anti-inflammatory responses. However, our cytokine data only show slight anti-inflammatory effects in the presence of ACh and Gal. In ACh-only treated macrophages, IL-6 release was inhibited in acutely treated U937 Mo macrophages whereas IL-10 release was increased in chronically treated THP-1 M1 macrophages. In the presence of both ACh and Gal, IL-6 release was once again inhibited in acutely treated U937 Mo macrophages whereas TNF-α was inhibited in chronically treated THP-1 Mo macrophages. Lastly, in Gal-only treated macrophages, the only significant effect was the inhibition of IL-1β in chronically treated THP-1 Mo macrophages.

Since many studies have demonstrated ACh's anti-inflammatory properties, ACh was expected to have greater anti-inflammatory effects than those observed, especially in the presence of an AChE inhibitor. Considering our Western Blot and PCR results suggest the presence of BChE in THP-1 and U937 macrophages, it is possible that BChE is further degrading ACh, decreasing its ability to bind to AChRs and overall, reducing its anti-inflammatory capabilities. Therefore, in future studies, a BChE inhibitor should also be included to ensure no ACh is being degraded. Furthermore, the lack of α7 nAChR mRNA observed in the THP-1 and U937 macrophages could influence the overall anti-inflammatory effect of ACh within these cells, especially considering many studies suggest ACh's anti-inflammatory effect is produced by binding to the α7 subunit[155,161,189,218]. Finally, though ACh is capable of binding α7 nAChRs and produce anti-inflammatory effects, it may also bind mAChRs and induce pro-inflammatory effects. Hence, the inflammatory effect observed upon ACh treatment may depend on which receptor it interacts with.

The treatment of another AChR agonist, Ch, was additionally assessed in acute and chronic treatments in THP-1 and U937 macrophages. Similar to ACh, Ch did not have significant effects on cytokine release. In fact, according to our cytokine data, Ch only inhibited IL-10 in U937 M1 macrophages, thus having a more pro-inflammatory effect in these cells. These results were unexpected since, in various studies, Ch has been shown to bind to the α7 nAChR and produce anti-inflammatory effects[222–224]. As previously described for ACh, the lack of α7 nAChR mRNA observed in the THP-1 and U937 macrophages could also influence the overall anti-inflammatory effect of Ch within these cells. Interestingly, a study also demonstrated that Ch at a concentration of 50 mM had the most significant effect on TNF-α release in human whole blood and 1mM in human macrophages. Therefore, future studies with high Ch treatments

could be implemented to further assess Ch's anti-inflammatory roles in THP-1 and U937 macrophages[170].

Afterwards, the cytotoxicity of THP-1 and U937 macrophages treated with acute (Figure 23) and chronic (Figure 28) pharmacological treatments was assessed. After incubation with the various treatments, the collection of cell supernatant required for cytokine profiling was also used in an LDH cytotoxicity assay. The LDH measurements from each sample were analyzed using a fluorescent LDH cytotoxicity assay and the fluorescence was measured using the Cytation 5 imaging reader. Upon cell death, LDH is released from the cells and is therefore a good representation of overall cellular cytotoxicity. According to Figure 23, no significant differences in cytotoxicity were observed in comparison to the LPS + DMSO control group in acute treatments of THP-1 and U937 macrophages. However, in chronic treatments (Figure 28), the cytotoxicity levels of THP-1 Mo treated with p-CF_3 diEPP was significantly lower in comparison to the LPS + DMSO group. The decrease in cytotoxicity in p-CF_3 diEPP could account for some of its anti-inflammatory effect previously described. Overall, in all differentiated THP-1 and U937 macrophages (Mo and M1), p-CF_3 diEPP was the only treatment to have significantly lower cytotoxicity in THP-1 Mo macrophages. Hence, the anti-inflammatory effects of the acute and chronic pharmacological treatments observed within THP-1 and U937 macrophages is likely not due to cell death.

Lastly, the relative normalized expression (normalized to LPS or LPS + DMSO group) of cell markers in THP-1 and U937 macrophages upon chronic treatments of agonists (Ach, Ch, Nic and p-CF_3 diEPP) and cholinergic inhibitors (Gal, ML352 and α-NETA) in the presence of LPS were additionally assessed (Figures 29-32). To determine the mRNA expression of cell markers, RNA was isolated from the treated/stimulated macrophages and a qPCR with primers targeting

various markers were utilized. As previously discussed, M1 and M2 polarized macrophages have distinguishing features, one of them being their expression of cell markers. M1 macrophages typically have higher expression of CD80, and CXCL10. On the contrary, M2 macrophages typically have a higher expression of MRC1 (CD206) and CD163. Other general macrophage / monocyte markers include CCR2, CD14, ITGAM (CD11b) and CX3CR1.

Amongst the cell markers assessed, only CCR2, CD80, CX3CR1 and CXCL10 showed significant effects upon the various chronic pharmacological treatments. First, CCR2, a monocyte / macrophage marker, was more highly expressed in the untreated group of THP-1 Mo and M1 macrophages, in comparison to the LPS treated group. These results were unexpected considering, as a monocyte / macrophage marker, it was not expected to be significantly influenced by LPS. However, a study by Phillips *et al*. showed that THP-1 undifferentiated cells express very high levels of CCR2 which is diminished upon THP-1 differentiation into macrophages[225]. Since LPS is known to polarize THP-1 macrophages into a more M1 state, perhaps its further differentiation promotes more macrophage-like features and reduces CCR2 levels. In addition, a study by Parker *et al*. also found that activation of the TLR4 (by LPS) in THP-1 monocytes, down-regulated CCR2 expression[226]. Such findings align with our CCR2 expression data which demonstrates the reduction of CCR2 expression upon LPS treatments in THP-1 macrophages.

Secondly, the expression of CD80 and CXCL10 were shown to be significantly lower in most of the untreated group in comparison to the LPS-treated group. Considering both markers are generally more expressed by M1 macrophages and that LPS is often used to polarize the macrophages into an M1 state, it is not surprising that CD80 expression increases upon LPS treatment.

Lastly, the expression of CX3CR1 was assessed and was significantly higher in the untreated groups of THP-1 Mo and M1 macrophages, in comparison to the LPS group. It is also important to note that U937 derived macrophages failed to express detectable amounts of CX3CR1 mRNA. The increase in CX3CR1 expression in THP-1 macrophages was once again not expected to be significantly influenced by LPS. As not many studies have focused on CX3CR1 expression and LPS, the reason for this effect remains unclear. Although, Montague *et al*. suggested a novel interaction between CX3CR1 and CCR2 in monocytes and its role in a model of pain[227]. Perhaps the increase in CCR2 expression previously described, also leads to the increase in CX3CR1 expression.

The expression level of cell markers was expected to be significantly different in some treatment groups in comparison to the LPS / LPS + DMSO control group, however this was not the case. Since treatment groups like nicotine, ML352, p-CF_3 diEPP and α-NETA inhibited cytokine release in the differentiated macrophages, it was hypothesized that they would have also altered cell marker levels. For example, since p-CF_3 diEPP showed anti-inflammatory properties by inhibiting cytokines, it was expected that p-CF_3 diEPP would increase anti-inflammatory markers (M2) and decrease pro-inflammatory markers (M1). However, based on the data obtained, the altered cytokine secretion seen is likely due to direct effects of agonists and cholinergic inhibitors on cytokine secretion, and not due to changes in polarization state. Interestingly, one study demonstrated that nicotine dose-dependently induced M2 macrophage polarization in vitro starting at 2 µg/mL for 24 hours in resting macrophages[220]. However, in *Mycobacterium avium* subspecies *paratuberculosis* (MAP)-infected macrophages, nicotine did not have significant effects on cell markers and did not induce M2 macrophage polarization[220]. Therefore, it would be of interest to study the treatment groups both in the presence and the

absence of LPS to further confirm their ability to induce macrophage polarization. In addition, since LPS is known to induce M1 macrophage polarization in THP-1 and U937 cells, it would be interesting to stimulate the cells with another immune stimulant that is not commonly used for macrophage polarization.

Our initial proposal to study cell surface markers was to use fluorescent antibodies against the cell markers of interest and quantify the expression levels using flow cytometry. However, the differentiated macrophages were very strongly adhered to the culture plates making them extremely difficult to remove, even with trypsin. Since most of the cell markers of interest are cell surface receptors, scraping the cells would result in significant damage to the cell surface markers, affecting our overall results. Thus, we decided to quantify the cell markers using qPCRs. If perhaps a new strategy to remove the macrophages safely from the plates was determined, it would be of interest to validate our results using fluorescent antibodies and the flow cytometer. Additionally, another method to quantify and validate the results obtained by qPCR would be via Western Blot.

Conclusion

Taken together, this study provides insights on various cholinergic proteins (AChE, BChE, ChT, ChAT, VAChT, nAChRs) expressed by THP-1 and U937 macrophages. This study also reports for the first time the anti-inflammatory effects of nAChR silent agonism (p-CF_3 diEPP, m-bromo PEP, m-$CONH_2$ Iodide) in LPS-stimulated THP-1 and U937 differentiated macrophages. Furthermore, our findings demonstrate anti-inflammatory and pro-inflammatory effects of various nAChR agonist (Ach, Ch, Nic and p-CF_3 diEPP) and cholinergic inhibitors (Gal, ML352 and α-NETA) in LPS-stimulated THP-1 and U937 macrophages. More specifically, nicotine, ChT inhibition and silent agonism seems to have the most significant anti-inflammatory effect whereas ChAT inhibition seems to have the most significant pro-inflammatory effect in the differentiated macrophages. While the chronic pharmacological treatments were not shown to significantly influence cell marker expression, further optimization will allow for a better interpretation.

Despite findings obtained in this study, much work is still required. Our Western Blot and PCR data should be further validated in conditional knock-out cells to validate primer and antibody specificity. Furthermore, once experiments assessing cell marker expression in the presence of pharmacological treatment has been optimized, future studies investigating intracellular signaling events in the presence of the pharmacological treatments should be carried out. This would provide further insights on how exactly the pharmacological treatments influence cytokine release from the cells. The results presented in this study provides further insights on the functional role of the cholinergic system within immune cells and reveal the potential of nAChR silent agonism for pharmacological treatment of auto-immune diseases.

References

1. Charles A Janeway, J., Travers, P., Walport, M. & Shlomchik, M. J. Principles of innate and adaptive immunity. in *Immunology: The Immune System in Health and Disease* (2001).
2. Marshall, J. S., Warrington, R., Watson, W. & Kim, H. L. An introduction to immunology and immunopathology. *Allergy Asthma Clin Immunol* **14**, (2018).
3. Sattler, S. The Role of the Immune System Beyond the Fight Against Infection. *Adv Exp Med Biol* **1003**, 3–14 (2017).
4. Iwasaki, A. & Medzhitov, R. Control of adaptive immunity by the innate immune system. *Nat Immunol* **16**, 343–353 (2015).
5. Akira, S., Uematsu, S. & Takeuchi, O. Pathogen recognition and innate immunity. *Cell* **124**, 783–801 (2006).
6. Medzhitov, R. & Janeway, C. Innate immunity. *N Engl J Med* **343**, 338–344 (2000).
7. Li, D. & Wu, M. Pattern recognition receptors in health and diseases. *Sig Transduct Target Ther* **6**, 1–24 (2021).
8. Turvey, S. E. & Broide, D. H. Chapter 2: Innate Immunity. *J Allergy Clin Immunol* **125**, S24–S32 (2010).
9. Wynn, T. A., Chawla, A. & Pollard, J. W. Macrophage biology in development, homeostasis and disease. *Nature* **496**, 445–455 (2013).
10. Murray, P. J. & Wynn, T. A. Protective and pathogenic functions of macrophage subsets. *Nat Rev Immunol* **11**, 723–737 (2011).
11. Gordon, S. The macrophage: past, present and future. *Eur J Immunol* **37 Suppl 1**, S9-17 (2007).

12. Taylor, P. R. *et al.* Macrophage receptors and immune recognition. *Annu Rev Immunol* **23**, 901–944 (2005).
13. Martinez, F. O., Helming, L. & Gordon, S. Alternative activation of macrophages: an immunologic functional perspective. *Annu Rev Immunol* **27**, 451–483 (2009).
14. Van Dyken, S. J. & Locksley, R. M. Interleukin-4- and interleukin-13-mediated alternatively activated macrophages: roles in homeostasis and disease. *Annu Rev Immunol* **31**, 317–343 (2013).
15. Mosser, D. & Edwards, J. Exploring the full spectrum of macrophage activation | Nature Reviews Immunology. *Nature Reviews Immunology* **8**, 958–969 (2008).
16. Mishra, M. K. & Yong, V. W. Myeloid cells - targets of medication in multiple sclerosis. *Nat Rev Neurol* **12**, 539–551 (2016).
17. Laskin, D. L., Sunil, V. R., Gardner, C. R. & Laskin, J. D. Macrophages and tissue injury: agents of defense or destruction? *Annu Rev Pharmacol Toxicol* **51**, 267–288 (2011).
18. Mittal, M., Siddiqui, M. R., Tran, K., Reddy, S. P. & Malik, A. B. Reactive Oxygen Species in Inflammation and Tissue Injury. *Antioxid Redox Signal* **20**, 1126–1167 (2014).
19. Bertani, F. R. *et al.* Classification of M1/M2-polarized human macrophages by label-free hyperspectral reflectance confocal microscopy and multivariate analysis. *Sci Rep* **7**, 8965 (2017).
20. Surdziel, E. *et al.* Multidimensional pooled shRNA screens in human THP-1 cells identify candidate modulators of macrophage polarization. *PLoS One* **12**, (2017).
21. Wheeler, K. C. *et al.* VEGF may contribute to macrophage recruitment and M2 polarization in the decidua. *PLoS One* **13**, (2018).

22. Xuan, W., Qu, Q., Zheng, B., Xiong, S. & Fan, G.-H. The chemotaxis of M1 and M2 macrophages is regulated by different chemokines. *J Leukoc Biol* **97**, 61–69 (2015).
23. Moehle, M. S. & West, A. B. M1 and M2 Immune Activation in Parkinson's Disease: Foe and Ally? *Neuroscience* **302**, 59–73 (2015).
24. Lu, J. *et al.* Discrete functions of M2a and M2c macrophage subsets determine their relative efficacy in treating chronic kidney disease. *Kidney Int* **84**, 745–755 (2013).
25. Fiorentino, D. F., Bond, M. W. & Mosmann, T. R. Two types of mouse T helper cell. IV. Th2 clones secrete a factor that inhibits cytokine production by Th1 clones. *J Exp Med* **170**, 2081–2095 (1989).
26. Glocker, E.-O. *et al.* Inflammatory bowel disease and mutations affecting the interleukin-10 receptor. *N Engl J Med* **361**, 2033–2045 (2009).
27. Rőszer, T. Understanding the Mysterious M2 Macrophage through Activation Markers and Effector Mechanisms. *Mediators of Inflammation* **2015**, e816460 (2015).
28. Tan, H.-Y. *et al.* The Reactive Oxygen Species in Macrophage Polarization: Reflecting Its Dual Role in Progression and Treatment of Human Diseases. *Oxid Med Cell Longev* **2016**, (2016).
29. Genin, M., Clement, F., Fattaccioli, A., Raes, M. & Michiels, C. M1 and M2 macrophages derived from THP-1 cells differentially modulate the response of cancer cells to etoposide. *BMC Cancer* **15**, 577 (2015).
30. Morón Calvente, V. *Inhibitor of apoptosis proteins (IAPs) expression in monocyte to macrophage differentiation and M1/M2 polarization*. (Universidad de Granada, 2018).
31. Zhang, J.-M. & An, J. Cytokines, Inflammation and Pain. *Int Anesthesiol Clin* **45**, 27–37 (2007).

32. Dinarello, C. A. Immunological and inflammatory functions of the interleukin-1 family. *Annu Rev Immunol* **27**, 519–550 (2009).

33. Turner, M. D., Nedjai, B., Hurst, T. & Pennington, D. J. Cytokines and chemokines: At the crossroads of cell signalling and inflammatory disease. *Biochim Biophys Acta* **1843**, 2563–2582 (2014).

34. Meng, F. & Lowell, C. A. Lipopolysaccharide (LPS)-induced Macrophage Activation and Signal Transduction in the Absence of Src-Family Kinases Hck, Fgr, and Lyn. *J Exp Med* **185**, 1661–1670 (1997).

35. Wright, S. D., Ramos, R. A., Tobias, P. S., Ulevitch, R. J. & Mathison, J. C. CD14, a receptor for complexes of lipopolysaccharide (LPS) and LPS binding protein. *Science* **249**, 1431–1433 (1990).

36. Pålsson-McDermott, E. M. & O'Neill, L. A. J. Signal transduction by the lipopolysaccharide receptor, Toll-like receptor-4. *Immunology* **113**, 153–162 (2004).

37. Caldwell, A. B., Cheng, Z., Vargas, J. D., Birnbaum, H. A. & Hoffmann, A. Network dynamics determine the autocrine and paracrine signaling functions of TNF. *Genes Dev.* **28**, 2120–2133 (2014).

38. Stillie, R. & Stadnyk, A. W. Role of TNF receptors, TNFR1 and TNFR2, in dextran sodium sulfate-induced colitis: *Inflammatory Bowel Diseases* **15**, 1515–1525 (2009).

39. Parameswaran, N. & Patial, S. Tumor Necrosis Factor-α Signaling in Macrophages. *Crit Rev Eukaryot Gene Expr* **20**, 87–103 (2010).

40. Bradley, J. R. TNF-mediated inflammatory disease. *J Pathol* **214**, 149–160 (2008).

41. Jücker, M. *et al.* Expression of interleukin-6 and interleukin-6 receptor in Hodgkin's disease. *Blood* **77**, 2413–2418 (1991).

42. Kishimoto, T. IL-6: from its discovery to clinical applications. *Int Immunol* **22**, 347–352 (2010).
43. Peters, M., Müller, A. M. & Rose-John, S. Interleukin-6 and soluble interleukin-6 receptor: direct stimulation of gp130 and hematopoiesis. *Blood* **92**, 3495–3504 (1998).
44. Taga, T. & Kishimoto, T. Gp130 and the interleukin-6 family of cytokines. *Annu Rev Immunol* **15**, 797–819 (1997).
45. Goette, N. P. *et al.* Abnormal regulation of soluble and anchored IL-6 receptor in monocytes from patients with essential thrombocythemia. *Exp Hematol* **38**, 868-876.e1 (2010).
46. Arend, W. P., Palmer, G. & Gabay, C. IL-1, IL-18, and IL-33 families of cytokines. *Immunol Rev* **223**, 20–38 (2008).
47. Lopez-Castejon, G. & Brough, D. Understanding the mechanism of IL-1β secretion. *Cytokine Growth Factor Rev* **22**, 189–195 (2011).
48. Murray, M. F. Chapter 39 - Susceptibility and Response to Infection. in *Emery and Rimoin's Principles and Practice of Medical Genetics* (eds. Rimoin, D., Pyeritz, R. & Korf, B.) 1–24 (Academic Press, 2013). doi:10.1016/B978-0-12-383834-6.00047-1.
49. Kaneko, N., Kurata, M., Yamamoto, T., Morikawa, S. & Masumoto, J. The role of interleukin-1 in general pathology. *Inflammation and Regeneration* **39**, 12 (2019).
50. Peters, V. A., Joesting, J. J. & Freund, G. G. IL-1 receptor 2 (IL-1R2) and its role in immune regulation. *Brain Behav Immun* **32**, 1–8 (2013).
51. Iyer, S. S. & Cheng, G. Role of Interleukin 10 Transcriptional Regulation in Inflammation and Autoimmune Disease. *Crit Rev Immunol* **32**, 23–63 (2012).
52. Srinivasan, L., Harris, M. C. & Kilpatrick, L. E. 128 - Cytokines and Inflammatory Response in the Fetus and Neonate. in *Fetal and Neonatal Physiology (Fifth Edition)* (eds. Polin, R.

A., Abman, S. H., Rowitch, D. H., Benitz, W. E. & Fox, W. W.) 1241-1254.e4 (Elsevier, 2017). doi:10.1016/B978-0-323-35214-7.00128-1.

53. Aristizábal, B. & González, Á. *Innate immune system*. *Autoimmunity: From Bench to Bedside [Internet]* (El Rosario University Press, 2013).
54. Chen, L. *et al.* Inflammatory responses and inflammation-associated diseases in organs. *Oncotarget* **9**, 7204–7218 (2017).
55. Abdulkhaleq, L. A. *et al.* The crucial roles of inflammatory mediators in inflammation: A review. *Vet World* **11**, 627–635 (2018).
56. Weiss, U. Inflammation. *Nature* **454**, 427 (2008).
57. Information, N. C. for B., Pike, U. S. N. L. of M. 8600 R., MD, B. & Usa, 20894. *The innate and adaptive immune systems*. *InformedHealth.org [Internet]* (Institute for Quality and Efficiency in Health Care (IQWiG), 2020).
58. Bonilla, F. A. & Oettgen, H. C. Adaptive immunity. *J Allergy Clin Immunol* **125**, S33-40 (2010).
59. Alberts, B. *et al.* The Adaptive Immune System. *Molecular Biology of the Cell. 4th edition* (2002).
60. Kondělková, K. *et al.* Regulatory T cells (TREG) and their roles in immune system with respect to immunopathological disorders. *Acta Medica (Hradec Kralove)* **53**, 73–77 (2010).
61. Kumar, B. V., Connors, T. & Farber, D. L. Human T cell development, localization, and function throughout life. *Immunity* **48**, 202–213 (2018).
62. Alberts, B. *et al.* B Cells and Antibodies. *Molecular Biology of the Cell. 4th edition* (2002).
63. Smith, D. A. & Germolec, D. R. Introduction to immunology and autoimmunity. *Environ Health Perspect* **107**, 661–665 (1999).

64. Rosenblum, M. D., Remedios, K. A. & Abbas, A. K. Mechanisms of human autoimmunity. *J Clin Invest* **125**, 2228–2233 (2015).

65. Buckner, J. H. Mechanisms of impaired regulation by CD4(+)CD25(+)FOXP3(+) regulatory T cells in human autoimmune diseases. *Nat Rev Immunol* **10**, 849–859 (2010).

66. Kukreja, A. *et al.* Multiple immuno-regulatory defects in type-1 diabetes. *J Clin Invest* **109**, 131–140 (2002).

67. Miyara, M. *et al.* Global natural regulatory T cell depletion in active systemic lupus erythematosus. *J Immunol* **175**, 8392–8400 (2005).

68. Zhang, W., Rho, J., Roehrl, M. W., Roehrl, M. H. & Wang, J. Y. A repertoire of 124 potential autoantigens for autoimmune kidney diseases identified by dermatan sulfate affinity enrichment of kidney tissue proteins. *PLOS ONE* **14**, e0219018 (2019).

69. 't Hart, B. A., Luchicchi, A., Schenk, G. J., Killestein, J. & Geurts, J. J. G. Multiple sclerosis and drug discovery: A work of translation. *EBioMedicine* **68**, 103392 (2021).

70. Vidal-Jordana, A. & Montalban, X. Multiple Sclerosis: Epidemiologic, Clinical, and Therapeutic Aspects. *Neuroimaging Clin. N. Am.* **27**, 195–204 (2017).

71. Ghasemi, N., Razavi, S. & Nikzad, E. Multiple Sclerosis: Pathogenesis, Symptoms, Diagnoses and Cell-Based Therapy. *Cell J* **19**, 1–10 (2017).

72. Wasserman, A. M. Diagnosis and Management of Rheumatoid Arthritis. *Rheumatoid Arthritis* **84**, 8 (2011).

73. Silman, A. J. & Pearson, J. E. Epidemiology and genetics of rheumatoid arthritis. *Arthritis Res* **4**, S265–S272 (2002).

74. Li, P., Zheng, Y. & Chen, X. Drugs for Autoimmune Inflammatory Diseases: From Small Molecule Compounds to Anti-TNF Biologics. *Front Pharmacol* **8**, (2017).

75. Laine, L. Approaches to nonsteroidal anti-inflammatory drug use in the high-risk patient. *Gastroenterology* **120**, 594–606 (2001).

76. Simmons, D. L., Botting, R. M. & Hla, T. Cyclooxygenase isozymes: the biology of prostaglandin synthesis and inhibition. *Pharmacol Rev* **56**, 387–437 (2004).

77. Fujita, T., Kutsumi, H., Sanuki, T., Hayakumo, T. & Azuma, T. Adherence to the preventive strategies for nonsteroidal anti-inflammatory drug- or low-dose aspirin-induced gastrointestinal injuries. *J Gastroenterol* **48**, 559–573 (2013).

78. Murray, M. D. & Brater, D. C. Renal toxicity of the nonsteroidal anti-inflammatory drugs. *Annu Rev Pharmacol Toxicol* **33**, 435–465 (1993).

79. Ray, W. A. *et al.* COX-2 selective non-steroidal anti-inflammatory drugs and risk of serious coronary heart disease. *Lancet* **360**, 1071–1073 (2002).

80. Hermann, M. & Ruschitzka, F. Coxibs, non-steroidal anti-inflammatory drugs and cardiovascular risk. *Intern Med J* **36**, 308–319 (2006).

81. Barnes, P. J. Anti-inflammatory actions of glucocorticoids: molecular mechanisms. *Clin Sci (Lond)* **94**, 557–572 (1998).

82. Ethgen, O., de Lemos Esteves, F., Bruyere, O. & Reginster, J.-Y. What do we know about the safety of corticosteroids in rheumatoid arthritis? *Curr Med Res Opin* **29**, 1147–1160 (2013).

83. Giovannoni, G. Disease-modifying treatments for early and advanced multiple sclerosis: a new treatment paradigm. *Curr Opin Neurol* **31**, 233–243 (2018).

84. Markowitz, C. E. Interferon-beta: mechanism of action and dosing issues. *Neurology* **68**, S8-11 (2007).

85. Tabas, I. & Glass, C. K. Anti-inflammatory therapy in chronic disease: challenges and opportunities. *Science* **339**, 166–172 (2013).
86. Guarnera, C., Bramanti, P. & Mazzon, E. Alemtuzumab: a review of efficacy and risks in the treatment of relapsing remitting multiple sclerosis. *Ther Clin Risk Manag* **13**, 871–879 (2017).
87. Walther, E. U. & Hohlfeld, R. Multiple sclerosis: side effects of interferon beta therapy and their management. *Neurology* **53**, 1622–1627 (1999).
88. Cohan, S. L., Lucassen, E. B., Romba, M. C. & Linch, S. N. Daclizumab: Mechanisms of Action, Therapeutic Efficacy, Adverse Events and Its Uncovering the Potential Role of Innate Immune System Recruitment as a Treatment Strategy for Relapsing Multiple Sclerosis. *Biomedicines* **7**, 18 (2019).
89. Guo, Q. *et al.* Rheumatoid arthritis: pathological mechanisms and modern pharmacologic therapies. *Bone Res* **6**, (2018).
90. Navegantes, K. C. *et al.* Immune modulation of some autoimmune diseases: the critical role of macrophages and neutrophils in the innate and adaptive immunity. *Journal of Translational Medicine* **15**, 36 (2017).
91. Circu, M. L. & Aw, T. Y. Reactive oxygen species, cellular redox systems, and apoptosis. *Free Radic Biol Med* **48**, 749–762 (2010).
92. Neeli, I., Dwivedi, N., Khan, S. & Radic, M. Regulation of extracellular chromatin release from neutrophils. *J Innate Immun* **1**, 194–201 (2009).
93. Wegner, N. *et al.* Autoimmunity to specific citrullinated proteins gives the first clues to the etiology of rheumatoid arthritis. *Immunological Reviews* **233**, 34–54 (2010).

94. Herz, J., Filiano, A. J., Smith, A., Yogev, N. & Kipnis, J. Myeloid Cells in the Central Nervous System. *Immunity* **46**, 943–956 (2017).

95. Henderson, A. P. D., Barnett, M. H., Parratt, J. D. E. & Prineas, J. W. Multiple sclerosis: distribution of inflammatory cells in newly forming lesions. *Ann Neurol* **66**, 739–753 (2009).

96. Brück, W. *et al.* Macrophages in multiple sclerosis. *Immunobiology* **195**, 588–600 (1996).

97. Gordon, S. & Plüddemann, A. Chapter 11 - Role of Macrophages in Autoimmunity. in *The Autoimmune Diseases (Fifth Edition)* (eds. Rose, N. R. & Mackay, I. R.) 161–174 (Academic Press, 2014). doi:10.1016/B978-0-12-384929-8.00011-3.

98. Mikita, J. *et al.* Altered M1/M2 activation patterns of monocytes in severe relapsing experimental rat model of multiple sclerosis. Amelioration of clinical status by M2 activated monocyte administration. *Mult Scler* **17**, 2–15 (2011).

99. Maurer, S. V. & Williams, C. L. The Cholinergic System Modulates Memory and Hippocampal Plasticity via Its Interactions with Non-Neuronal Cells. *Front. Immunol.* **8**, (2017).

100. Black, S. A. G. & Rylett, R. J. Choline transporter CHT regulation and function in cholinergic neurons. *Cent Nerv Syst Agents Med Chem* **12**, 114–121 (2012).

101. Lee, N.-Y., Choi, H.-M. & Kang, Y.-S. Choline transport via choline transporter-like protein 1 in conditionally immortalized rat syncytiotrophoblast cell lines TR-TBT. *Placenta* **30**, 368–374 (2009).

102. Fisher, S. K. & Wonnacott, S. Chapter 13 - Acetylcholine. in *Basic Neurochemistry (Eighth Edition)* (eds. Brady, S. T., Siegel, G. J., Albers, R. W. & Price, D. L.) 258–282 (Academic Press, 2012). doi:10.1016/B978-0-12-374947-5.00013-4.

103. Tiwari, P., Dwivedi, S., Singh, M. P., Mishra, R. & Chandy, A. Basic and modern concepts on cholinergic receptor: A review. *Asian Pac J Trop Dis* **3**, 413–420 (2013).

104. Beckmann, J. & Lips, K. S. The non-neuronal cholinergic system in health and disease. *Pharmacology* **92**, 286–302 (2013).

105. Kawashima, K., Kajiyama, K., Fujimoto, K., Oohata, H. & Suzuki, T. Presence of acetylcholine in blood and its localization in circulating mononuclear leukocytes of humans. *Biogenic Amines* **9**, 251–258 (1993).

106. Kawashima, K., Oohata, H., Fujimoto, K. & Suzuki, T. Plasma concentration of acetylcholine in young women. *Neurosci Lett.* **80**, 339–342 (1987).

107. Kawashima, K., Oohata, H., Fujimoto, K. & Suzuki, T. Extraneuronal localization of acetylcholine and its release upon nicotinic stimulation in rabbits. *Neuroscience Letters* **104**, 336–339 (1989).

108. Fujii, T. *et al.* Species differences in the concentration of acetylcholine, a neurotransmitter, in whole blood and plasma. *Neuroscience Letters* **201**, 207–210 (1995).

109. Fujii, T. *et al.* Localization and synthesis of acetylcholine in human leukemic T cell lines. *J Neurosci Res.* **44**, 66–72 (1996).

110. Fujii, T. *et al.* Constitutive expression of mRNA for the same choline acetyltransferase as that in the nervous system, an acetylcholine-synthesizing enzyme, in human leukemic T-cell lines. *Neuroscience Letters* **259**, 71–74 (1999).

111. Rinner, I., Kawashima, K. & Schauenstein, K. Rat lymphocytes produce and secrete acetylcholine in dependence of differentiation and activation. *Journal of Neuroimmunology* **81**, 31–37 (1998).

112. Rinner, I. & Schauenstein, K. Detection of choline-acetyltransferase activity in lymphocytes. *J Neurosci Res.* **35**, 188–191 (1993).

113. Kawashima, K., Yoshikawa, K., Fujii, Y. X., Moriwaki, Y. & Misawa, H. Expression and function of genes encoding cholinergic components in murine immune cells. *Life Sciences* **80**, 2314–2319 (2007).

114. Koarai, A. *et al.* Expression of muscarinic receptors by human macrophages. *Europ. Resp Journal* **39**, 698–704 (2012).

115. Fujii, T. *et al.* Expression of Choline Acetyltransferase mRNA and Protein in T-Lymphocytes. *Proceedings of the Japan Academy, Series B* **71**, 231–235 (1995).

116. Kawashima, K. & Fujii, T. The lymphocytic cholinergic system and its biological function. *Life Sci.* **72**, 2101–2109 (2003).

117. Tayebati, S. K., El-Assouad, D., Ricci, A. & Amenta, F. Immunochemical and immunocytochemical characterization of cholinergic markers in human peripheral blood lymphocytes. *J Neuroimmunol* **132**, 147–155 (2002).

118. Fujii, T., Okuda, T., Haga, T. & Kawashima, K. Detection of the high-affinity choline transporter in the MOLT-3 human leukemic T-cell line. *Life Sci* **72**, 2131–2134 (2003).

119. Albuquerque, E. X. *et al.* Nicotinic receptor function in the mammalian central nervous system. *Ann N Y Acad Sci* **757**, 48–72 (1995).

120. Dani, J. A. & Bertrand, D. Nicotinic acetylcholine receptors and nicotinic cholinergic mechanisms of the central nervous system. *Annu Rev Pharmacol Toxicol* **47**, 699–729 (2007).

121. Gotti, C. & Clementi, F. Neuronal nicotinic receptors: from structure to pathology. *Prog Neurobiol* **74**, 363–396 (2004).

122. Black, J. Claude Bernard on the action of curare. *BMJ* **319**, 622 (1999).

123. Maehle, A.-H. "Receptive Substances": John Newport Langley (1852–1925) and his Path to a Receptor Theory of Drug Action. *Med Hist* **48**, 153–174 (2004).

124. Dale, H. H. The action of certain esters and ethers of choline and their relation to muscarine. *J of Pharma.and Exp. Therapeutics* **6**, 147–190 (1914).

125. Dale, H. H. The beginnings and the prospects of neurohumoral transmission. *Pharmacol Rev* **6**, 7–13 (1954).

126. Hurst, J. W., Fye, W. B. & Zimmer, H. Otto loewi and the chemical transmission of vagus stimulation in the heart. *Clin Cardiol* **29**, 135–136 (2006).

127. Tansey, E. M. Henry Dale and the discovery of acetylcholine. *Comptes Rendus Biologies* **329**, 419–425 (2006).

128. Albuquerque, E. X., Pereira, E. F. R., Alkondon, M. & Rogers, S. W. Mammalian Nicotinic Acetylcholine Receptors: From Structure to Function. *Physiol Rev* **89**, 73–120 (2009).

129. Unwin, N. Nicotinic acetylcholine receptor and the structural basis of neuromuscular transmission: insights from Torpedo postsynaptic membranes. *Q Rev Biophys* **46**, 283–322 (2013).

130. Lukas, R. J., Morimoto, H., Hanley, M. R. & Bennett, E. L. Radiolabeled alpha-bungarotoxin derivatives: kinetic interaction with nicotinic acetylcholine receptors. *Biochemistry* **20**, 7373–7378 (1981).

131. Servent, D. *et al.* Only snake curaremimetic toxins with a fifth disulfide bond have high affinity for the neuronal alpha7 nicotinic receptor. *J Biol Chem* **272**, 24279–24286 (1997).

132. Rajendran, B. K. *et al.* Pharmacoinformatic Approach to Explore the Antidote Potential of Phytochemicals on Bungarotoxin from Indian Krait, Bungarus caeruleus. *Comput Struct Biotechnol J* **16**, 450–461 (2018).

133. Hendrickson, L. M., Guildford, M. J. & Tapper, A. R. Neuronal Nicotinic Acetylcholine Receptors: Common Molecular Substrates of Nicotine and Alcohol Dependence. *Front Psychiatry* **4**, (2013).

134. Sine, S. M. The nicotinic receptor ligand binding domain. *J Neurobiol* **53**, 431–446 (2002).

135. Corringer, P. J., Le Novère, N. & Changeux, J. P. Nicotinic receptors at the amino acid level. *Annu Rev Pharmacol Toxicol* **40**, 431–458 (2000).

136. Millar, N. S. Assembly and subunit diversity of nicotinic acetylcholine receptors. *Biochem Soc Trans* **31**, 869–874 (2003).

137. Elgoyhen, A. B., Johnson, D. S., Boulter, J., Vetter, D. E. & Heinemann, S. α9: An acetylcholine receptor with novel pharmacological properties expressed in rat cochlear hair cells. *Cell* **79**, 705–715 (1994).

138. Couturier, S. *et al.* A neuronal nicotinic acetylcholine receptor subunit (alpha 7) is developmentally regulated and forms a homo-oligomeric channel blocked by alpha-BTX. *Neuron* **5**, 847–856 (1990).

139. Gerzanich, V., Anand, R. & Lindstrom, J. Homomers of alpha 8 and alpha 7 subunits of nicotinic receptors exhibit similar channel but contrasting binding site properties. *Mol Pharmacol* **45**, 212–220 (1994).

140. Gotti, C. *et al.* Pharmacology and biophysical properties of alpha 7 and alpha 7-alpha 8 alpha-bungarotoxin receptor subtypes immunopurified from the chick optic lobe. *Eur J Neurosci* **6**, 1281–1291 (1994).

141. McGehee, D. S. & Role, L. W. Physiological diversity of nicotinic acetylcholine receptors expressed by vertebrate neurons. *Annu Rev Physiol* **57**, 521–546 (1995).

142. Gotti, C. *et al.* Heterogeneity and complexity of native brain nicotinic receptors. *Biochem Pharmacol* **74**, 1102–1111 (2007).

143. Kalamida, D. *et al.* Muscle and neuronal nicotinic acetylcholine receptors. *The FEBS Journal* **274**, 3799–3845 (2007).

144. Benhammou, K. *et al.* [(3)H]Nicotine binding in peripheral blood cells of smokers is correlated with the number of cigarettes smoked per day. *Neuropharmacology* **39**, 2818–2829 (2000).

145. De Rosa, M. J., Dionisio, L., Agriello, E., Bouzat, C. & Esandi, M. D. C. Alpha 7 nicotinic acetylcholine receptor modulates lymphocyte activation. *Life Sci* **85**, 444–449 (2009).

146. De Rosa, M. J., Esandi, M. D. C., Garelli, A., Rayes, D. & Bouzat, C. Relationship between alpha 7 nAChR and apoptosis in human lymphocytes. *J Neuroimmunol* **160**, 154–161 (2005).

147. Fujii, T., Takada-Takatori, Y. & Kawashima, K. Basic and clinical aspects of non-neuronal acetylcholine: expression of an independent, non-neuronal cholinergic system in lymphocytes and its clinical significance in immunotherapy. *J Pharmacol Sci* **106**, 186–192 (2008).

148. Sato, K. Z. *et al.* Diversity of mRNA expression for muscarinic acetylcholine receptor subtypes and neuronal nicotinic acetylcholine receptor subunits in human mononuclear leukocytes and leukemic cell lines. *Neurosci Lett* **266**, 17–20 (1999).

149. Yoshikawa, H. *et al.* Nicotine inhibits the production of proinflammatory mediators in human monocytes by suppression of I-kappaB phosphorylation and nuclear factor-kappaB transcriptional activity through nicotinic acetylcholine receptor alpha7. *Clin Exp Immunol* **146**, 116–123 (2006).

150. de Jonge, W. J. *et al.* Stimulation of the vagus nerve attenuates macrophage activation by activating the Jak2-STAT3 signaling pathway. *Nat Immunol* **6**, 844–851 (2005).

151. Matsunaga, K., Klein, T. W., Friedman, H. & Yamamoto, Y. Involvement of nicotinic acetylcholine receptors in suppression of antimicrobial activity and cytokine responses of alveolar macrophages to Legionella pneumophila infection by nicotine. *J Immunol* **167**, 6518–6524 (2001).

152. Wang, H. *et al.* Cholinergic agonists inhibit HMGB1 release and improve survival in experimental sepsis. *Nat Med* **10**, 1216–1221 (2004).

153. Wang, Y. *et al.* Human bronchial epithelial and endothelial cells express alpha7 nicotinic acetylcholine receptors. *Mol Pharmacol* **60**, 1201–1209 (2001).

154. Wilson, G. G. & Karlin, A. Acetylcholine receptor channel structure in the resting, open, and desensitized states probed with the substituted-cysteine-accessibility method. *PNAS* **98**, 1241–1248 (2001).

155. Borovikova, L. V. *et al.* Vagus nerve stimulation attenuates the systemic inflammatory response to endotoxin. *Nature* **405**, 458–462 (2000).

156. Papke, R. L. *et al.* The analgesic-like properties of the alpha7 nAChR silent agonist NS6740 is associated with non-conducting conformations of the receptor. *Neuropharmacology* **0**, 34–42 (2015).

157. Corradi, J. & Bouzat, C. Understanding the Bases of Function and Modulation of α7 Nicotinic Receptors: Implications for Drug Discovery. *Mol. Pharmacol.* **90**, 288–299 (2016).

158. Dineley, K. T., Pandya, A. A. & Yakel, J. L. Nicotinic ACh Receptors as Therapeutic Targets in CNS Disorders. *Trends Pharmacol Sci* **36**, 96–108 (2015).

159. Papke, R. L., Meyer, E., Nutter, T. & Uteshev, V. V. alpha7 receptor-selective agonists and modes of alpha7 receptor activation. *Eur J Pharmacol* **393**, 179–195 (2000).

160. Papke, R. L., Kem, W. R., Soti, F., López-Hernández, G. Y. & Horenstein, N. A. Activation and desensitization of nicotinic alpha7-type acetylcholine receptors by benzylidene anabaseines and nicotine. *J Pharmacol Exp Ther* **329**, 791–807 (2009).

161. Corradi, J. & Bouzat, C. Understanding the Bases of Function and Modulation of α7 Nicotinic Receptors: Implications for Drug Discovery. *Mol Pharmacol* **90**, 288–299 (2016).

162. Shen, J. & Yakel, J. L. Functional α7 Nicotinic ACh Receptors on Astrocytes in Rat Hippocampal CA1 Slices. *J Mol Neurosci* **48**, 14–21 (2012).

163. Hernandez, C. M. & Dineley, K. T. α7 nicotinic acetylcholine receptors in Alzheimer's disease: neuroprotective, neurotrophic or both? *Curr Drug Targets* **13**, 613–622 (2012).

164. Shen, J. & Yakel, J. L. Nicotinic acetylcholine receptor-mediated calcium signaling in the nervous system. *Acta Pharmacol Sin* **30**, 673–680 (2009).

165. Piao, W.-H. *et al.* Nicotine and inflammatory neurological disorders. *Acta Pharmacol. Sin.* **30**, 715–722 (2009).

166. Wang, H. *et al.* Nicotinic acetylcholine receptor alpha7 subunit is an essential regulator of inflammation. *Nature* **421**, 384–388 (2003).

167. Rosas-Ballina, M. *et al.* Acetylcholine-Synthesizing T Cells Relay Neural Signals in a Vagus Nerve Circuit. *Science* **334**, 98–101 (2011).

168. Olofsson, P. S. *et al.* α7 Nicotinic Acetylcholine Receptor (α7nAChR) Expression in Bone Marrow-Derived Non-T Cells Is Required for the Inflammatory Reflex. *Mol Med* **18**, 539–543 (2012).

169. Pavlov, V. A. *et al.* Brain acetylcholinesterase activity controls systemic cytokine levels through the cholinergic anti-inflammatory pathway. *Brain Behav Immun* **23**, 41–45 (2009).

170. Parrish, W. R. *et al.* Modulation of TNF Release by Choline Requires α7 Subunit Nicotinic Acetylcholine Receptor-Mediated Signaling. *Mol Med* **14**, 567–574 (2008).

171. Fujii, Y. X. *et al.* Enhanced serum antigen-specific IgG1 and proinflammatory cytokine production in nicotinic acetylcholine receptor alpha7 subunit gene knockout mice. *J Neuroimmunol* **189**, 69–74 (2007).

172. Hao, J. *et al.* Attenuation of CNS inflammatory responses by nicotine involves α7 and non-α7 nicotinic receptors,. *Exp Neurol* **227**, 110–119 (2011).

173. Liu, Q. *et al.* Dissecting the signaling pathway of nicotine-mediated neuroprotection in a mouse Alzheimer disease model. *FASEB J* **21**, 61–73 (2007).

174. Richter, K. *et al.* Comparison of two unconventional nicotinic acetylcholine receptor ligands, phosphocholine and pCF3-diEPP. *Manuscript in Preparation*.

175. Papke, R. L., Andleeb, H., Stokes, C., Quadri, M. & Horenstein, N. A. Selective agonists and antagonists of a9 nicotinic acetylcholine receptors. *Submitted to ACS Neuroscience*.

176. Richter, K. *et al.* Phosphocholine - an agonist of metabotropic but not of ionotropic functions of α9-containing nicotinic acetylcholine receptors. *Sci Rep* **6**, 28660 (2016).

177. Papke, R. L. *et al.* Persistent activation of α7 nicotinic ACh receptors associated with stable induction of different desensitized states. *Br J Pharmacol* **175**, 1838–1854 (2018).

178. Quadri, M. *et al.* The Antinociceptive and Anti-Inflammatory Properties of the α7 nAChR Weak Partial Agonist p-CF3 N,N-diethyl-N′-phenylpiperazine. *J Pharmacol Exp Ther* **367**, 203–214 (2018).

179. Horenstein, N. A. & Papke, R. L. Anti-inflammatory Silent Agonists. *ACS Med Chem Lett* **8**, 989–991 (2017).

180. Godin, J.-R. *et al.* A silent agonist of α7 nicotinic acetylcholine receptors modulates inflammation ex vivo and attenuates EAE. *Brain Behav Immun* **87**, 286–300 (2020).

181. Espinosa, E. Identifying the anti-inflammatory potential of α7 nicotinic receptor silent agonists in human blood immune cells. *Manuscript in Preparation*.

182. Thomsen, M. S. & Mikkelsen, J. D. The α7 nicotinic acetylcholine receptor ligands methyllycaconitine, NS6740 and GTS-21 reduce lipopolysaccharide-induced TNF-α release from microglia. *J Neuroimmunol* **251**, 65–72 (2012).

183. Quadri, M., Papke, R. L. & Horenstein, N. A. Dissection of N,N-diethyl-N′-phenylpiperazines as α7 nicotinic receptor silent agonists. *Bioorg Med Chem* **24**, 286–293 (2016).

184. Borovikova, L. V. *et al.* Vagus nerve stimulation attenuates the systemic inflammatory response to endotoxin. *Nature* **405**, 458–462 (2000).

185. Waldburger, J.-M., Boyle, D. L., Pavlov, V. A., Tracey, K. J. & Firestein, G. S. Acetylcholine regulation of synoviocyte cytokine expression by the alpha7 nicotinic receptor. *Arthritis Rheum* **58**, 3439–3449 (2008).

186. Czura, C. J., Friedman, S. G. & Tracey, K. J. Neural inhibition of inflammation: the cholinergic anti-inflammatory pathway. *J Endotoxin Res* **9**, 409–413 (2003).

187. Gilboa-Geffen, A. *et al.* The thymic theme of acetylcholinesterase splice variants in myasthenia gravis. *Blood* **109**, 4383–4391 (2007).

188. García-Ayllón, M.-S. *et al.* Altered Levels of Acetylcholinesterase in Alzheimer Plasma. *PLOS ONE* **5**, e8701 (2010).

189. Liu, E. Y. L. *et al.* Interacting with α7 nAChR is a new mechanism for AChE to enhance the inflammatory response in macrophages. *Acta Pharmaceutica Sinica B* **10**, 1926–1942 (2020).

190. Vijayaraghavan, S. *et al.* Regulated Extracellular Choline Acetyltransferase Activity—The Plausible Missing Link of the Distant Action of Acetylcholine in the Cholinergic Anti-Inflammatory Pathway. *PLOS ONE* **8**, e65936 (2013).

191. Oda, Y. Choline acetyltransferase: The structure, distribution and pathologic changes in the central nervous system. *Pathol Int.* **49**, 921–937 (1999).

192. Tooyama, I. & Kimura, H. A protein encoded by an alternative splice variant of choline acetyltransferase mRNA is localized preferentially in peripheral nerve cells and fibers. *Journal of Chemical Neuroanatomy* **17**, 217–226 (2000).

193. Grosman, D. D., Lorenzi, M. V., Trinidad, A. C. & Strauss, W. L. The Human Choline Acetyltransferase Gene Encodes Two Proteins. *J Neurochem.* **65**, 484–491 (1995).

194. Bergeron, A., Schrader, A., Yang, D., Osman, A. & Simmons, D. The Final Stage of Cholinergic Differentiation Occurs Below Inner Hair Cells During Development of the Rodent Cochlea. *Journal of the Association for Research in Otolaryngology : JARO* **6**, 401–15 (2006).

195. Tata, A. M. *et al.* Subpopulations of Rat Dorsal Root Ganglion Neurons Express Active Vesicular Acetylcholine Transporter. *Journal of neuroscience research* **75**, 194–202 (2004).

196. Kljakic, O. *et al.* Cholinergic transmission from the basal forebrain modulates social memory in male mice. *Eur J Neurosci* **54**, 6075–6092 (2021).

197. Tassone, A. *et al.* Vesicular Acetylcholine Transporter Alters Cholinergic Tone and Synaptic Plasticity in DYT1 Dystonia. *Mov Disord* (2021) doi:10.1002/mds.28698.

198. Nossal, G. J. V. & Ada, G. L. CHAPTER 8 - INTERACTION OF ANTIGENS WITH CELLS OF THE RETICULOENDOTHELIAL SYSTEM. in *Antigens, Lymphoid Cells and the Immune Response* (eds. Nossal, G. J. V. & Ada, G. L.) 142–169 (Academic Press, 1971). doi:10.1016/B978-0-12-521950-1.50015-7.

199. Reale, M. & Costantini, E. Cholinergic Modulation of the Immune System in Neuroinflammatory Diseases. *Diseases* **9**, 29 (2021).

200. Fujii, T. *et al.* Induction of choline acetyltransferase mRNA in human mononuclear leukocytes stimulated by phytohemagglutinin, a T-cell activator. *J Neuroimmunol* **82**, 101–107 (1998).

201. Ye, J. *et al.* Primer-BLAST: A tool to design target-specific primers for polymerase chain reaction. *BMC Bioinformatics* **13**, 134 (2012).

202. Siniavin, A. E. *et al.* Activation of α7 Nicotinic Acetylcholine Receptor Upregulates HLA-DR and Macrophage Receptors: Potential Role in Adaptive Immunity and in Preventing Immunosuppression. *Biomolecules* **10**, 507 (2020).

203. Chernyavsky, A. I., Arredondo, J., Skok, M. & Grando, S. A. AUTO/PARACRINE CONTROL OF INFLAMMATORY CYTOKINES BY ACETYLCHOLINE IN MACROPHAGE-LIKE U937 CELLS THROUGH NICOTINIC RECEPTORS. *Int Immunopharmacol* **10**, 308–315 (2010).

204. Ihnatovych, I. *et al.* iPSC model of CHRFAM7A effect on α7 nicotinic acetylcholine receptor function in the human context. *Transl Psychiatry* **9**, 1–11 (2019).

205. Lucas-Cerrillo, A. M. de *et al.* Function of Partially Duplicated Human α7 Nicotinic Receptor Subunit CHRFAM7A Gene: POTENTIAL IMPLICATIONS FOR THE CHOLINERGIC ANTI-INFLAMMATORY RESPONSE *. *Journal of Biological Chemistry* **286**, 594–606 (2011).

206. Araud, T. *et al.* The chimeric gene CHRFAM7A, a partial duplication of the CHRNA7 gene, is a dominant negative regulator of α7*nAChR function. *Biochemical Pharmacology* **82**, 904–914 (2011).

207. Soreq, H. & Seidman, S. Acetylcholinesterase--new roles for an old actor. *Nat Rev Neurosci* **2**, 294–302 (2001).

208. Matsuo, A. *et al.* Nuclear Choline Acetyltransferase Activates Transcription of a High-affinity Choline Transporter. *Journal of Biological Chemistry* **286**, 5836–5845 (2011).

209. Misawa, H., Matsuura, J., Oda, Y., Takahashi, R. & Deguchi, T. Human choline acetyltransferase mRNAs with different 5'-region produce a 69-kDa major translation product. *Brain Res Mol Brain Res* **44**, 323–333 (1997).

210. Lockridge, O. Review of human butyrylcholinesterase structure, function, genetic variants, history of use in the clinic, and potential therapeutic uses. *Pharmacology & Therapeutics* **148**, 34–46 (2015).

211. Jasiecki, J. *et al.* Haplotypes of butyrylcholinesterase K-variant and their influence on the enzyme activity. *Chem Biol Interact* **307**, 154–157 (2019).

212. Traiffort, E., Ruat, M., O'Regan, S. & Meunier, F. M. Molecular characterization of the family of choline transporter-like proteins and their splice variants. *J Neurochem* **92**, 1116–1125 (2005).

213. Machová, E. *et al.* Detection of choline transporter-like 1 protein CTL1 in neuroblastoma × glioma cells and in the CNS, and its role in choline uptake. *Journal of Neurochemistry* **110**, 1297–1309 (2009).

214. Joviano-Santos, J. V. *et al.* Motoneuron-specific loss of VAChT mimics neuromuscular defects seen in congenital myasthenic syndrome. *FEBS J* **288**, 5331–5349 (2021).

215. Ennis, E. A. *et al.* Identification and Characterization of ML352: A Novel, Noncompetitive Inhibitor of the Presynaptic Choline Transporter. *ACS Chem Neurosci* **6**, 417–427 (2015).

216. Nizri, E., Hamra-Amitay, Y., Sicsic, C., Lavon, I. & Brenner, T. Anti-inflammatory properties of cholinergic up-regulation: A new role for acetylcholinesterase inhibitors. *Neuropharmacology* **50**, 540–547 (2006).

217. Karakiulakis, G. & Roth, M. Muscarinic Receptors and Their Antagonists in COPD: Anti-Inflammatory and Antiremodeling Effects. *Mediators Inflamm* **2012**, 409580 (2012).

218. Youssef, M. E., Moustafa, Y. & Abdelrazek, H. Molecular mechanisms of α7-nAchR-mediated anti-inflammatory effects. *IJPP* **64**, 158–173 (2021).

219. Sopori, M. Effects of cigarette smoke on the immune system. *Nat Rev Immunol* **2**, 372–377 (2002).

220. AlQasrawi, D., Abdelli, L. S. & Naser, S. A. Mystery Solved: Why Smoke Extract Worsens Disease in Smokers with Crohn's Disease and Not Ulcerative Colitis? Gut MAP! *Microorganisms* **8**, E666 (2020).

221. Kumar, R., Kumar, A., Långström, B. & Darreh-Shori, T. Discovery of novel choline acetyltransferase inhibitors using structure-based virtual screening. *Sci Rep* **7**, 16287 (2017).

222. Rowley, T. J., McKinstry, A., Greenidge, E., Smith, W. & Flood, P. Antinociceptive and anti-inflammatory effects of choline in a mouse model of postoperative pain. *Br J Anaesth* **105**, 201–207 (2010).

223. Parrish, W. R. *et al.* CHOLINE SUPPRESSES INFLAMMATORY RESPONSES. *Shock* **25**, 45 (2006).

224. Liu, L. *et al.* Choline ameliorates cardiovascular damage by improving vagal activity and inhibiting the inflammatory response in spontaneously hypertensive rats. *Sci Rep* **7**, 42553 (2017).

225. Phillips, R. J., Lutz, M. & Premack, B. Differential signaling mechanisms regulate expression of CC chemokine receptor-2 during monocyte maturation. *Journal of Inflammation* **2**, 14 (2005).

226. Parker, L. C., Whyte, M. K. B., Vogel, S. N., Dower, S. K. & Sabroe, I. Toll-Like Receptor (TLR)2 and TLR4 Agonists Regulate CCR Expression in Human Monocytic Cells. *J Immunol* **172**, 4977–4986 (2004).

227. Montague, K., Simeoli, R., Valente, J. & Malcangio, M. A novel interaction between CX3CR1 and CCR2 signalling in monocytes constitutes an underlying mechanism for persistent vincristine-induced pain. *Journal of Neuroinflammation* **15**, 101 (2018).

Appendices

Appendix A. Raw Cytokine Data of THP-1 and U937 Macrophages Treated with the Silent Agonists in the Presence of LPS

IL-1β				
Treatment	**Mean (ng/mL)**			
	THP-1 Mo	**THP-1 M1**	**U937 Mo**	**U937 M1**
DMSO	0.0	0.0	N/A	N/A
LPS + DMSO	155.2	197.2	N/A	N/A
LPS + p-CF3 diEPP	169.0	189.1	N/A	N/A
LPS + m-bromo PEP	146.6	161.3	N/A	N/A
LPS + CONH2 Iodide	163.3	190.4	N/A	N/A

TNF-α				
Treatment	**Mean (ng/mL)**			
	THP-1 Mo	**THP-1 M1**	**U937 Mo**	**U937 M1**
DMSO	1.4	0.0	4.7	0
LPS + DMSO	4361.4	7571.6	21914.9	22736.1
LPS + p-CF3 diEPP	2563.3	2955.7	17479.1	10477.3
LPS + m-bromo PEP	4985.2	8201.7	23163.6	20723.4
LPS + CONH2 Iodide	3584.4	6367.2	22066.1	19290.5

IL-10				
Treatment	**Mean (ng/mL)**			
	THP-1 Mo	**THP-1 M1**	**U937 Mo**	**U937 M1**
DMSO	0.1	0.0	54.2	31.6
LPS + DMSO	46.8	45.8	2520.5	3167.4
LPS + p-CF3 diEPP	37.8	43.9	2093.9	2751.8
LPS + m-bromo PEP	39.9	45.2	2307.2	2533.4
LPS + CONH2 Iodide	43.4	44.8	2115.5	2346.0

IL-6				
Treatment	**Mean (ng/mL)**			
	THP-1 Mo	**THP-1 M1**	**U937 Mo**	**U937 M1**
DMSO	0.0	0.0	8.9	0.0
LPS + DMSO	1402.1	2775.0	9445.7	10614.6
LPS + p-CF3 diEPP	1543.1	2646.9	7739.1	9491.5
LPS + m-bromo PEP	1420.0	2815.4	7761.9	8985.5
LPS + CONH2 Iodide	1273.4	2606.8	7697.1	8106.2

Appendix A. Raw Cytokine Data of THP-1 and U937 Macrophages Treated Acutely with Agonists and Cholinergic Inhibitors in the Presence of LPS

IL-1β				
Treatment	**Mean (ng/mL)**			
	THP-1 Mo	**THP-1 M1**	**U937 Mo**	**U937 M1**
Control	2.2	0.0	N/A	N/A
LPS	154.5	130.8	N/A	N/A
LPS + ACh	170.1	150.7	N/A	N/A
LPS + ACh + Gal	162.7	150.4	N/A	N/A
LPS + Gal	150.8	131.4	N/A	N/A
LPS + Ch	151.6	143.5	N/A	N/A
LPS + Nic	165.4	149.6	N/A	N/A
LPS + ML352	125.7	133.3	N/A	N/A
LPS + DMSO	172.9	159.1	N/A	N/A
LPS + p-CF3 diEPP	150.6	145.1	N/A	N/A
LPS + α-NETA	130.7	123.1	N/A	N/A

TNF-α				
Treatment	**Mean (ng/mL)**			
	THP-1 Mo	**THP-1 M1**	**U937 Mo**	**U937 M1**
Control	0.1	0.4	321.8	16.7
LPS	2730.2	2510.3	3308.8	483.1
LPS + ACh	3722.9	3599.0	3085.0	422.5
LPS + ACh + Gal	2964.8	2976.9	2837.6	531.3
LPS + Gal	2185.5	2966.8	3064.5	766.4
LPS + Ch	2799.1	2775.0	2855.8	489.9
LPS + Nic	2710.3	3182.0	2673.1	361.6
LPS + ML352	1385.2	1502.3	2202.8	144.9
LPS + DMSO	3349.5	3139.3	2962.5	692.3
LPS + p-CF3 diEPP	2950.9	2006.0	3173.7	743.7
LPS + α-NETA	3424.5	2998.5	3530.6	989.2

IL-10				
Treatment	**Mean (ng/mL)**			
	THP-1 Mo	**THP-1 M1**	**U937 Mo**	**U937 M1**
Control	2.1	4.5	72.1	80.7
LPS	80.9	220.3	1159.4	443.9
LPS + ACh	89.4	212.8	1154.5	412.6
LPS + ACh + Gal	98.0	239.7	994.0	397.6
LPS + Gal	81.7	193.8	1153.8	438.3

LPS + Ch	73.7	208.5	1010.3	399.8
LPS + Nic	83.4	221.2	970.0	340.5
LPS + ML352	58.5	174.2	852.0	300.1
LPS + DMSO	72.9	178.4	1007.6	430.3
LPS + p-CF3 diEPP	82.3	214.5	898.6	428.6
LPS + α-NETA	54.2	151.9	941.7	451.5

IL-6				
Treatment	**Mean (ng/mL)**			
	THP-1 Mo	**THP-1 M1**	**U937 Mo**	**U937 M1**
Control	1.4	0.0	0.1	1.6
LPS	490.4	454.7	456.9	115.5
LPS + ACh	466.7	486.6	378.6	93.2
LPS + ACh + Gal	469.5	471.7	355.3	102.0
LPS + Gal	457.0	439.3	394.1	147.4
LPS + Ch	474.9	445.7	393.3	100.2
LPS + Nic	520.3	485.4	322.3	102.7
LPS + ML352	349.7	338.4	261.9	74.8
LPS + DMSO	507.4	445.4	368.3	97.5
LPS + p-CF_3 diEPP	470.3	492.7	398.0	122.8
LPS + α-NETA	483.7	414.7	439.0	131.0

Appendix B. Raw Cytokine Data of THP-1 and U937 Macrophages Treated Chronically with Agonists and Cholinergic Inhibitors in the Presence of LPS

IL-1β				
Treatment	**Mean (ng/mL)**			
	THP-1 Mo	**THP-1 M1**	**U937 Mo**	**U937 M1**
Control	0.1	15.8	N/A	N/A
LPS	216.6	111.8	N/A	N/A
LPS + ACh	226.0	133.1	N/A	N/A
LPS + ACh + Gal	189.4	125.4	N/A	N/A
LPS + Gal	182.6	117.0	N/A	N/A
LPS + Ch	230.6	137.9	N/A	N/A
LPS + Nic	250.0	145.7	N/A	N/A
LPS + ML352	200.3	122.2	N/A	N/A
LPS + DMSO	202.2	109.4	N/A	N/A
LPS + p-CF_3 diEPP	162.0	88.7	N/A	N/A
LPS + α-NETA	136.2	68.4	N/A	N/A

TNF-α				
Treatment	**Mean (ng/mL)**			
	THP-1 Mo	**THP-1 M1**	**U937 Mo**	**U937 M1**
Control	0.1	0.0	39.3	18.7
LPS	5828.5	4856.1	3230.0	3184.7
LPS + ACh	5159.8	5497.7	2796.4	2808.9
LPS + ACh + Gal	5249.6	4147.0	3111.9	3310.7
LPS + Gal	5234.2	4575.2	3218.1	3420.6
LPS + Ch	4664.4	5322.7	2797.9	2695.7
LPS + Nic	4360.9	3439.2	2535.5	2242.7
LPS + ML352	3925.3	4036.8	2774.0	2109.2
LPS + DMSO	4419.2	4072.8	2672.7	2247.5
LPS + p-CF_3 diEPP	3886.9	4227.3	1553.4	1448.1
LPS + α-NETA	4947.5	4214.2	2936.0	2718.7

IL-10				
Treatment	**Mean (ng/mL)**			
	THP-1 Mo	**THP-1 M1**	**U937 Mo**	**U937 M1**
Control	2.2	0.3	51.4	89.7
LPS	146.0	136.4	787.6	865.8
LPS + ACh	153.4	173.2	702.9	866.1
LPS + ACh + Gal	146.5	157.3	685.3	839.3
LPS + Gal	151.8	164.0	680.6	904.8
LPS + Ch	136.8	155.8	644.9	790.8
LPS + Nic	136.0	162.5	542.3	678.7
LPS + ML352	128.0	133.3	598.3	778.4
LPS + DMSO	183.8	134.0	697.5	818.7
LPS + p-CF_3 diEPP	209.9	152.4	432.1	555.2
LPS + α-NETA	114.7	67.9	536.4	660.1

IL-6				
Treatment	**Mean (ng/mL)**			
	THP-1 Mo	**THP-1 M1**	**U937 Mo**	**U937 M1**
Control	0.0	6.5	1.8	0.8
LPS	1111.9	371.9	377.6	244.2
LPS + ACh	1046.4	390.9	338.8	247.2
LPS + ACh + Gal	966.8	387.8	355.0	252.4
LPS + Gal	966.2	365.7	331.3	250.6
LPS + Ch	1025.5	391.1	322.0	245.8
LPS + Nic	1070.8	322.3	270.8	212.4
LPS + ML352	930.5	369.6	241.1	185.9

LPS + DMSO	972.2	372.8	303.6	238.6
LPS + p-CF_3 diEPP	1127.5	445.7	226.0	178.9
LPS + α-NETA	863.5	404.8	337.6	225.8